2(P)

DEVELOPMENT OF OPTIMIZED TECHNIQUES AND REQUIREMENTS FOR COMPUTER ENHANCEMENT OF STRUCTURAL WELD RADIOGRAPHS

ESL-TM213
VOLUME I

TECHNICAL REPORT

Prepared under Contract No. NAS8-25590

John R. Adams
Sandra W. Hawley
Glenn R. Peterson
Sheldon S. Salinger
Ronald A. Workman

ESL INCORPORATED
495 Java Drive
Sunnyvale, California 94086

For: CR-123814

NASA - GEORGE C. MARSHALL SPACE FLIGHT CENTER
Huntsville, Alabama

This document consists of 152 pages.
Copy No. 8 of 25 copies.

March 5, 1971

DEVELOPMENT OF OPTIMIZED TECHNIQUES AND REQUIREMENTS FOR COMPUTER ENHANCEMENT OF STRUCTURAL WELD RADIOGRAPHS

ESL-TM213
VOLUME I

TECHNICAL REPORT

Prepared under Contract No. NAS8-25590

John R. Adams
Sandra W. Hawley
Glenn R. Peterson
Sheldon S. Salinger
Ronald A. Workman

ESL INCORPORATED
495 Java Drive
Sunnyvale, California 94086

For:

NASA - GEORGE C. MARSHALL SPACE FLIGHT CENTER
Huntsville, Alabama

This document consists of 152 pages.
Copy No. 8 of 25 copies.

March 5, 1971

CONTENTS

CONTENTS --Continued

CONTENTS --Continued

1. INTRODUCTION.

The achievement of a manned space maintenance capability on earth orbital and deep space missions requires an intimate knowledge of the initial condition of structural welds, as well as any changes in condition that they might undergo as a result of loads and environment encountered during the missions.

Radiography has long been employed as the primary tool for weld analyses. However, the physical limitations of this nondestructive testing method have introduced many opportunities for errors in judgement due to the presence of unsharp images. The requirement for the detection of cracks and crack-like defects such as porosity with a sharp "tail", chain porosity (porosity connected by a crack), lack of sidewall fusion, and the incomplete penetration of two weld beads in plate material welded from both sides has become imperative because of low safety factors. Radiography, unfortunately, is not well suited to the detection of these defects since the mass of the weld metal is only slightly distorted by their presence. Any technique which may be applied to enable the sound analysis and judgement of weld discontinuities will materially enhance the reliability of flight vehicles.

The application of computer enhancement methods which have been developed offer promise in this regard. For this reason the present study of digital enhancement of radiographs was undertaken.

1.1 Study Objective.

The objective of this study is to develop a hardware and software specification covering requirements for the computer enhancement of structural weld radiographs.

1.2 Approach.

Three scanning systems were used to digitize more than 15 weld radiographs. The performance of these systems was evaluated by determining modulation transfer functions and noise characteristics. Enhancement techniques were developed and applied to the digitized radiographs. The scanning parameters of spot size and spacing and film density were studied to optimize the information content of the digital representation of the image. Hardware requirements for

1.2 --Continued.

an X-ray enhancement system were determined and the system configuration was specified.

1.3 Summary and Conclusions.

The results of this study led to the following conclusions:

(1) The digitizing obtained for this study contained so little information that enhancement techniques could not restore the data. In no case was the definition of a weld fault as clear as could be obtained by enlarging the original radiograph.

(2) Although a wide range of spot size and spacing combinations were used in the digitizing, a meaningful emperical specification of the optimum combination could not be made because of the lack of resolvable detail in the digital data. Within the spot size range that the study was restricted to (10 μm to 25 μm) the best results based on visual comparisons were achieved with scanning spot sizes in the range 10 μm to 12 μm.

(3) Excessive system noise was found to be the major contributor to the degradation of the digital radiograph data. Thus it was demonstrated that, as presently operated, the commercial scanners used in this study are inadequate for processing weld radiographs.

(4) Many operational difficulties were encountered in obtaining the film scanning required for this study; e.g., it was not possible to send out films on a routine basis and receive consistent results. Attempts were made to acquaint the operators of the commercial scanners with the need to accurately scan the low contrast radiographs, the need to minimize environmental effects (e.g., the effects of dust, RFI, etc.), and the need to maximize the performance of the scanning system. The contractual relationship with the

1.3 --Continued.

scanning companies was such that ESL could not exercise complete control over the scanning process. However, the best scanning was obtained when ESL personnel were present. Thus it is concluded that direct tasking by NASA could lead to improved performance by the companies providing scanning services. Furthermore, through such an arrangement NASA could independently evaluate scanner performance.

(5) Because the quality of the digital data precluded meaningful visual comparisons, analytical and software tools were developed to provide a means to quantitatively evaluate the performance of scanners. Using these tools the Modulation Transfer Function and noise characteristics of the scanners were derived. The noise characteristics can be studied by calculating the standard deviations of gray levels when scanning an all black or all white area. These results, as well as the MTF's, are presented for the six scanner/lens systems used in this study. These results allow direct comparison between the different systems.

(6) A method of combining the standard deviations with the MTF's is presented. Using this method curves were developed which show the minimum number of gray levels required as a function of detail size for each of the scanner systems. The Signal/Noise ratio for threshold visibility is a parameter in determining these curves; a value of 5 as suggested in reference 1 was used to determine the curves shown.

(7) Effects of film density were studied and it was determined that radiographic information can be recorded on film at a density which is within the specified best operating range of available scanners. This density range was determined to be 1.0 to 1.4 for type M radiographic film.

(8) The scanner performance and film density analysis led to a recommendation for a feature not available on the scanners used in this study; this feature is a selectable

1.3 --Continued.

density/transmittance window. The relationship between the selection of density or transmission mode scanning and the selectable window is given. The recommended option is for a scanner with a transmittance window of selectable width and center and the capability of scanning in equal transmittance steps.

(9) Enhancement techniques were developed and applied to non-radiographic as well as radiographic data. Routines were developed which show that improved resolution can be achieved by correcting for the poor MTF's; however, this improvement is limited by the excessive noise. Digital pictures of scans with average contrast excursions verified that the enhancement routines function properly, i.e., they provide the expected improvement. These routines provide a valuable enhancement capability that can be used when better weld fault digitizing can be obtained.

(10) The analysis tools developed as part of this study are novel and should be used to analyze the performance of other scanners before undertaking expensive digitizing and processing. In addition, these tools should be used to simulate the performance of hypothetical scanners and thus establish a basis for specifying the design parameters for a scanner to meet NASA's special needs.

1.4 Report Organization.

This report consists of two separately bound volumes. Volume I contains the final technical report and Volume II contains the programmers manual. These were bound separately to permit the programmers to use the programmer's manual without having to carry along the bulk of the final report; the programmer's manual contains listings and descriptions of the enhancement routines used to process the data obtained for this study.

Volume I is divided into a final technical report and Appendix A which provides theoretical background for the report. The technical report contains six sections in addition to the present one. The contents of these sections are summarized in the following.

A detailed description of the evaluation of scanner performance is given in Section 2. This includes a summary of the capabilities of the scanners studied and the techniques developed to determine their Modulation Transfer Functions (MTF's) and noise characteristics.

Section 3 contains the results of the investigation of the role that film density and scanner spot size and spacing play in obtaining an accurate digital representation of the optical data.

Section 4 presents a complete summary of all of the digitizing obtained and processed for this study. The pertinent factors of film density, spot size and spacing, number of sample points and the scanned area are given as well as a general evaluation of each picture scanned. A number of examples of the digitized pictures and of processed pictures are given.

Section 5 contains an overview of the software routines and the total system logic flow chart. The detailed program descriptions, including listings, are bound separately in Volume II which serves as a programmer's manual.

The hardware-software, on-line versus off-line, configurations are presented in Section 6. This includes a functional description of an image processing system for radiographs and deals specifically with the central processor requirements, trade-offs in peripheral equipment, the rationale involved in selecting the special-purpose hardware, and the operating parameters for film scanner-recorders.

1.4 --Continued.

Appendix A contains the analytical background necessary for this study. It has three major sections. Section A.1 gives an overview of scanning and recording in two parts; the first part describes the scanner/recorder operation and the second part analytically considers scanner noise and accuracy. Section A.2 gives the development of the scanner evaluation techniques, and Section A.3 considers the analysis of film grain and gray level quantization.

2. SCANNER/RECORDER EVALUATION.

Two essential steps in the digital enhancement of radiographs are the digitization of the X-ray films (the input images) and the display and recording of the digitally processed images at various stages of enhancement. The optical-to-digital (O/D) conversion process is accomplished with a digital film scanner. The final hard-copy photographic record of digitally processed X-rays can be obtained with a digitally controlled film recorder, or by photographing a video display of the digital image.

If the digital image enhancement process is to be successful, it is necessary that the radiographic information be neither lost, degraded, nor distorted during the film scanning process. Information lost in film scanning is excluded from enhancement and further use, while image degradations and distortions place additional requirements upon the digital enhancement process. Because of their fundamental role in the digital processing of radiographs, the general nature and operation of film scanner/recorders are described in Section A.1.1 of the appendix. Section A.1.2 of the appendix provides the general background for the consideration of noise and accuracy of scanner/recorders.

During the course of this study the quality of the digitizing made it evident that it was necessary to develop accurate and meaningful methods to evaluate the performance of the three commercial film scanner/recorders used to digitize the radiographs. The method developed in this study is based on deriving the Modulation Transfer Function of the scanner. Section 2.1 summarizes the specifications of the three scanning systems. Section 2.2 discusses the problems encountered in obtaining the digitizing. Section 2.3 discusses the method for determining the Modulation Transfer Function and shows the results for each of the three systems. The problem of system noise is considered and the noise characteristics of each system is shown in Section 2.4. Section 2.5 completes the scanner evaluation by considering the spatial resolution that can be expected with each system. The digital-to-optical conversion step is discussed in Section 2.6.

2.1 Specifications of Scanners Used.

A requirement of the study performed by ESL was to investigate the effects of spot size (in the range 10 μm to 25 μm), spot spacing, and film density on digitization. Three commercially available film-scanner systems were selected for

2.1 --Continued.

use in this investigation. These systems are maintained by Information International Incorporated (I.I.I.), Link Division of Singer, and Dicomed. The I.I.I. and Link systems are flying spot scanners and the Dicomed system is an image dissector. The vendor specified capabilities of these three systems are summarized in Table 2-1.

Table 2-1. Summary of Scanner Capabilities.

System	Lens	Minimum Distance Between Spot Centers	Maximum Scanning Area	Spot Size Range	Density Range	Number of Gray Levels
I. I. I.	125:1	4.3 μm	70x70 mm	2 μm to 160 μm	0 to 4.0	64, 128, 256, 512
	3:1	1.5 μm	25x25 mm			
	7.25:1	0.6 μm	10x10 mm			
Link	1:1	8 μm	100x128 mm	13 μm to 200 μm	0 to 2.5	64, 256
	3:1	2.5 μm	23x36 mm			
Dicomed	1:1	25 μm	50x50 mm	13μm;25μm	0.05 - 2.25	16, 32, 64

An important consideration in film scanning is the time required to perform the digitizing. The time required to scan an X-ray involves two factors: job preparation and film scan time. The job preparation may include any or all of the following:

(1) film cutting or sprocketing,
(2) film mounting in the film holder,
(3) area specification (by marks on the film or by coordinate determination),
(4) photomultiplier voltage adjustment,
(5) film positioning.

2.1 --Continued.

Of the above items, it was found that 4 and 5 were the most important. For example, because routine procedures have not been established at Link, the 4 pictures scanned with the 3 to 1 lens required an average of one hour each to determine the proper adjustments and to position the film. The most satisfactory voltage level must be determined through experience with film of any particular density.

After the job is prepared, the time required for scanning depends on the scanner and the number of bits of data being obtained. Table 2-2 gives the scan times for the three systems used in this study.

Table 2-2. Scanning Times for Systems Used.

Scanning Company	No. of Bits of Data	Scan Time for One Million Points	Limiting Factor
I.I.I.	6 9*	2.5 min. 20 min.	Tape limited Computer limited
Link	6 8	1.7 min. 1.7 min.	Computer limited -- this includes software to provide histograms
Dicomed	4 5 6	1.1 min. 2 min. 3.8 min.	Scanner limited

* I.I.I. has an improved hardware capability which is expected to be operational in early 1971. This would reduce the 9-bit scan time to 30 seconds and would be computer limited.

2.2 Problems Encountered in Digitizing.

The most basic requirement of any system involving the digital processing of photographic data is the high quality conversion of the photograph to digital form. Many problems were encountered under this contract in obtaining sufficiently high quality in the digitizing. A few of these problems are discussed below.

Noise introduced by dirt and dust can be a significant problem. Any film to be digitized must be handled with sufficient care to prevent collecting tiny scratches, fingerprints and dust. Without complete control of the scanning system this is difficult to achieve. While a scratch on the negative can in general be differentiated from information in the original film such differentiation does require time and information on the part of the weld analyst. Analyzing several radiographs of the same area provides a check on any suspect information, but is extremely inefficient.

Dust can be removed from the film before scanning but may still be present within the optics of the system. Neither Link, I.I.I. nor Dicomed attempt to scan in a dust-free environment. If it is not possible to perform the digitizing in a clean room, then it can be expected that some degradation of information content will result. An open aperture scan was obtained from Link and Dicomed but insufficient time and funds prevented analyses of the dust problem.

Radio frequency interference can cause positional errors in the scanning process. I.I.I., Link, and Dicomed indicate that there is no significant interference as a result of RF. The Link scanning, however, shows significant geometric distortion, streaking and "herringbone" effects (See Figure 2-11) which are attributed to RFI. Re-recording done at Link under another contract also revealed positional distortion. The presence of any geometric distortion is not tolerable in the analysis of weld data. The streaking and "herringbone" effect can create spurious nonexistent defects. The effect can be removed by providing shielding against RF frequencies in the area of the scanner.

If only a section of a radiograph is to be scanned it is necessary to develop a method of specifying the coordinates so that the area can be quickly and accurately positioned in the center of the aperture. Because the standard film holder holders used by I.I.I. and Link required that the radiograph be cut and mounted, it was found that the only way to ensure that the scanning did cover the area of interest was to mark the film. This procedure accomplished two things:

(1) the scanner operator could see the mark on his on-line

2.2 --Continued.

display device and could adjust the film position until it was properly centered, and

(2) the image analyst could see the mark on the display of his original data and could be assured that the desired area had been scanned.

Prior to establishing this procedure several scans were not properly positioned by the operators.

To obtain a sharp digital image of the photographic data the scanner must be accurately focused. Both Link and I.I.I. have extensive experience with single emulsion film. Every attempt was made to insure proper focus on the double emulsion films used in this study. However it is recommended that a sharp black/white image on Type M film should be used to determine the optimum focusing techniques for any particular scanner. The practical experience gained in this study indicates that it will be necessary to verify proper focus for each frame being scanned.

Many factors can produce a distorted spot. Periodic scanning of a standard black and white pattern is suggested to check for problems such as spot flare (encountered once in this contract) or halation. The contrast of the images in the radiographs is too slight to allow visual detection of these problems.

2.3 Modulation Transfer Function.

This section gives a detailed discussion of the method used to determine the Modulation Transfer Function (MTF) of the scanning systems. The resulting MTF's are shown for each of the scanner-lens combinations that were used for the digitizing. A detailed theoretical discussion of the Modulation Transfer Function and its characteristics is contained in Section A.2.1 of the appendix.

The basic input to the program that calculates the MTF (see page 51 of Vol. II) is the digital representation of a black/white edge. A high contrast Air Force Resolution chart was digitized by each of the 6 scanner-lens systems (3 for I.I.I., 2 for Link and 1 for Dicomed) used in this study. The Air Force chart is a test pattern made up to sets of parallel alternately white and black bars. From each of the

2.3 --Continued.

scanned charts both a vertical and horizontal black/white transition were selected such that the transition was approximately centered in a 128 x 128 data set. Figure 2-1 shows the vertical transitions used to determine the MTF's for the I.I.I. system with the 1.25:1 lens, the Link 1:1 scanning system and the Dicomed scanning system.

The MTF's were calculated by the MTF program (see page 51, Vol. II) from these data sets in the following way. Since each line of data represents the edge trace response of the scanner system being studied, the first step is to calculate the one-dimensional spatial derivative of each line; the result is the line spread function of the system. Then, for each line, the Fourier transform of the derivative is formed and the magnitude of the frequency components scaled so that the DC term is unity. The MTF program outputs the average value of each frequency component. Knowledge of the point-to-point spacing allows the determination of the scale factor to convert from the Fourier frequency domain to the spatial frequency domain. The MTF curve is obtained by plotting the magnitude of the frequency component versus the spatial frequency.

Applying the above technique to transitions scanned with the six scanner-lens systems studied gives the curves labeled "1" in Figures 2-2 through 2-7. As discussed in Section A.2.2 of the appendix, the MTF should decrease monotonically. However, curves "1" of Figures 2-2 to 2-6 decrease to a minimum value and then increase. The latter feature indicates the presence of noise. As the analysis in Section A.2.1 shows, taking the spatial derivative of the original data introduces a multiplicative sine function in the Fourier transform. The MTF can be corrected by subtracting out a noise-constant times the sine wave; see Section A.2.1 and in particular Figure A.2-6. The results of making this correction are the shown as curves labeled "2" in Figures 2-2 to 2-6. The data shown in Figure 2-7 could not be corrected, i.e., the noise constant could not be determined because of the limited spatial frequency range covered by the data.

A second way to calculate a noise-free MTF is to perform a smoothing of the original line spread function before taking the Fourier transform. The smoothing operation consist of aligning the black/white transition and then averaging all of the lines together. The resulting noise-free MTF's agree well with those obtained by the first method described. Figure 2-8 illustrates this agreement for the Link 3:1 scanner. Both methods are applied by the MTF program (see page 51, Vol. II).

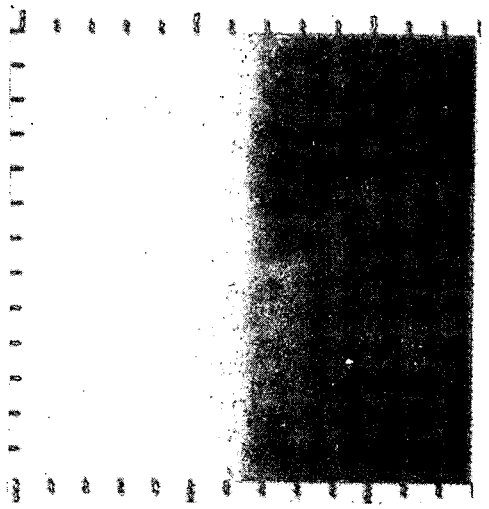

I.I.I. 1.25:1 lens

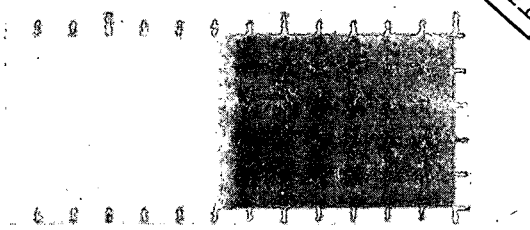

Link 1:1 lens

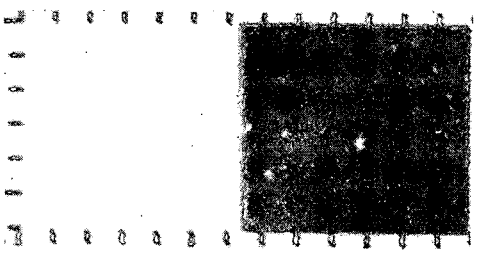

Dicomed 1:1 lens

Figure 2-1. Black to White Transitions Used as Input for Determining the System MTF Curves.

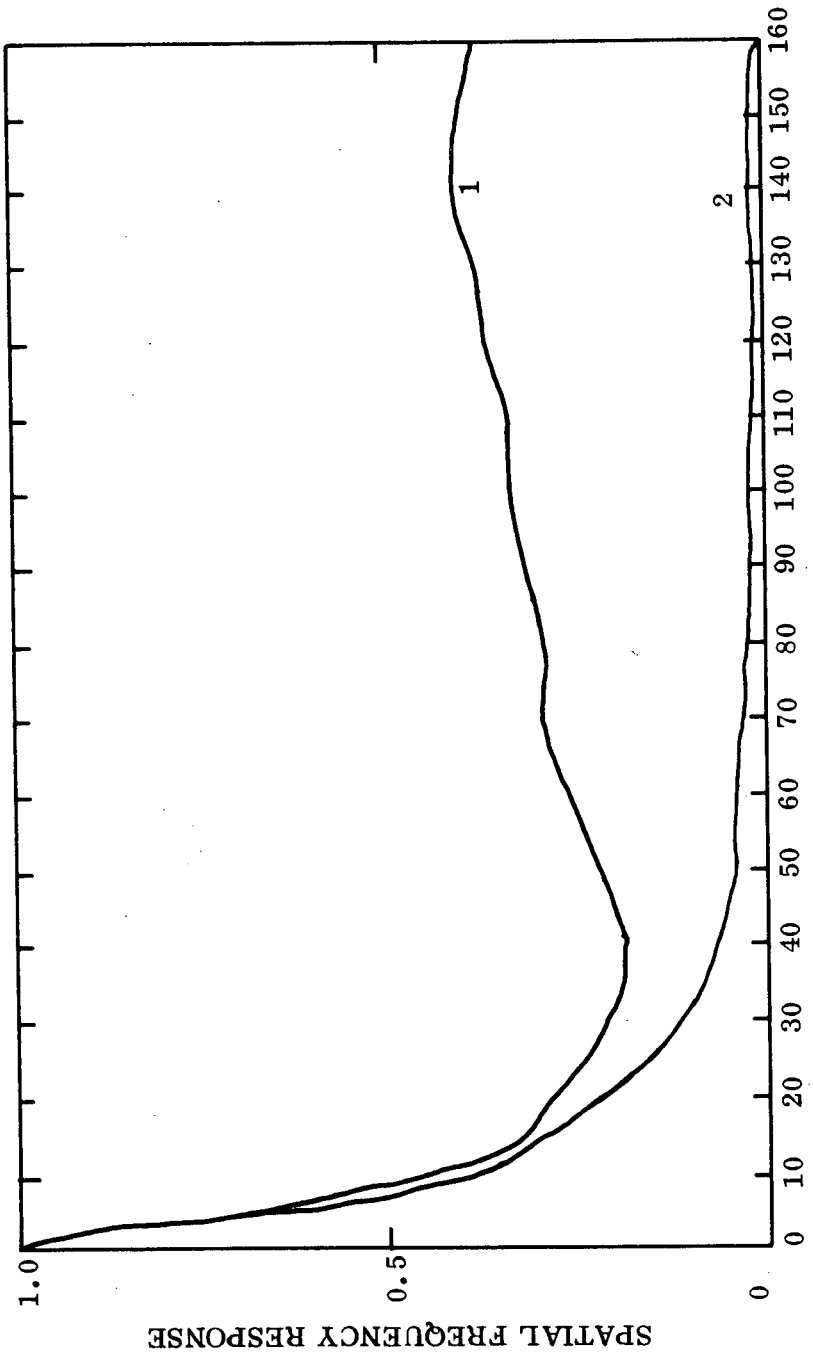

Figure 2-2. Calculated MTF for I.I.I. 1.25:1 System. Curve 1 shows the MTF with noise. Curve 2 shows the result of subtracting the product of the noise constant and the sine function from Curve 1.

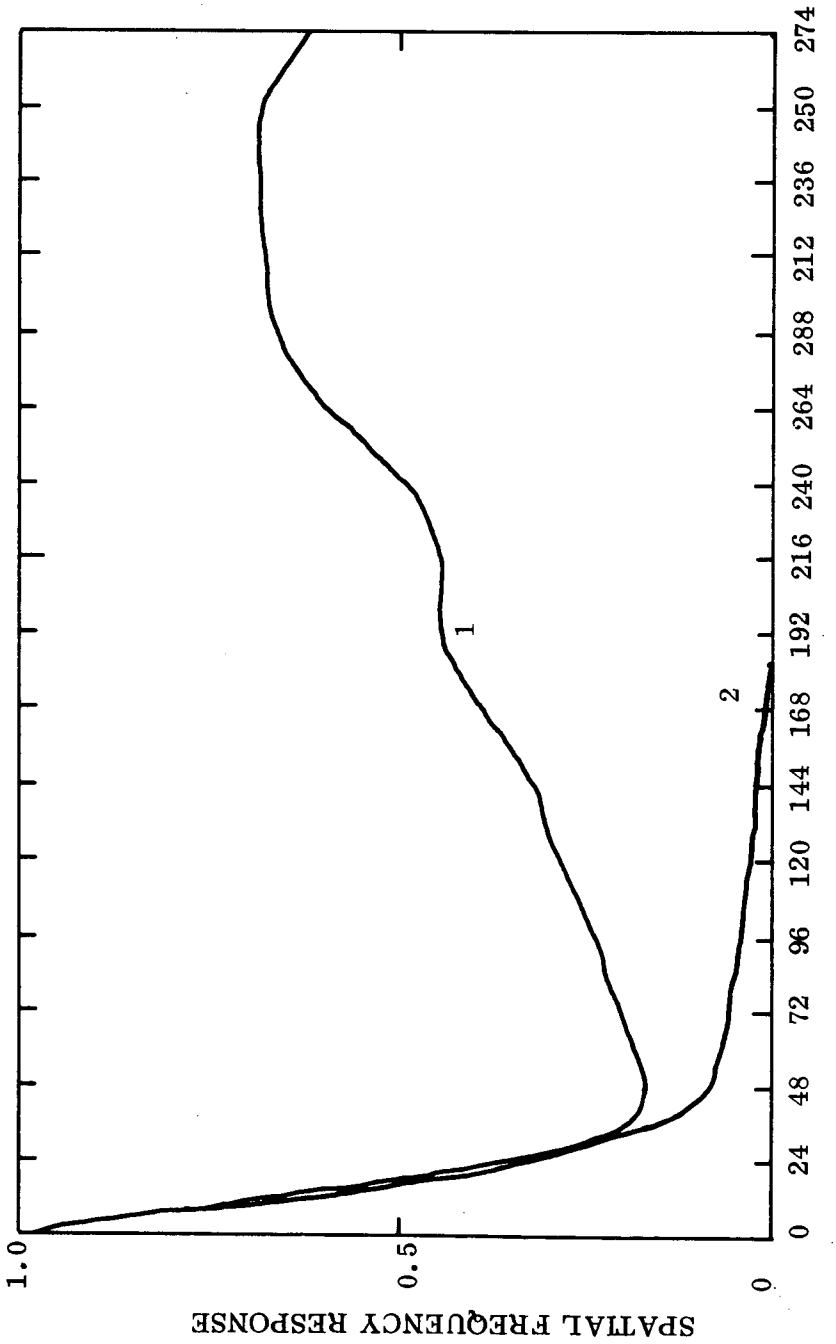

Figure 2-3. Calculated MTF for I.I.I. 3:1 System. Curve 1 shows the MTF with noise. Curve 2 shows the result of subtracting the product of the noise constant and the sine function from Curve 1.

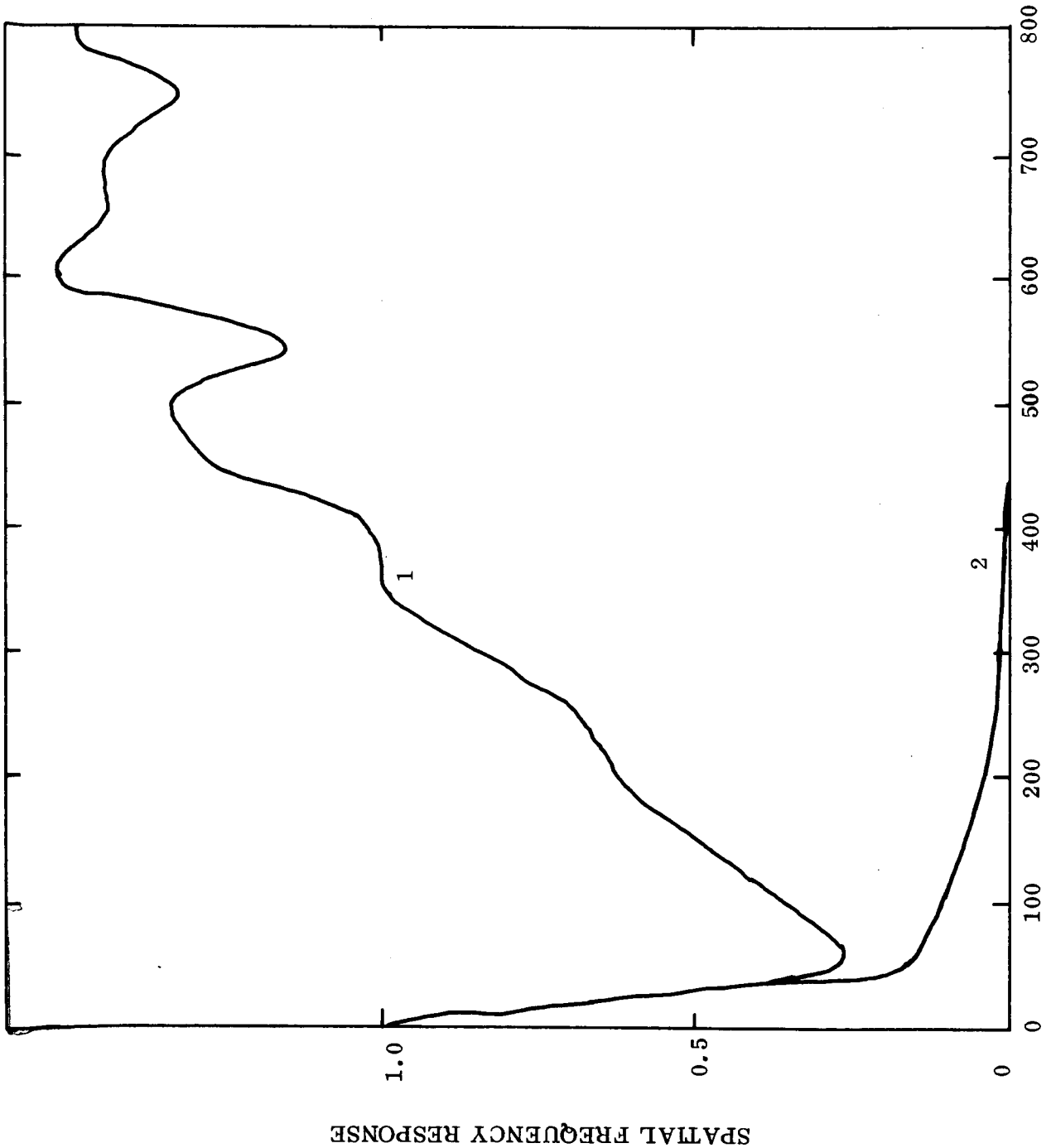

Figure 2-4. Calculated MTF for I.I.I. 7.25:1 System. Curve 1 shows the MTF with noise. Curve 2 shows the result of subtracting the product of the noise constant and the sine function from Curve 1.

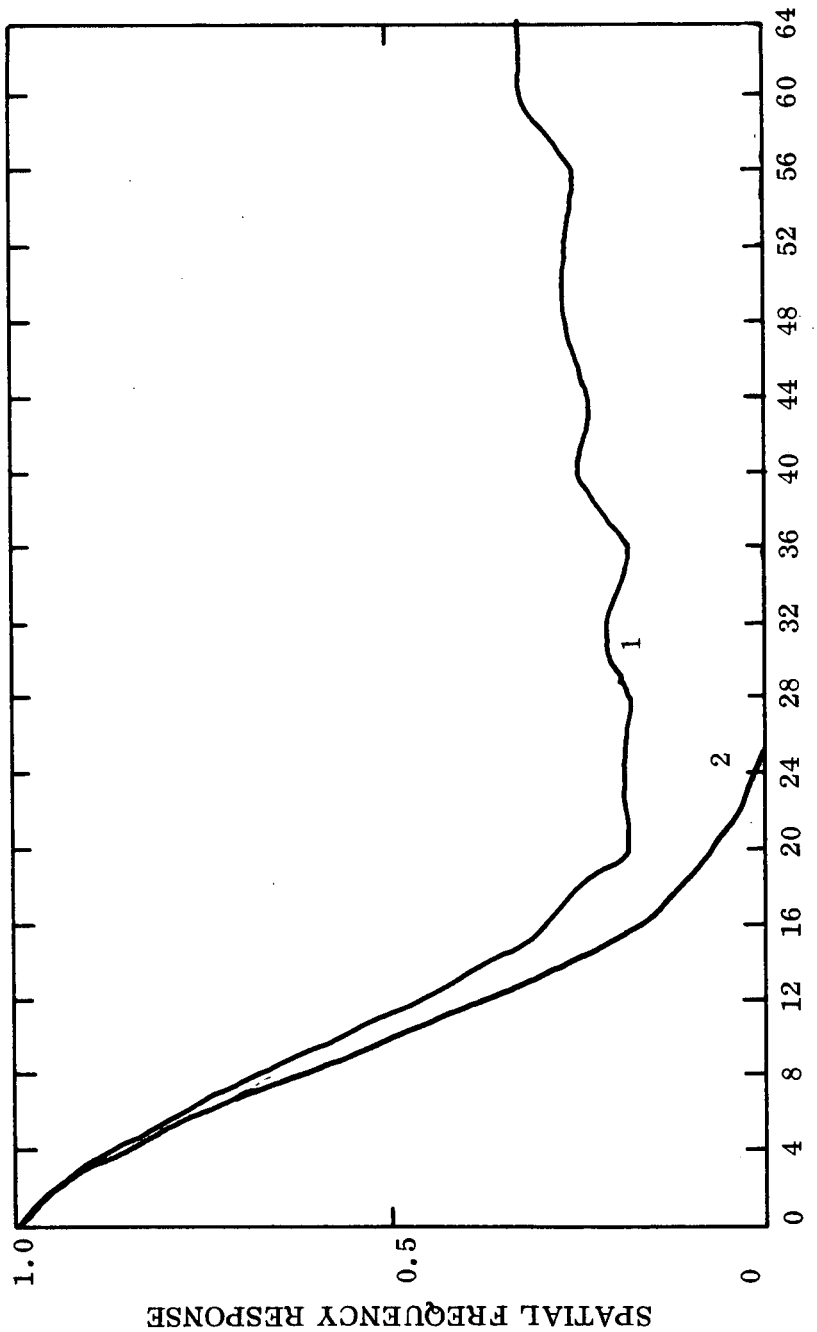

Figure 2-5. Calculated MTF for Link 1:1 System. Curve 1 shows the MTF with noise. Curve 2 shows the result of subtracting the product of the noise constant and the sine function from Curve 1.

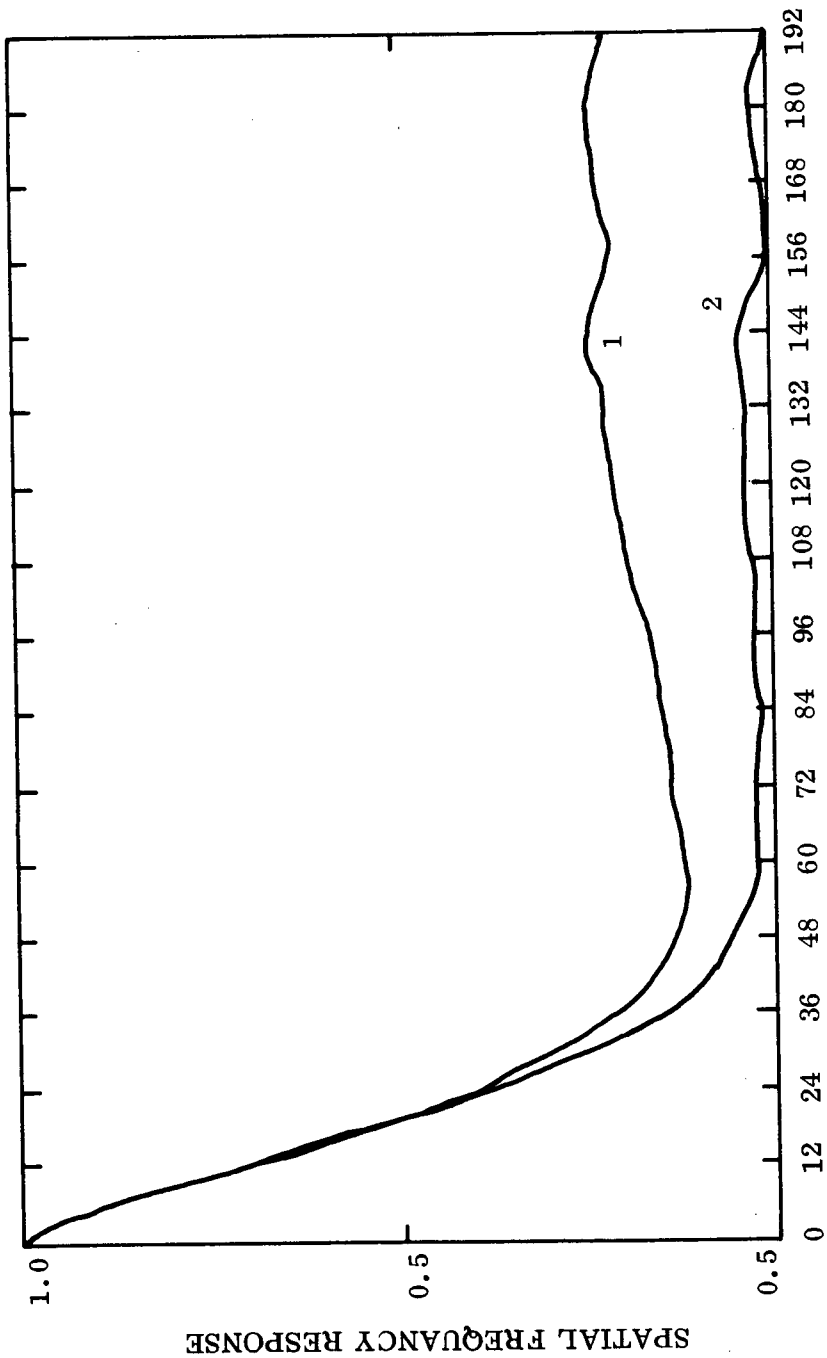

Figure 2-6. Calculated MTF for Link 3:1 System. Curve 1 shows the MTF with noise. Curve 2 shows the result of subtracting the product of the noise constant and the sine function from Curve 1.

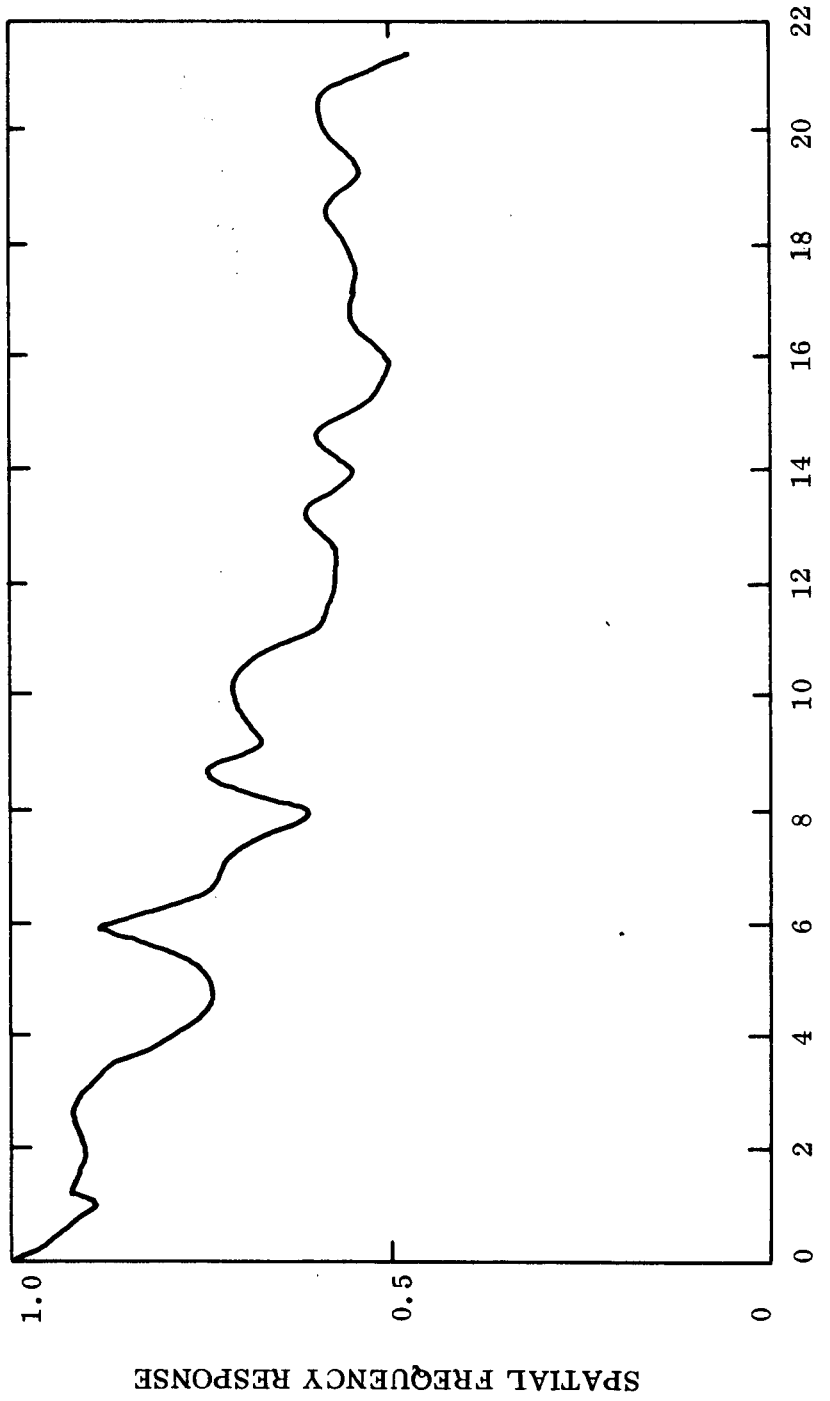

Figure 2-7. Calculated MTF for the Dicomed System.

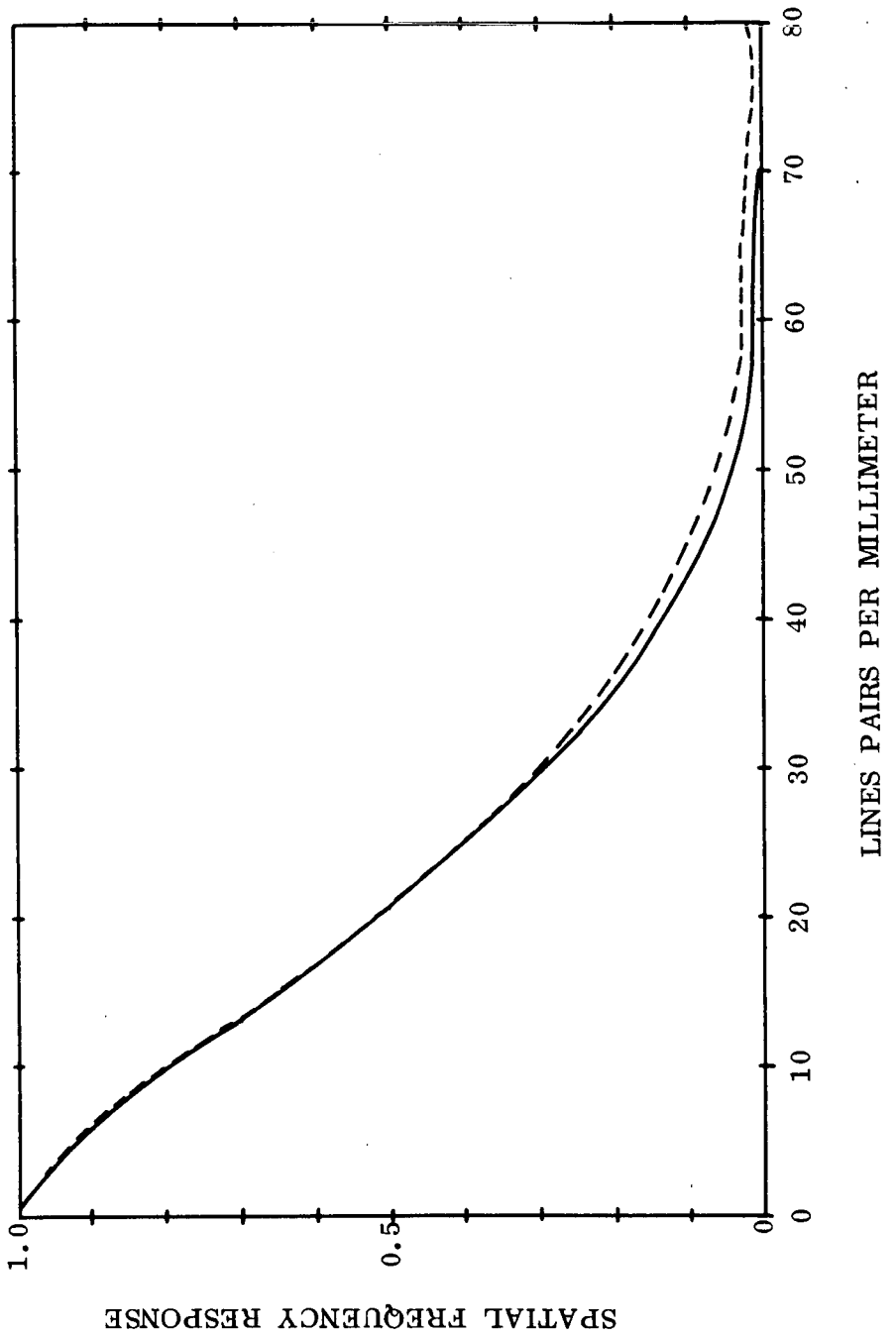

Figure 2-8. Comparison of the two techniques to remove the effect of noise from the MTF for the Link 3:1 scanner. The solid curve was calculated by subtracting a noise constant times a sine function. The dashed curve was calculated by aligning the black/white transition.

2.3 --Continued.

The primary purpose for determining the MTF's was to provide a means of evaluating system performance. These curves in conjunction with the system Signal-to-Noise ratio (SNR) allow the comparison of the resolution capability of the six systems. The noise evaluation is discussed in Section 2.4 and the evaluation of the complete system is treated in detail in Section 2.5.

A second use for the MTF's is that they allow the generation of an inverse filter which can be applied to all the scanning performed by that system. This inverse filter will improve the modulation of the data to as great an extent as the noise in the system will permit; in this sense it is the optimum filter that can be generated.

The improvement that can be gained by applying the inverse filter can be seen by filtering the black/white transition and then determining a new MTF from the sharper black/white edge. This new MTF will be as close an approximation to the ideal transfer function (which is unity) out to the limiting spatial frequency as can be obtained. This improvement is demonstrated in Figures 2-9, 2-10, and 2-11. The improvements shown in Figures 2-9 and 2-10 are substantial enough to indicate that inverse filtering could be a valuable enhancement technique for data such as that obtained with the Link and I.I.I. systems. However, the curves in Figure 2-11 show that inverse filtering data scanned with the Dicomed system is not justified since relatively little improvement in the MTF can be achieved. The primary limiting factor in the successful use of the inverse filter is the noise introduced into the data by the scanning system.

An example of the visual improvement obtainable by inverse filtering is shown in Figure 2-12. The top picture (a) is a display of the original digitizing of a section of an Air Force Resolution chart as scanned with the Link 3:1 lens and the bottom picture (b) shows the same section after inverse filtering. The improved resolution is apparent. The departures from the straight lines defining the black/white transitions are caused by radio frequency interference as discussed in Section 2.2.

2.4 Noise Evaluation.

The presence of noise is a critical factor in the enhancement of X-ray data because of weak signals found on the radiograph film. Although some system

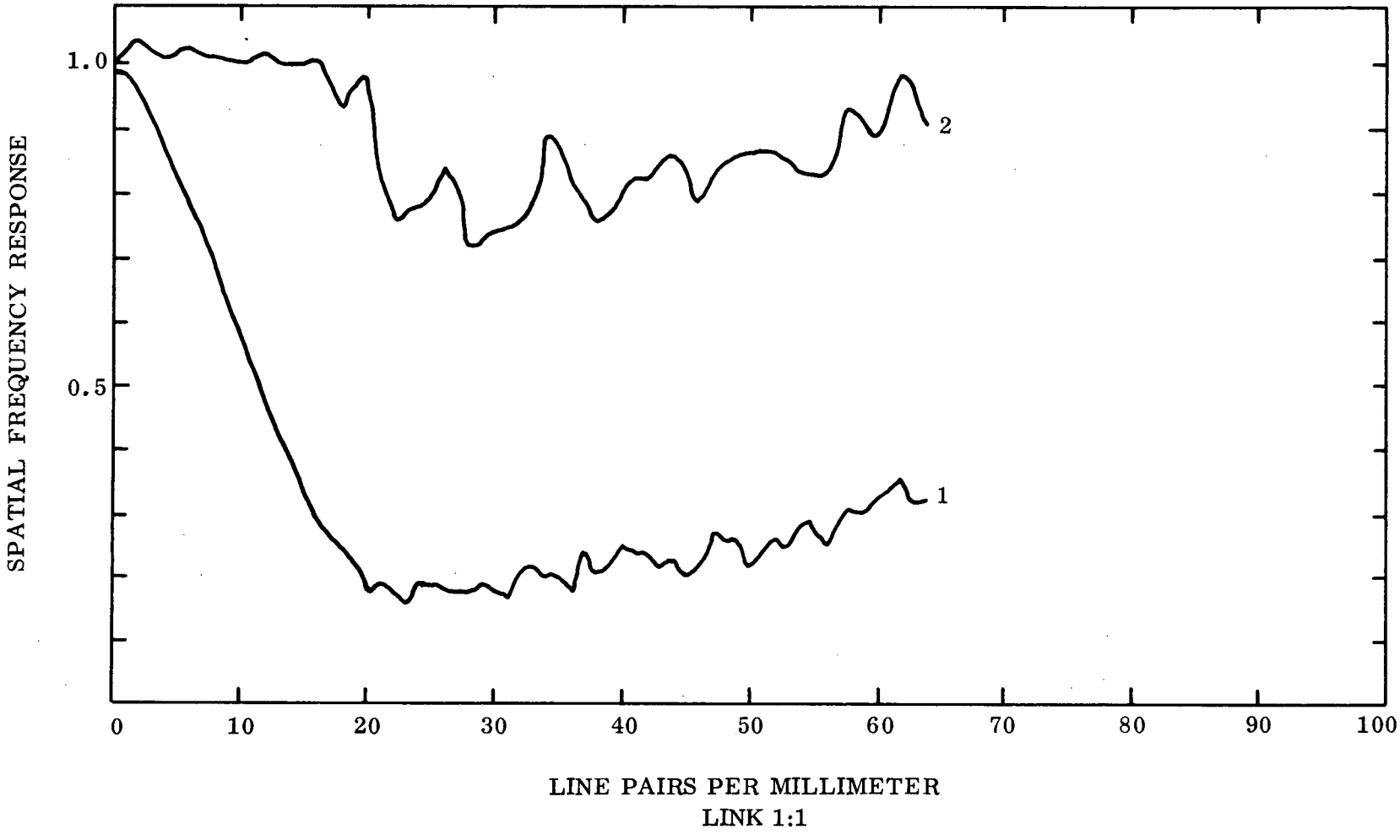

Figure 2-9 . Curve 1 is the MTF calculated from the original black to white transistion; Curve 2 is the MTF calculated from the filtered black to white transition.

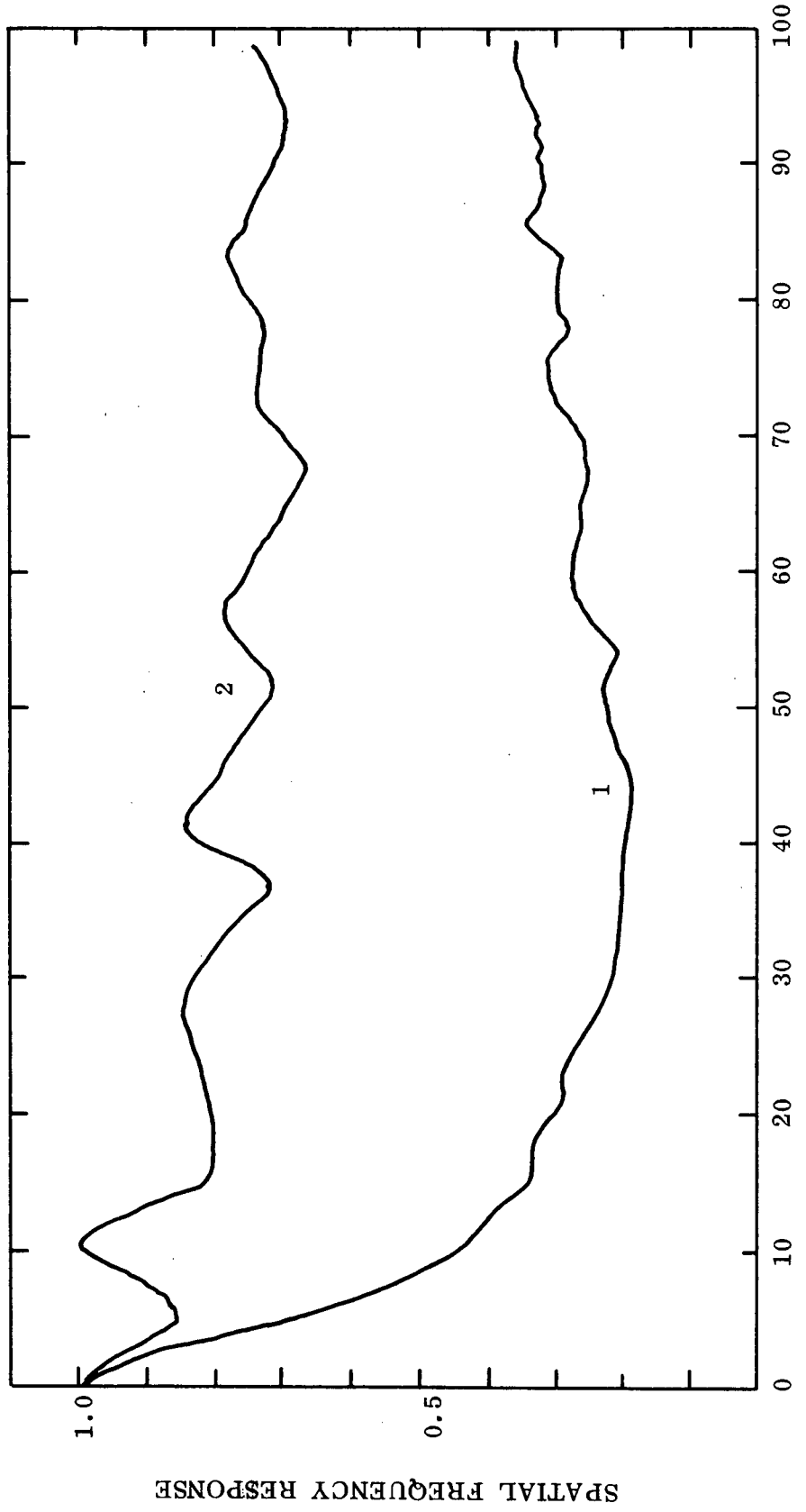

Figure 2-10. Curve 1 is the MTF calculated from the original black to white transition; Curve 2 is the MTF calculated from the filtered black to white transition.

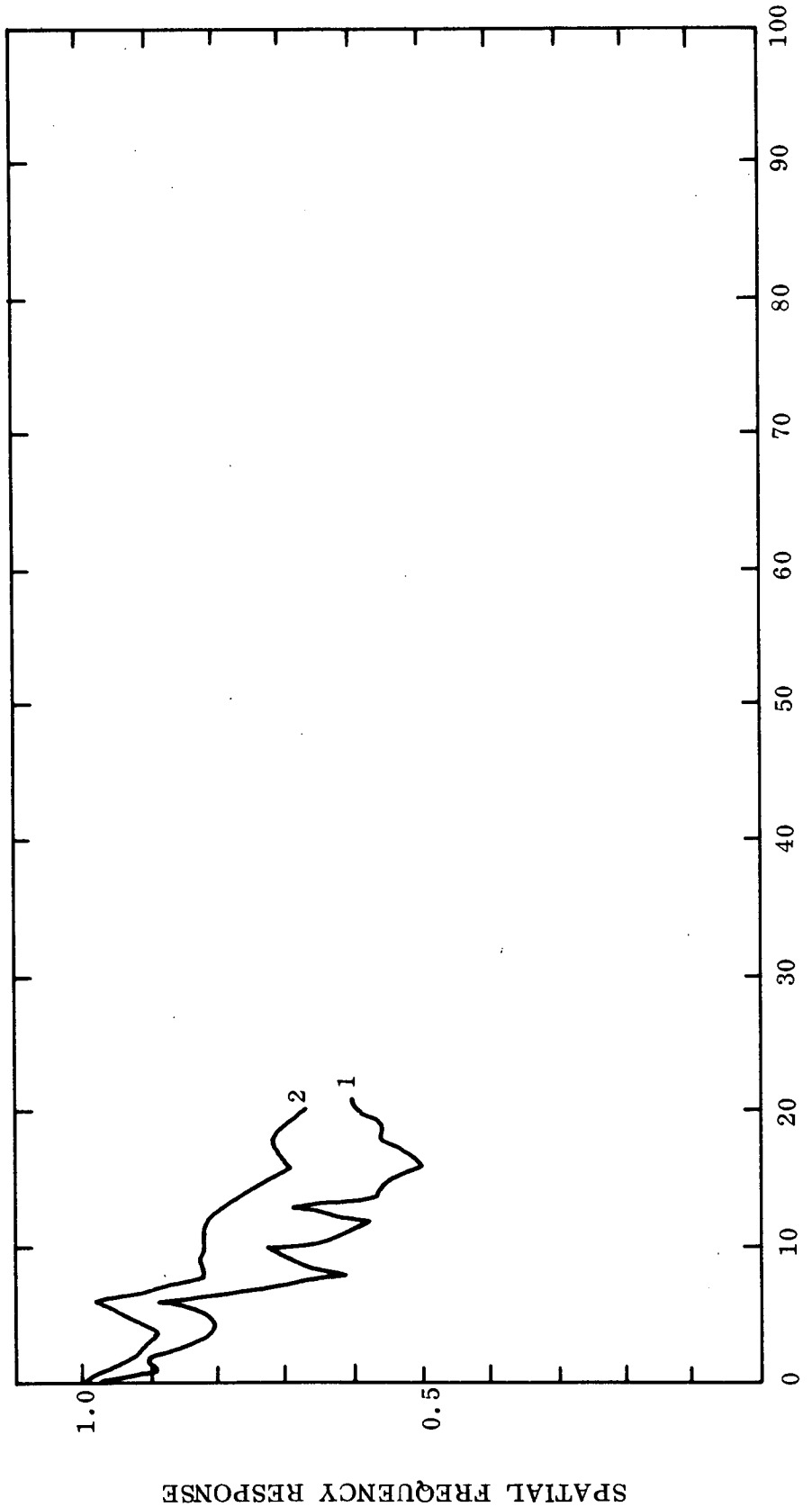

Figure 2-11. Curve 1 is the MTF calculated from the original black to white transition; Curve 2 is the MTF calculated from the filtered black to white transition.

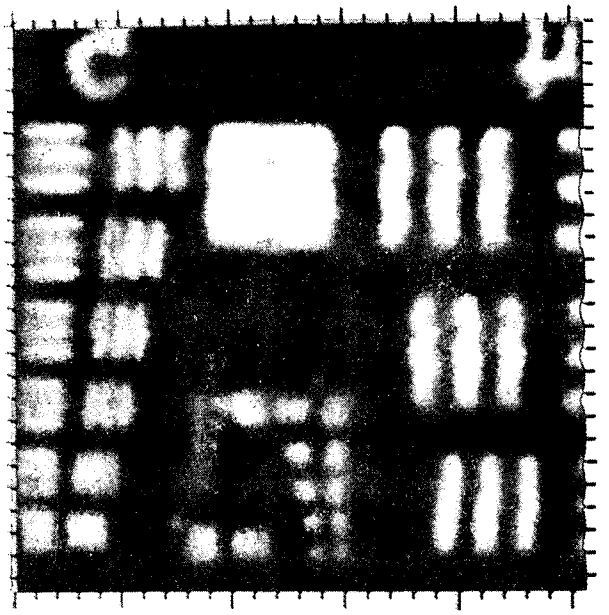

(a) before filtering

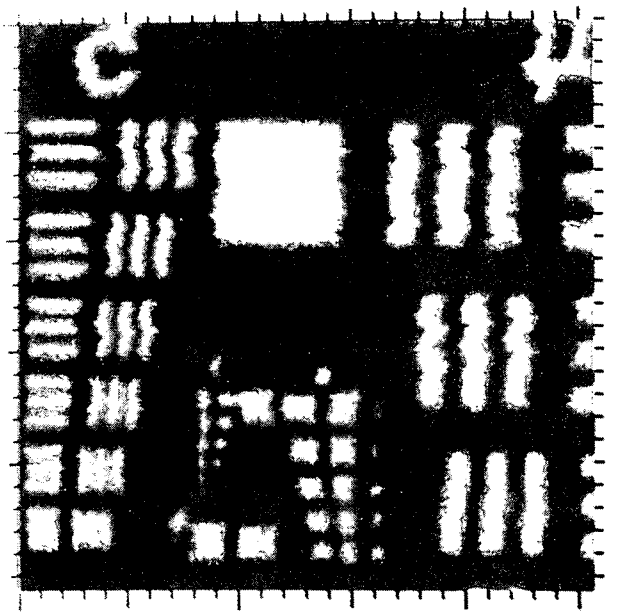

(b) after filtering

Figure 2-12. Resolution chart scanned with the Link 3:1 System.

2.4 --Continued.

noise was anticipated in the evaluation of film scanners it was found that the hardware introduces excessive noise; the various sources of hardware noise are discussed in the appendix in Section A.1.1. Furthermore, the MTF's generated from the resolution charts clearly demonstrated that there is an appreciable difference in the noise introduced by different systems. The principal factors contributing to the overall noise in the scanning process are:

(1) lack of clean room environment,
(2) radio frequency interference,
(3) electronic hardware noise, and
(4) quantization noise.

The relative quantitative affects of each of these noise sources can only be determined by performing scanning under conditions in which the effects of a clean room and an RF shielded room could be studied separately. These results could then be combined with a parametric model of a CRT scanner to evaluate hardware and quantization noise. This is an important study but beyond the scope of the present work.

The scanning done by I.I.I. showed significant differences in the noise contribution when the lens systems were changed; compare Figures 2-2, 2-3, and 2-4. This is primarily caused by the reduced amount of energy reaching the photomultiplier tube. The most significant increase in noise occurred with the 7:1 lens system which delivers the lowest energy to the photomultiplier tube. This fact is supported qualitatively by the results of the MTF evaluation. The Link system shows no significant dependence on the lens system.

A meaningful way to analyze the degradation introduced by a scanner is to consider the deviations in intensity levels that occur on scanning a flat field (an all black or all white area). Such an analysis tool was developed and applied in the following way. The noise program is described in Vol. II, page 61.

From each of the data sets containing the black/white transitions the mean values of the black areas and white areas sections were computed. This calculation was performed on both a horizontal and a vertical transition for each of the six scanner-lens systems; there was no significant difference between the horizontal and vertical cases. Table 2-3 summarizes the standard deviations for each system, normalized to the maximum possible value of 255.

Table 2-3. Standard Deviations of the Black Areas and White Areas for the Six Systems.

Scanner System	Lens	Normalized Standard Deviation (σ) (percentage) White Area	Black Area
Link	1:1	1.01	1.28
	3:1	0.28	0.92
I.I.I.	1.25:1	1.30	1.78
	3:1	0.47	2.15
	7.25:1	4.40	6.08
Dicomed	1:1	0.85	5.04

It should be stressed that the values shown in Table 2-3 have been determined from flat fields on extremely fine grain, high resolution film. Therefore, none of the variations in gray level are caused by film grain effects; or by degradations introduced by the X-ray imaging system. Thus the results in Table 2-3 give a direct quantitative measure of scanner system noise.

Knowledge of the standard deviation of the scanner noise can be used in combination with the MTF to determine the resolution capability of each system. This is considered in the following section.

2.5 Scanner Resolution Capability.

To complete the scanner analysis in this section the tools previously discussed (the MTF and the standard deviation of the noise) are used to model the effect of the scanner on an ideal input. By varying the input (detail size) and specifying the required signal-to-noise ratio for the output picture the number of gray levels ($N(\omega)$) required to resolve a detail with spatial frequency ω can be determined. In particular

$$N(\omega) = \frac{(S/N) \bullet \sigma}{RANGE} ,$$

where σ is obtained from Table 2-3 and "RANGE" is determined as follows: the Fourier transform of an ideal (computer generated) input is multiplied by the system MTF. This models the system effect on the frequency domain of the input original. The inverse transform of this product represents, in the spatial domain, the input signal after being degraded by the system. The original picture had a normalized signal that varied from 0 to 1.0 to represent the detail of interest. The degraded picture will represent the detail with a signal that varies from a to b where

$$o \leq a \leq b \leq 1.0$$

The difference b-a is the value of "RANGE".

Figure 2-13 shows plots of $N(\omega)$ for each of the six systems. For these figures S/N is 5, the value required to discriminate the signal from the background.[1] The data for Figure 2-13 were obtained using the program size (Vol. II, page 65). These results which are for non-radiographic film agree with the results of scanning weld images. In particular the scanning performed by Link with the 3:1 lens did contain the most information, and the I.I.I. 3:1 lens gave the next best result. Note that Figure 2-13 shows that for higher frequencies the I.I.I. 1.25 to 1 lens requires fewer gray levels to resolve detail than the 7.25:1 lens. This is because of the high noise level in the 7.25:1 lens system and is an important result since the larger spot size with the 1.25:1 lens allows faster scanning and fewer data samples.

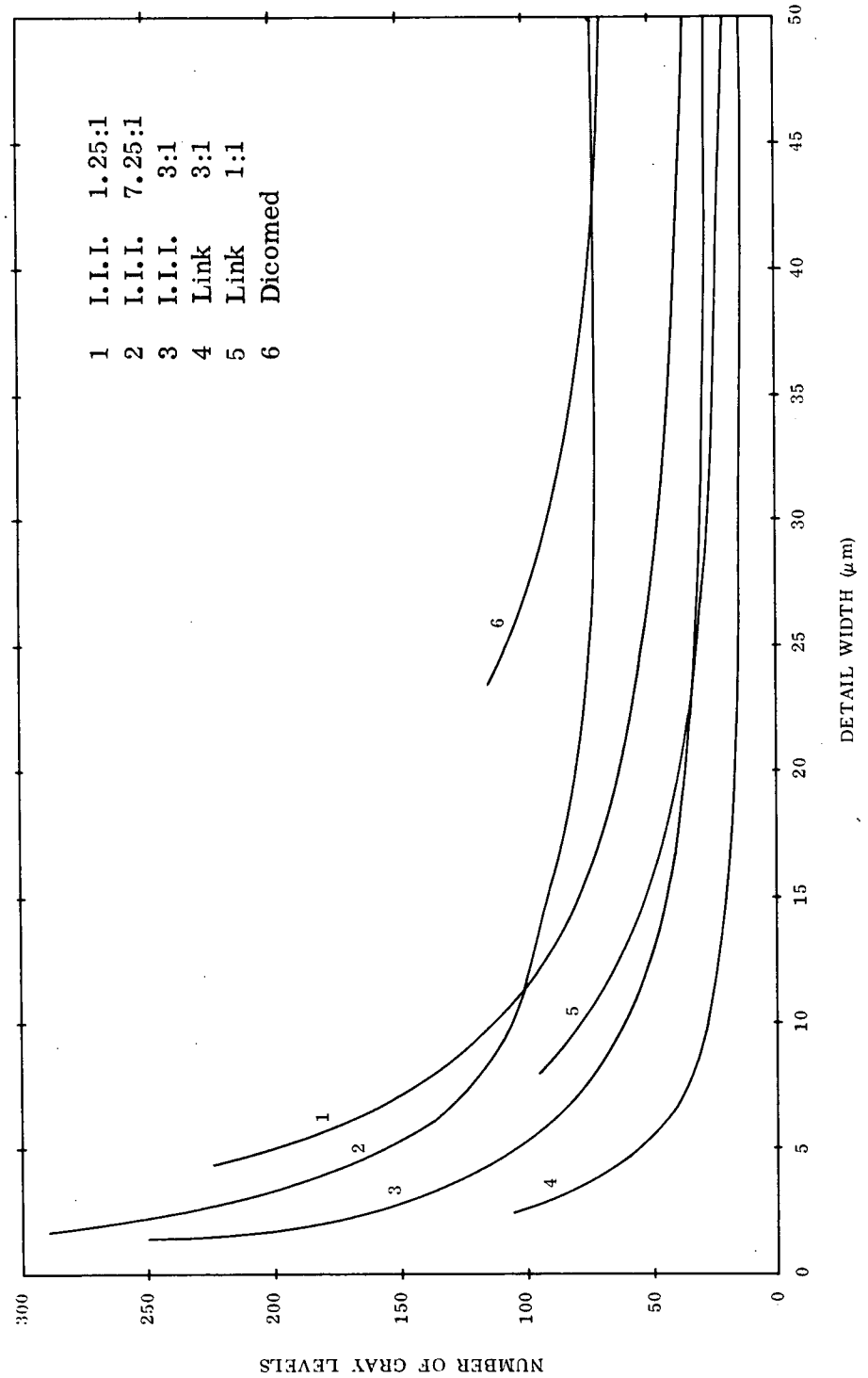

Figure 2-13. Number of gray levels required to resolve a detail of varying width (in microns) with a Signal/Noise of 5.0. Assumes 255 gray levels are available.

2.5 --Continued.

The curves in Figure 2-13 provide a basis for making comparisions between the scanners studied. However, it must be emphasized that these results do not indicate the resolvability of weld fault data. The reasons for this are as follows:

(1) The input signal to the program that produced the data for Figure 2-13 was a perfect square wave, where the width of the input was varied to correspond to the detail size of interest. In distinction radiograph signals are not square waves and they are degraded by the modulation transfer function of the x-ray system. As a result the accutance value of the actual input to the scanners would be greatly degraded and resolvability is a function of accutance. Reference 9 (page 73) gives an excellent discussion of this fact and compares the difference in resolvability of penetrameter holes and natural cavities.

(2) The curves shown in Figure 2-13 are based on one-dimensional analysis, i.e., the signal has a finite width but an infinite length. The two-dimensional analogue (which is more realistic) would show that more gray levels are required when the eye does not have the long signal over which to integrate.

2.6 Digital to Optical Conversion.

Two methods of obtaining hard copy results of processing were used during this study. A Dicomed 30 video display unit is an essential part of the ESL image processing system. This unit has a raster size of 1024 x 1024 and 64 gray levels. Although it has an undesirably small dynamic range it is adequate for the majority of pictures. The low cost of displaying a picture and photographing it made it possible to handle the large quantity of data which had to be iteratively processed during this study.

The second method used to get a picture of the digitally processed data was to record the desired pictures on tape and to send the data to be recorded on film by one of the scanner/recorder systems being used. There are two main reasons

2.6 --Continued.

for having the pictures recorded by a film scanner/recorder. These are improved resolution and larger raster size. Under ideal conditions there are also two disadvantages of this method, namely the turn around time and great expense. Several examples of recording with the Link scanner and the 1:1 lens on a previous contract showed that the low frequency jitter in their unshielded system was beyond the tolerable limit. Several pictures were sent to I.I.I. so that the original digitizing on large areas could be studied and some enhanced sections could be compared to the originals. The general poor quality of the digitizing and the expense (approximately $100/picture) did not justify further use of this recording method.

3. DETERMINATION OF OPTIMUM SCAN PARAMETERS.

In this section, results of studying optimum parameters and modes of operation for the film scanners are presented. The importance of optimizing the performance of the film scanner for minimum loss and distortion of information have already been discussed, but cannot be overemphasized.

Scanner performance factors that are considered here include operating film density, and scanning spot size.

3.1 Film Density.

A discussion of the optimum film density for a scanning system can be divided into two parts. The first concerns the relationship between the film density and the information content of the film. This relationship is independent of the scanning system. The second part concerns the relationship between film density and the accuracy of digitizing the film. Ideally, the usable density range of the scanning system should allow digitizing at the density which had been determined to contain the maximum amount of information. The ideal digitizing could not be achieved for the combination of film scanners and film type used in this study. The selected film density involved a compromise to meet conflicting requirements.

Section 3.1.1 discusses the relationship between density and the information characteristics of the film. Section 3.1.2 discusses the role that density plays

3.1 --Continued.

in the digitizing process and Section 3.1.3 shows the method used to determine the optimum density range (1.0 - 1.4) based on a tradeoff of the conflicting density requirements.

3.1.1 Density Characteristics of X-Ray Film.

The curve of net density of developed film versus exposure for X-rays is significantly different from that of net density versus exposure for visible light.[2] In particular the density - versus - exposure curve of X-ray film at low densities is a straight line passing through the origin. This is because of the extremely high probability that each X-ray quantum impinging upon the film will sensitize at least one grain. When the density is plotted versus the logarithm of the exposure, the conventional D-log E characteristic curve is obtained. Characteristic curves for various Kodak Industrial X-ray films are shown in Figure 3-1. All analyses and evaluation on the present study were performed using Kodak type M films exposed and processed at MSFC. Figure 3-1 shows that the gradient of the D-log E curve for X-ray films is monotonically increasing. For a linear D - versus - E characteristic, this gradient should vary as $G = 2.3\ D$.[2] Calculations have shown that for X-ray films the gradient of the characteristic curve is close to $G = 2.3\ D$ for the densities treated in this study.[2]

Since increasing the gradient of the D-log E curve results in increased contrast in the exposed and developed radiographs, the proportionality of G to D explains the desirability of exposing X-ray film at as high a density as possible (short of film saturation) for visual study of film detail. A film density as high as possible should also be used to minimize degradation of the signal-to-noise ratio due to film graininess effects; see Section A.3 of the appendix for a detailed discussion. Specifically for type M film a density in the range between 2.2 and 2.7 density units will optimize the film information content for an "ideal" scanner and covers a linear section of the curve shown in Figure 3-1.

3.1.2 Density Considerations in Film Scanners.

The optical-to-digital conversion step requires the accurate measurement of the light transmitted when the film surface is illuminated by a very small spot. (See Section A.1 and Figure A-1 of the appendix for a general description of the scanning operation.) When scanning film of zero density (or an open aperture

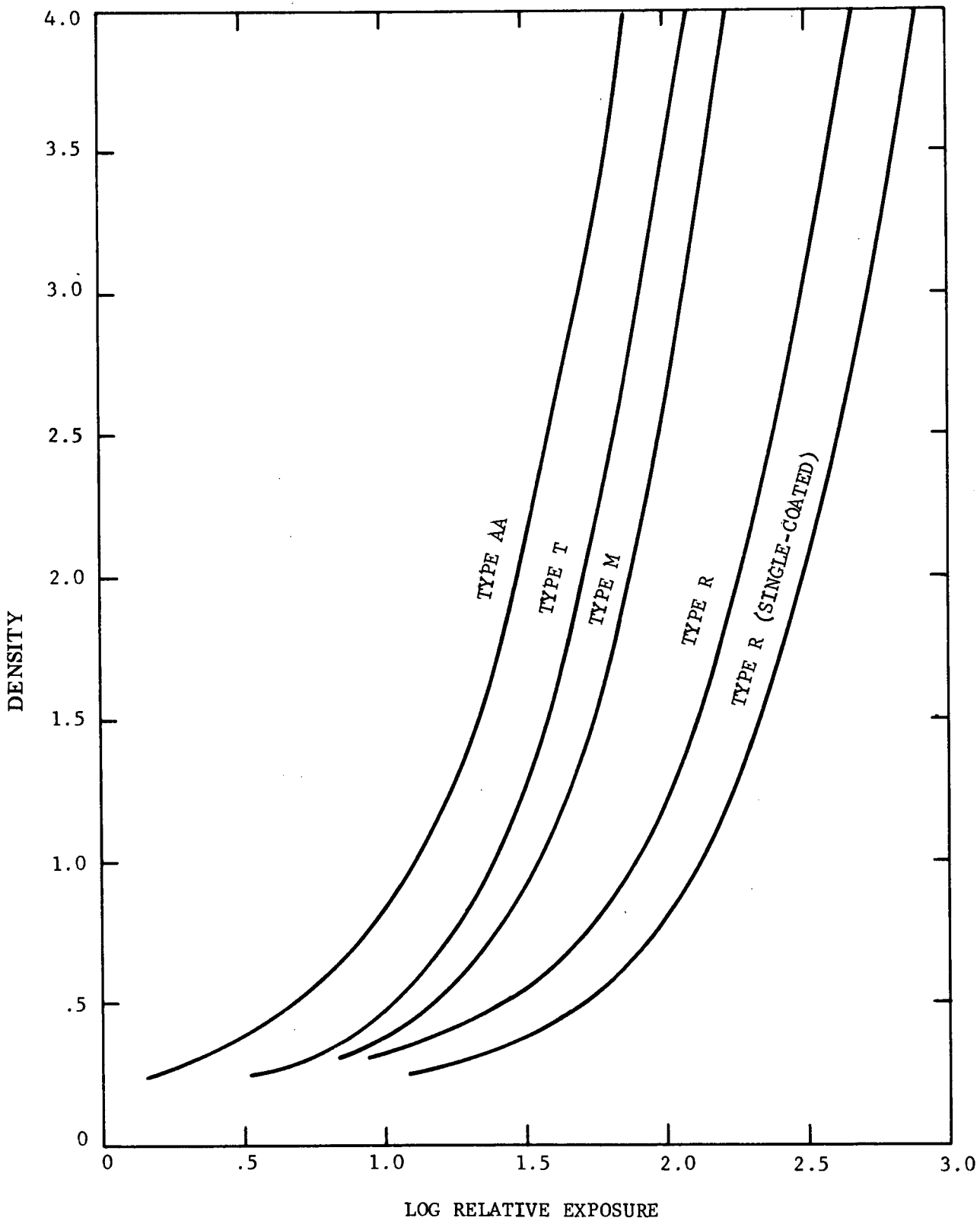

Figure 3-1. Characteristic curves for Kodak Industrial X-ray films.

3.1.2 --Continued.

scan with no film) 100 percent of the light is transmitted to the collecting lens. For film with a density of 1, 10 percent of the light is transmitted while a density of 2 transmits one percent of the light and a density of 3 transmits only 0.1 percent. The transmitted light is imaged onto the face of the photomultiplier tube and the corresponding photomultiplier current is integrated over the dwell time of the spot on the film. As the film density is increased causing the intensity of the transmitted light to decrease exponentially, it becomes necessary to increase the voltage to the photomultiplier tube so that a non-zero value can be obtained for the digital value of the spot on the film. The photomultiplier performs best in a certain voltage range. For this reason there are limits to the film density through which sufficient light can be transmitted while maintaining the operating voltage levels in the designed range.

Consideration must also be given to the relationship between the film density and the scanner signal-to-noise ratio. In particular, as the density of the transparency increases, the S/N decreases. For example, for the Link system increasing the film density from 0 to 1 to 2 decreases the S/N from 50 db to 40 db to 30 db.

These two factors show that the scanners will perform best when the film being scanned has a very low density. The requirement is in conflict with the requirements discussed in the previous section. Therefore a tradeoff must be made.

3.1.3 Selection of Optimum Scanning Density for Type M Film.

The manufacturers specifications of the density range that can be handled by each of the three scanning systems was shown in Table 2-1. It should be recognized the density specifications can be either diffuse or specular (that is they do or do not depend on measurements that include the scattered light). A series of experiments performed at Link for this study showed that a diffuse (using a densitometer) reading of 1.54 on the type M film corresponded to a specular (using the 3:1 lens on the Link scanner) reading of 2.01. This difference must be kept in mind when considering the values in Table 2-1 which are apparently specular measurements. The upper density limit as determined with a densitometer (the most common method) was found from these experiments to be approximately 1.8 for the Link scanning system.

3.1.3 --Continued.

A final density experiment was performed at Link to determine the density range that was optimum for the X-ray digitizing process, i.e., the range that provided the most information in the digital representation of a weld fault. From the series of weld faults done at densities of 0.84, 0.99, 1.19, 1.31, 1.58 and 1.75, three were selected (0.84, 1.19, 1.58). Each of these three films was positioned in the scanner and several lines across the film were scanned with the 3-to-1 lens; care was taken to insure that the same fault area was used in each case. Each scan was performed for a series of voltage levels and a histogram was generated for each level. Analysis of these histograms resulted in the selection of the 1.2 density film as having the most gray level spread from a voltage reading that Link personnel considered to be in the best signal-to-noise range of their scanner. It should be noted that there is not a single "optimum" density but instead a density range that allows the extraction of the same amount of information from the film. This range has been determined to be 1.0 to 1.4 for the Link scanning system.

The scanning equipment built by I.I.I. has wider density range than that built by Link. (See manufacturers specifications in Table 2-1.) This range is generally sufficient to digitize films of density 2.4 (determined by a densitometer), but equipment difficulties occurred on one occasion that made such high density films unreadable. As noted in the summary of the I.I.I. digitizing performed under this contract, all six of the weld fault areas were scanned from the 2.4 density film. Ideally, visual comparisons of scanning done at several densities using the same lens could be the basis for the determination of the density range which gave the best digitizing. It is difficult, however, to directly compare the information content of the scanning by I.I.I. on the high and low density films because of the excessive noise in the digitized data. In addition the data were obtained under different operating conditions because I.I.I. was improving their system performance over the eight months of the contract; the 2.4 density film was scanned in the second month and the 1.0 film was digitized in the seventh month. Also, a direct comparison between digitizing by Link and I.I.I. on different density films is difficult because the scanning performed by I.I.I. was done in equal density steps while that done by Link was in equal transmittance steps (see Section 6 for a discussion of transmittance mode and density mode scanning). The best digitizing obtained from I.I.I. was on the 1.0 density film of the weld faults. However, because of the factors mentioned it cannot be unequivocably stated that a density of 1.0 is optimum.

3.1.3 --Continued.

In summary, neither Link nor I.I.I. was capable of producing their best scanning in the density range (2.2 - 2.7) determined, on the basis of the results presented in Section 3.1.1, to be best for the information content of the film. This study can only conclude that film with a density between 1.0 and 1.4 allows either Link or I.I.I. to digitally convert the photographic data contained in the film without serious degradations caused by film density.

One of the original objectives of this study was to determine an optimum spot size and spacing for the scanning system. Spot sizes ranging from 10 μm to 25 μm were to be used. Optimum is used here in the sense of retaining all of the film data possible with a minimum number of samples. Ideally this spot size and spacing would be independent of the radiograph processing (exposure time, development time and temperature, and source power level) and independent of the scanning system. However, since no limit has been placed on the smallest dimension that defines a weld fault, specifying the spot size needed to resolve all the data on the film reduces to (1) determining the smallest detail that can be recorded on radiographic film, and (2) determining the relationship between film detail and the spot size needed to resolve that detail.

The second question can be answered. In particular, it is known that if there is sufficient contrast between the detail and the background then it is necessary to have at least two spots within the detail to detect it and at least six spots to be able to identify it.[3] Therefore a general rule can be stated -- the spot size (or equivalently the distance between spot centers) should be no more than 1/6 the dimension of the finest detail of interest.

Answering the first question is more complicated because the size of the resolvable detail size depends on film grain and clumping effects. The complexity of these effects is discussed in Section A.3 of the appendix. Because the digitizing for this study was severely limited by noise, no definitive optimum spot size or spacing could be determined emperically by comparing scanning done at different spot sizes. However, within the spot size range considered (10 μm to 25 μm) the best results were obtained with a spot size of 10 μm and a distance of 2.5 μm between spot centers.

4. RADIOGRAPH PROCESSING.

Negatives of resolution charts and radiographs were digitized for this contract. The analysis and processing of the resolution charts has been discussed in Section 3. Tables 4-1, 4-2 and 4-3 summarize the scanning performed for this study. The scanning parameters of spot size and spacing as well as the area dimensions and film density are listed. Comments concerning the relative quality of the scanning are included.

The radiographs can be divided into two types; wedge slit penetrameters and weld faults. Section 4.1 discusses the processing of the pentrameter, including the result of directional filtering. Section 4.2 gives 44 examples of the fault radiographs. These examples include prints made from the original negatives, prints of the digitized pictures before computer processing (as displayed by both the Dicomed and the scanner), and prints of the digital pictures after various processing steps. Section 4.3 contains a summary of the processing conclusions.

The examples of processing are intended to illustrate the method of selecting processing parameters as well as to illustrate the quality of the digitized data. Unfortunately the poor quality of the initial scanning makes it impossible to demonstrate significant enhancement of radiographic images. However, each of the processing algorithms was applied to non-radiographic images with average density excursions and the expected enhancement was demonstrated. Evaluation of the degree of enhancement that can be achieved on radiographic images cannot be made until the images can be faithfully converted in the digitizing step.

4.1 Wedge Slit Penetrameters.

The wedge slit penetrameter was constructed as a test object simulating a linear crack with width varying from 0.2 to 5.6 mils. The slit has a depth of 2 mils in a plate with a thickness of 250 mils. Of the penetrameters shown in the scanning summary (Tables 4-1 and 4-2) the slit could be detected in numbers 1 and 2 of Table 4-2. Because of the limited enhancement that can be achieved by inverse filtering noisy data all those cases in which it was not possible to detect the slit with a series of contrast stretches were not processed further.

Table 4-1. Summary of Scanning Performed by I. I. I. *

No.	Bits	Picture	Dimension (inches)	No. of Samples	Film Density	Spot Size (μ)	Spot Spacing (μ)	Comments
1	6	Resolution Chart	$0.025 \times 0.025 = 6.25 \times 10^{-4}$	$1026 \times 1026 = 1.05 \times 10^{6}$	High contrast	1.75	0.6	bad scan - flared spot. Second attempt OK but low contrast.
2	6	Wedge Penetrameter (narrow end)	$0.06 \times 0.186 = 0.0115$	$2600 \times 2600 = 6.75 \times 10^{6}$	1.5	1.75	0.6	Wedge slit not detectable, noise in 7.25:1 lens too great, more bits of data required.
3	6	Wedge Penetrameter (wide end)	$0.062 \times 0.8 = 0.0496$	$438 \times 2730 = 1.20 \times 10^{6}$	1.5	3.5	3.5	
4	9	Area 1	$0.727 \times 0.187 = 0.136$	$375 \times 1450 = 0.54 \times 10^{6}$	2.4	13	13	All weld faults look noisy-less data discrimination than expected.
5	9	Area 2A	$0.125 \times 0.125 = 0.016$	$250 \times 250 = 0.07 \times 10^{6}$	2.4	13	13	
6	9	Area 2B	$0.125 \times 0.125 = 0.016$	$250 \times 250 = 0.07 \times 10^{6}$	2.4	13	13	
7	9	Area 3	$1.375 \times 0.56 = 0.773$	$1120 \times 1376 = 3.1 \times 10^{6}$ (two sections)	2.4	13	13	
8	9	Area 4	$0.25 \times 0.25 = 0.063$	$500 \times 500 = 0.25 \times 10^{6}$	2.4	13	13	
9	9	Area 5	$0.125 \times 0.125 = 0.016$	$250 \times 250 = 0.07 \times 10^{6}$	2.4	13	13	
10	9	Area 1	$0.727 \times 0.187 = 0.136$	$375 \times 1450 = 0.54 \times 10^{6}$	0.5	13	13	Film density too low. Noise from fog level.

* Information International, Incorporated
12435 West Olympic Boulevard
Los Angeles, California 90064

Table 4-1. --Continued.

No.	Bits	Picture	Dimension (inches)	No. of Samples	Film Density	Spot Size (μ)	Spot Spacing(μ)	Comments
11	9	Area 2A	0.125x0.125 =0.016	$250x250_6$ $0.07x10^6$	0.5	13	13	Film density too low-noise from film fog level.
12	9	Area 2B	0.125x0.125 =0.016	$250x250_6$ $=0.07x10^6$	0.5	13	13	
13	6	Resolution Chart (7:1)	$0.025x0.025_4$ $=6.25x10^4$	$1026x1026_6$ $=1.05x10^6$	High contrast	1.75	0.6	Used to determine the MTF's of the three lenses. In general less contrast and more noise than expected.
14	6	Resolution Chart (3:1)	0.063x0.063 =0.0039	$1026x1026_6$ $=1.05 \times 10^6$	High contrast	6	1.55	
15	6	Resolution Chart (1.25:1)	0.122x0.122 =0.0149	$1026x1026_6$ $= 1.05x10^6$	High contrast	13	4.3	
16	9	Wedge Penetrameter	0.062x0.5 = 0.031	1251x2730	1.5	1.75	1.75	No slit detectable-done with 7:1 lens.
17	9	Area 2A	0.125x1.125 =0.016	$1000x1000_6$ $= 1 \times 10^6$	1.0	6	3	Best I.I.I. scanning of a weld but no flaws clearly resolvable
18	9	Area 2B	0.125x0.125 =0.016	$1000x1000_6$ $= 1x10^6$	1.0	6	3	Blurry data-apparently not focused.
19	9	Wedge Penetrameter	0.125x1.0 =0.125	$1000x1000_6$ $= 1x10^6$	1.5	6	3 on line 6 between lines	No slit detectable-done with 3:1 lens. Data too noisy.

Table 4-2. Summary of Scanning Performed by Link. *

No.	Bits	Picture	Dimension (inches)	No. of Samples	Film Density	Spot Size (μ)	Spot Spacing (μ)	Comments
1	8	Wedge Penetrameter	3.0 x 0.2 = 0.6	1200x320 $=0.39 \times 10^6$	1.5	30	16 on line 64 between lines	Slit can be detected.
2	8	Wedge Penetrameter	3.0 x 0.2 = 0.6	1200x320 $=0.39 \times 10^6$	3.0 inverted to 0.5	30	16 on line 64 between lines	Slit definition nearly as well as (1).
3	8	Wedge Penetrameter (3 files)	9.0 x 0.6 =5.4	3600x960 $= 3.5 \times 10^6$	1.5 enlarge three times	30	16 on line 64 between lines	No improvement in slit definition over (1)
4	8	Resolution Chart	0.22 x 0.22 = 0.05	2200x2200 $= 4,84 \times 10^6$	High contrast	10	2.5	Good bi-modal distribution but visible geometric distortion.
5	8	Area 1	.2 x 0.75 = 0.15	1000x3750 $= 3.75 \times 10^6$	1.19	10	2.5	Less flaw definition than (6) and (7).
6	8	Area 2A	0.2 x 0.2 = 0.04	2000x2000 $= 4.0 \times 10^6$	1.19	10	2.5	Best LINK scanning but no sharp flaw definition - nonexistent "flaw" introduced in (6).
7	8	Area 2B	0.17 x 0.15 = 0.026	1700x1500 $= 2.55 \times 10^6$	1.19	10	2.5	

* Singer - Link
1077 E. Arques Street
Sunnyvale, California 94086

Table 4-3. Summary of Scanning Performed by Dicomed. *

No.	Bits	Picture	Dimension (inches)	No. of Samples	Film Density	Size (μ)	Spot Spot Spacing (μ)	Comments
1	6	Resolution Chart	1.0 x 1.0 = 1.0	1024x1024 = 1.05×10^6	High contrast	25	25	Good bi modal distribution.
2	6	Area 1	1.0 x 1.0 = 1.0	1024x1024 = 2.1×10^6	0.8	25	12.5 on line 25 between lines	Noisy data-presence of dust-low resolution because of large spot and spacing dimensions.
3	6	Area 2A	1.0 x 1.0 = 1.0	1024x1024 = 2.1×10^6	0.8	25	12.5 on line 25 between lines	
4	6	Area 2B	1.0 x 1.0 = 1.0	1024x1024 = 2.1×10^6	0.8	25	12.5 on line 25 between lines	

* Dicomed Corporation
4600 W. 77th Street
Minneapolis, Minnesota

4.1 --Continued.

A print from the original radiograph of the wedge slit penetrameter is shown in Figure 4-1. Note that the slit can be seen for half the length of Figure 4-1; the visible slit width varies from 5.6 mils to 3.0 mils.

Picture 1 of Table 4-2 showed the best slit definition. The scanning was performed by Link with a 1.2 mil (30 μm) spot and a 50 percent overlap along a line. The best contrast stretch resultd in the pictures shown in Figure 4-2(a). This stretch was selected in the following way.

A general technique for selecting parameters to be used in the stretch routine had been developed from previous processing experience. These values are determined from the three gray levels that best describe the histogram (the minimum, the maximum, and the average) and the standard deviation of the distribution. In the remainder of this report "standard stretch" means a linear intensity mapping with gray level "W" and below going to white, gray level "B" and above to black, and the levels between "W" and "B" being linearly scaled between white and black. Table 4-4 defines the six sets of standard stretch parameters in terms of the standard deviation (Std) and the minimum (Min), maximum (Max) and average (Avg) gray levels of the original data.

Table 4-4. Standard Stretch Parameters

Stretch	Min	Avg-Std	Avg	Avg+Std	Max
1	W				B
2	W	B			
3	W		B		
4	W			B	
5			W		B
6				W	B

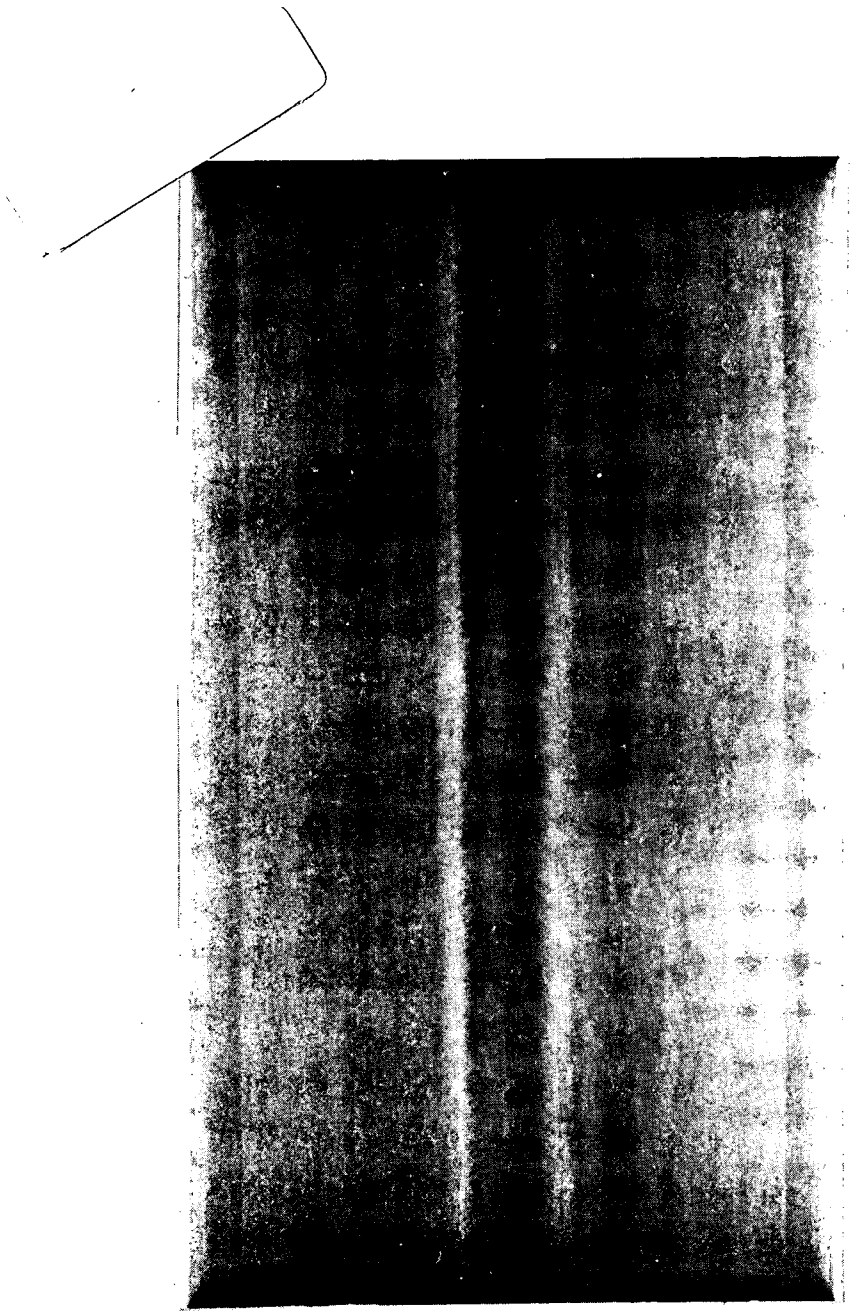

Figure 4-1. An enlargement made from the original radiograph of the wedge slit penetrameter.

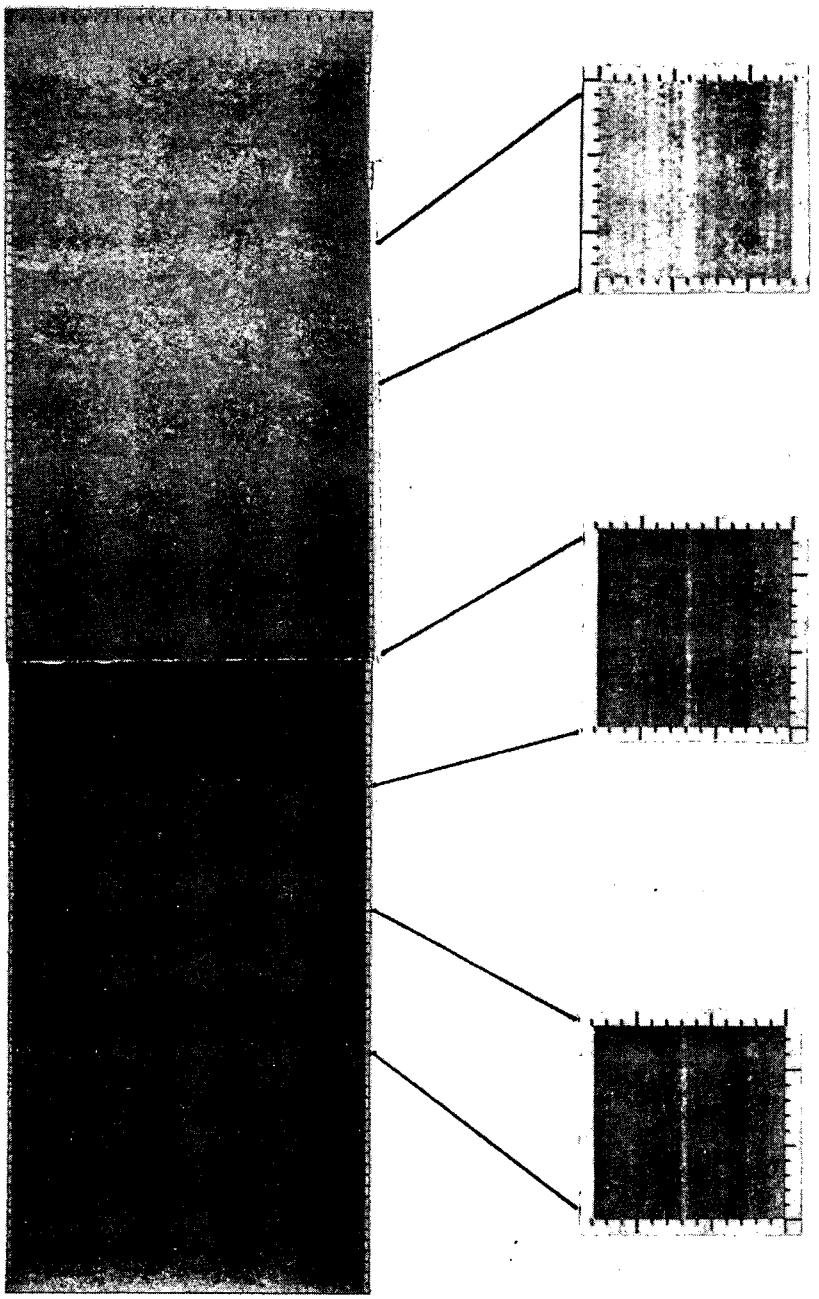

(a) (b)

Figure 4-2. (a) Wedge penetrameter digitized by Link after best contrast stretch (76, 112) (b) Three sections (128 x 128) from (a) after directional filtering.

4.1 --Continued.

The original version of the picture shown in Figure 4-2 (a) had an average gray level of 94, a standard deviation of 9, a minimum of 29 and a maximum of 128. Using these four values the six parameter combinations shown in Table 4-4 were applied to the picture and the results displayed. Of these, the best result was obtained with Stretch 5 of Table 4-4 (a linear display between the average gray level and the maximum gray level). On the basis of this result several more parameters for the stretch routine were selected by varying the upper and lower values. The greatest enhancement was achieved by using the values determined from the average minus twice the standard deviation (i.e., W = 76) and the average plus twice the standard deviation (i.e., B = 112).

Directional filtering was used to attempt to increase the slit definition. Because of the necessity of repeating the filtering for a variety of filter parameters, small areas (128 x 128) at three different slit widths were selected. The results are shown in Figure 4-2(b), and it can be seen that after filtering the slit is visible when the width of the slit is as small as 1.7 mils. Based on the discussion in Section 3.1.3, the limiting value of 1.7 mils is expected since approximately three spots lie within this width.

Directional filtering is a powerful tool but it does require a prior knowledge of the direction of a linear object. The present results provide a lower bound in the size of faults that can be detected with particular spot size and spacing used.

4.2 Weld Faults.

Six film specimens were provided for this study. The type of fault and the dimensions of the areas to be scanned are given in Table 4-5.

The specified areas were scanned at different densities with a variety of lenses, spot sizes and spacings (see Tables 4-1, 4-2 and 4-3). The pictures shown in this section include 2A, 2B, 1 and 3 in that order and consist of all of the scans in which the digitizing quality was sufficient to warrant more than minimal processing. Whereever possible the scanning results from more than one scanner are shown for direct visual comparison.

4.2 --Continued.

Table 4-5. Fault Type and Area Dimensions.

Specimen Number	Specimen Type	Dimension (inches)
1	Chain Porosity	0.727 x 0.187
2A	Tailed Porosity	0.125 x 0.125
2B	Tailed Porosity	0.125 x 0.125
3	Crater Cracks	1.375 x 0.562
4	Clustered Porosity	0.250 x 0.250
5	Tungsten Inclusion	0.125 x 0.125

Only Fourier inverse filtering results are presented. Convolution filtering was attempted with small filters on large pictures but the accuracy of the result imposed by the filter size was not sufficient to correct the MTF; accuracy and computing time considerations for convolution filtering are discussed in Section 6.2. The convolution software is included in the event that efficient convolution hardware is available to NASA-MSFC.

4.2.1 Results of Processing Area 2A.

4.2.1.1 Singer Link.

As described in Section 3. the optimum density for film scanned by the Link 3:1 lens system was determined to be between 1.0 and 1.4. Of the three areas scanned at a density of 1.2 with the 3:1 lens, Area 2A (number 6 of Table 4-2) has been selected as being of the greatest interest. For this reason a detailed discussion of the processing results for this specimen will be used to demonstrate the general approach.

4.2.1.1 --Continued.

Figure 4-3 is a display of the original Link data as recorded by I.I.I. The irregular areas around the edges are the ink lines on the negative which were used to define the area to be scanned. From the display of the entire original file, the coordinates of the area inside the ink lines were determined. The data set with these corordinates was then stored on the disk as the basic picture to be processed. The histogram for this picture is shown in Figure 4-4 and was used to determine the parameters for several contrast stretches. The results of each stretch were displayed and photographed (this required four pictures for each) in both positive and negative mode. A careful study of the 24 photos thus generated made it possible to determine an area 650 by 700 which contained the two flaws which could be seen on the negative under 12-power magnification. This area was then extracted and used as the basis for studying the results of the application of standard enhancement techniques. The original picture of this selected area and its histogram are shown in Figures 4-5 and 4-6. Note the reduced gray level range on the histogram of the selected portion.

Figures 4-7 and 4-8 show the standard stretches (Table 4-4) applied to Figure 4-5. From the study of Figures 4-7 and 4-8, stretch 3 was selected from the standard stretches as providing the best display of the weld faults. The small area in the lower half of the picture containing the vertical object was selected for inverse filtering. Because of the processing time involved (see Table 6-4 and the accompanying discussion) the dimensions of the area of interest for preliminary filtering were 256 by 256. The inverse filter that was applied to this fault was that determined from a black-to-white transition on the resolution chart scanned by Link with the same scanning parameters as those used for this picture; see Figure 2-6 for the OTF determined from this black-to-white transition. The result of applying the inverse filter to the picture in one dimension is shown in Figure 4-9(b); Figure 4-9(a) is the original unstretched picture of this section of the radiograph.

The radiograph area shown in Figure 4-9 was scanned by both Link and I.I.I. Only in the Link-scanned picture did the long object become apparent. Close examination of the original radiograph and the I.I.I.-scanned picture revealed that the long object in Figure 4-9 is not a weld defect and must be an anomaly peculiar to the Link scanning. This anomalous object is probably a piece of dirt or dust.

The dimensions of objects in the picture can be calculated by multiplying the size of the object in number of samples by the spot spacing. For the picture being discussed this gives 256 x 0.1 mils = 25.6 mils on a side. Since in Figure 4-9(b) the long dimension of the linear shape is approximately 80 samples (the tics on the picture mask correspond to 10 samples) the "object" is approximately 8 mils long and 1 mil wide.

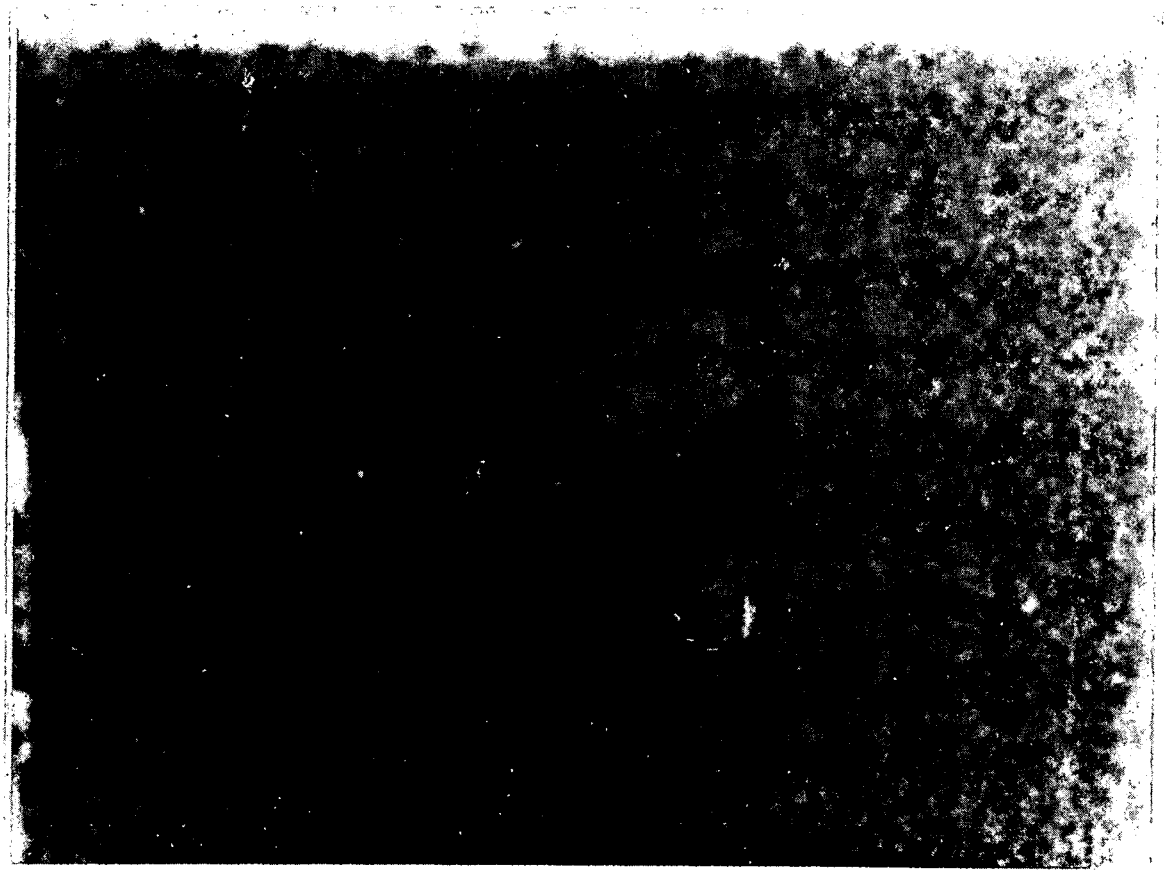

Figure 4-3. Film recording by I. I. I. of Link scan of Area 2A.

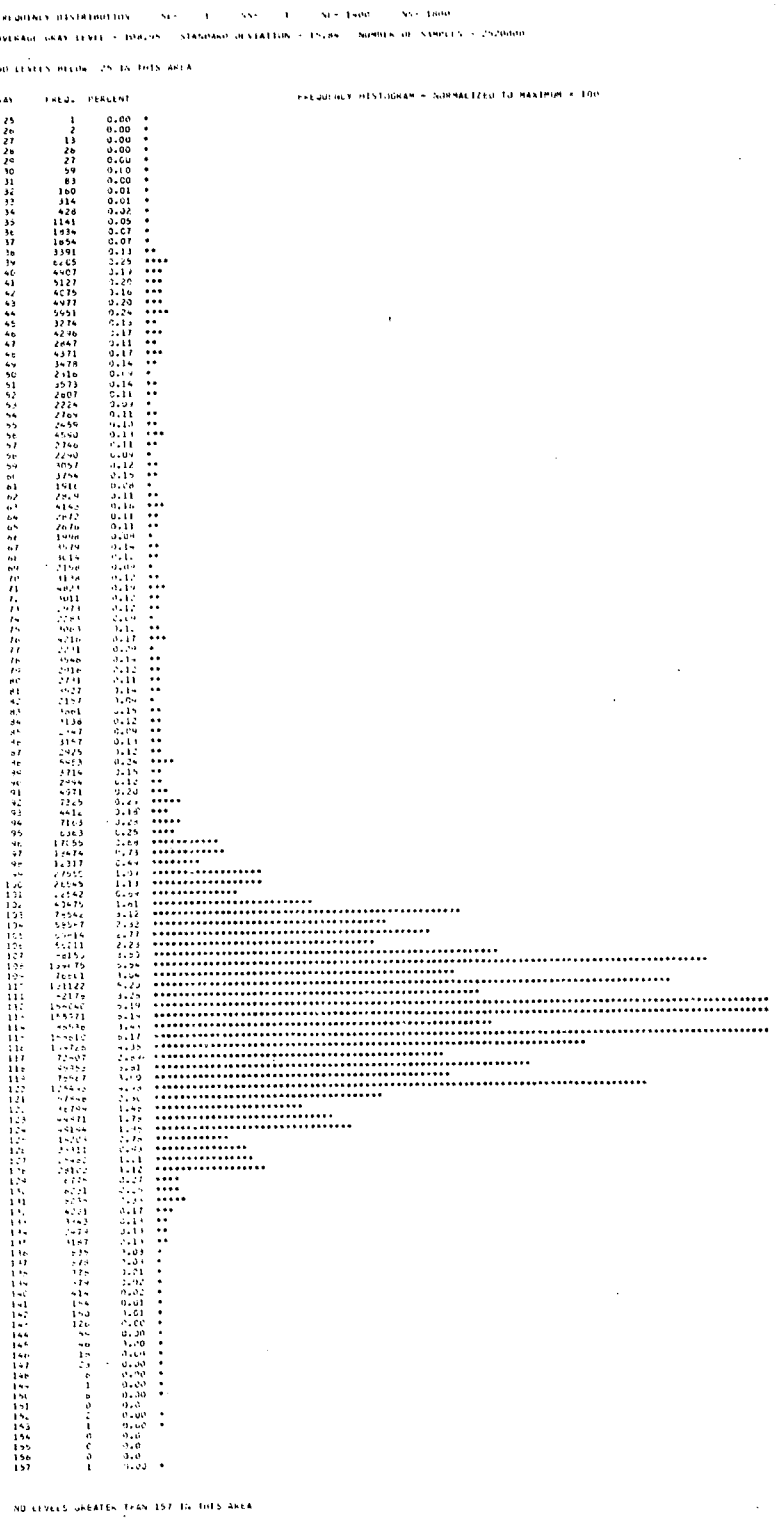

Figure 4-4 Histogram of Figure 4-4

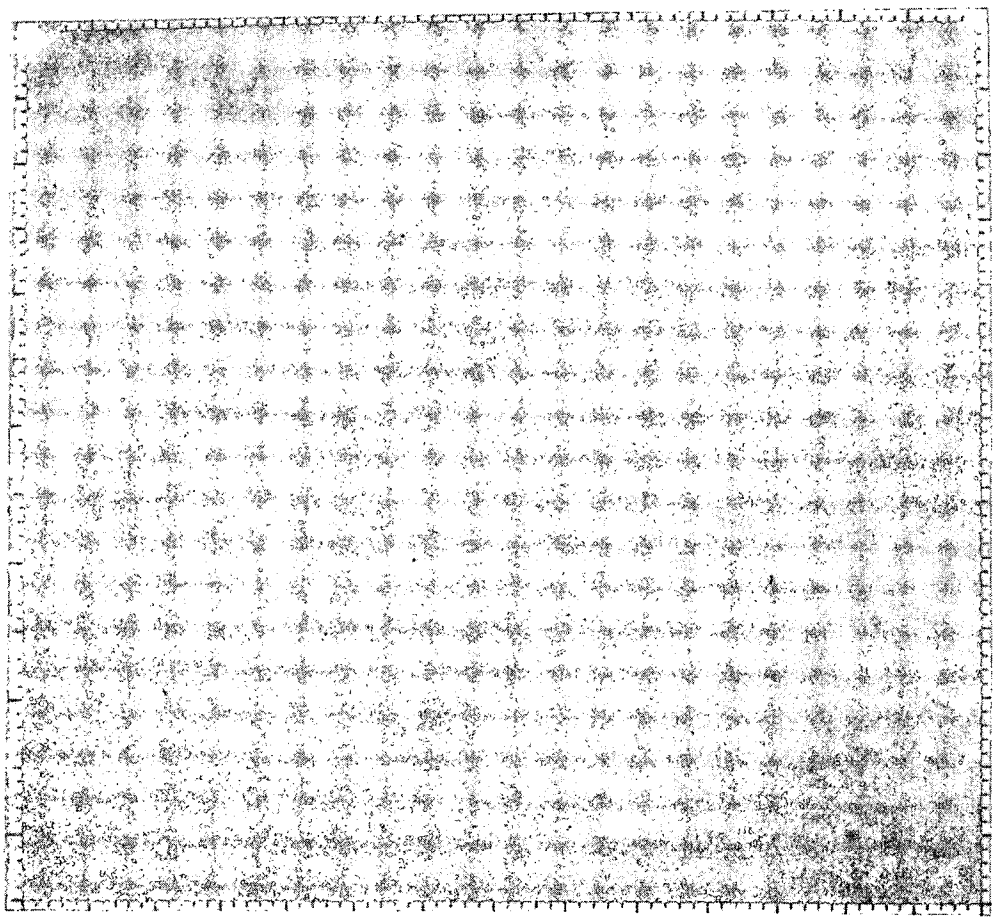

Figure 4-5. Section of Figure 4-4 used in processing.

FREQUENCY DISTRIBUTION SL= 1 SS= 1 NL= 650 NS= 700

AVERAGE GRAY LEVEL = 111.43 STANDARD DEVIATION = 8.21 NUMBER OF SAMPLES = 455000

NO LEVELS BELOW 63 IN THIS AREA

GRAY	FREQ.	PERCENT	FREQUENCY HISTOGRAM - NORMALIZED TO MAXIMUM = 100
63	1	0.00	*
64	7	0.00	*
65	7	0.00	*
66	6	0.00	*
67	12	0.00	*
68	8	0.00	*
69	12	0.00	*
70	24	0.01	*
71	39	0.01	*
72	24	0.01	*
73	29	0.01	*
74	19	0.00	*
75	27	0.01	*
76	43	0.01	*
77	32	0.01	*
78	37	0.01	*
79	41	0.01	*
80	31	0.01	*
81	54	0.01	*
82	44	0.01	*
83	71	0.02	*
84	93	0.02	*
85	81	0.02	*
86	102	0.02	*
87	168	0.04	*
88	591	0.13	**
89	571	0.13	**
90	534	0.12	**
91	1067	0.23	****
92	1881	0.41	*******
93	1256	0.28	*****
94	2195	0.48	********
95	1989	0.44	*******
96	5449	1.20	**********
97	5809	1.28	**********
98	3820	0.84	**********
99	8348	1.83	**********
100	8037	1.77	**********
101	6272	1.38	**********
102	10701	2.35	**********
103	19689	4.33	**********
104	13611	2.99	**********
105	15247	3.35	**********
106	12113	2.66	**********
107	18110	3.98	**********
108	27268	5.99	**********
109	14638	3.22	**********
110	24378	5.36	**********
111	14759	3.24	**********
112	27907	6.13	**********
113	27508	6.05	**********
114	14981	3.29	**********
115	26941	5.92	**********
116	19057	4.20	**********
117	12414	2.73	**********
118	16325	3.59	**********
119	12889	2.83	**********
120	21533	4.73	**********
121	10089	2.22	**********
122	6523	1.43	**********
123	7884	1.73	**********
124	8552	1.88	**********
125	3326	0.73	**********
126	4059	0.89	**********
127	4530	1.00	**********
128	4853	1.07	**********
129	1197	0.26	****
130	1050	0.23	****
131	1449	0.32	*****
132	693	0.15	**
133	539	0.12	**
134	414	0.09	*
135	493	0.11	**
136	103	0.02	*
137	117	0.03	*
138	52	0.01	*
139	46	0.01	*
140	48	0.01	*
141	13	0.00	*
142	8	0.00	*
143	7	0.00	*
144	7	0.00	*
145	2	0.00	*
146	2	0.00	*
147	3	0.00	*
148	1	0.00	*

NO LEVELS GREATER THAN 148 IN THIS AREA

Figure 4-6 Histogram of Figure 4-6

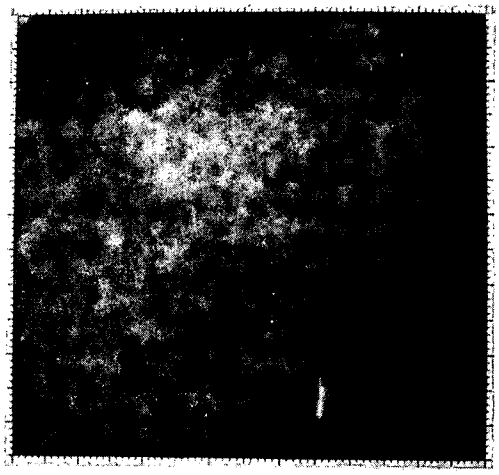

(a) Stretch 1

(b) Stretch 2

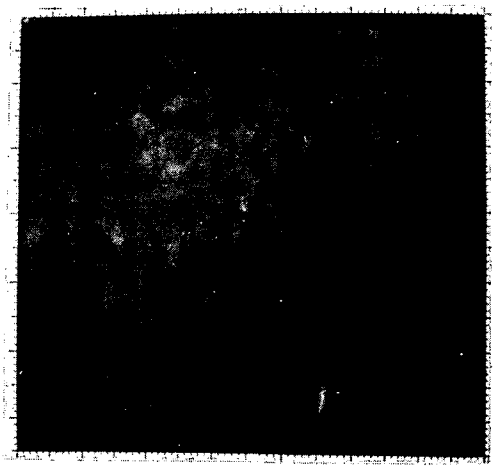

(c) Stretch 3

Figure 4-7. Stretches applied to Figure 4-5.

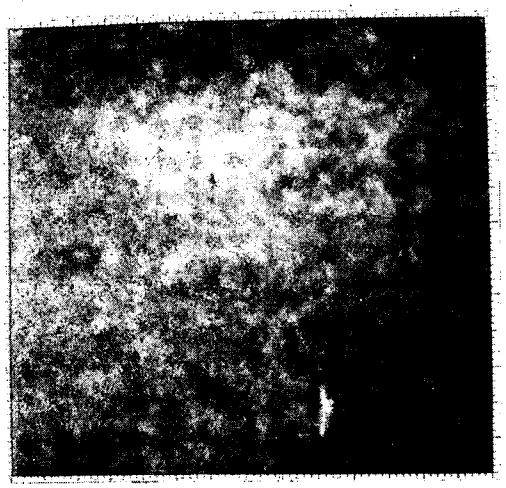

(a) Stretch 4

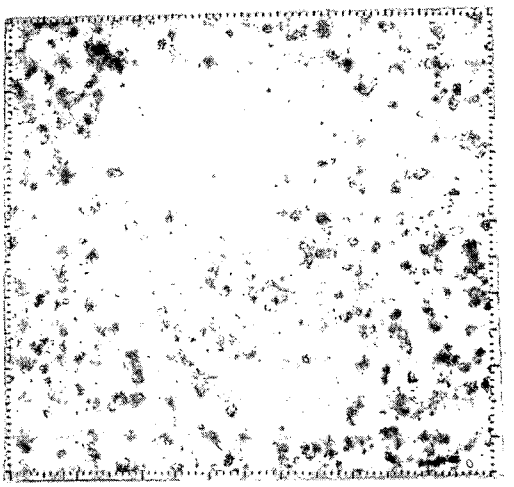

(b) Stretch 5

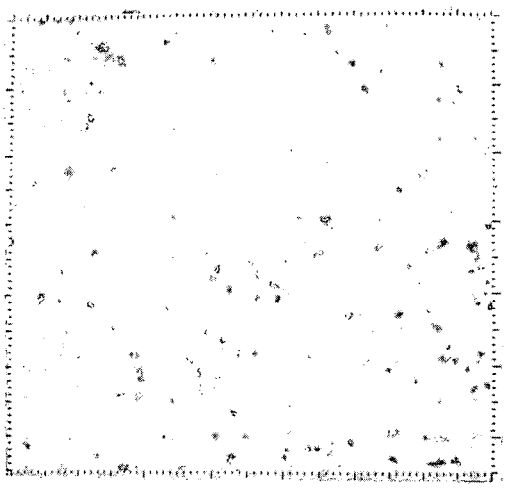

(c) Stretch 6

Figure 4-8. Stretches applied to Figure 4-5.

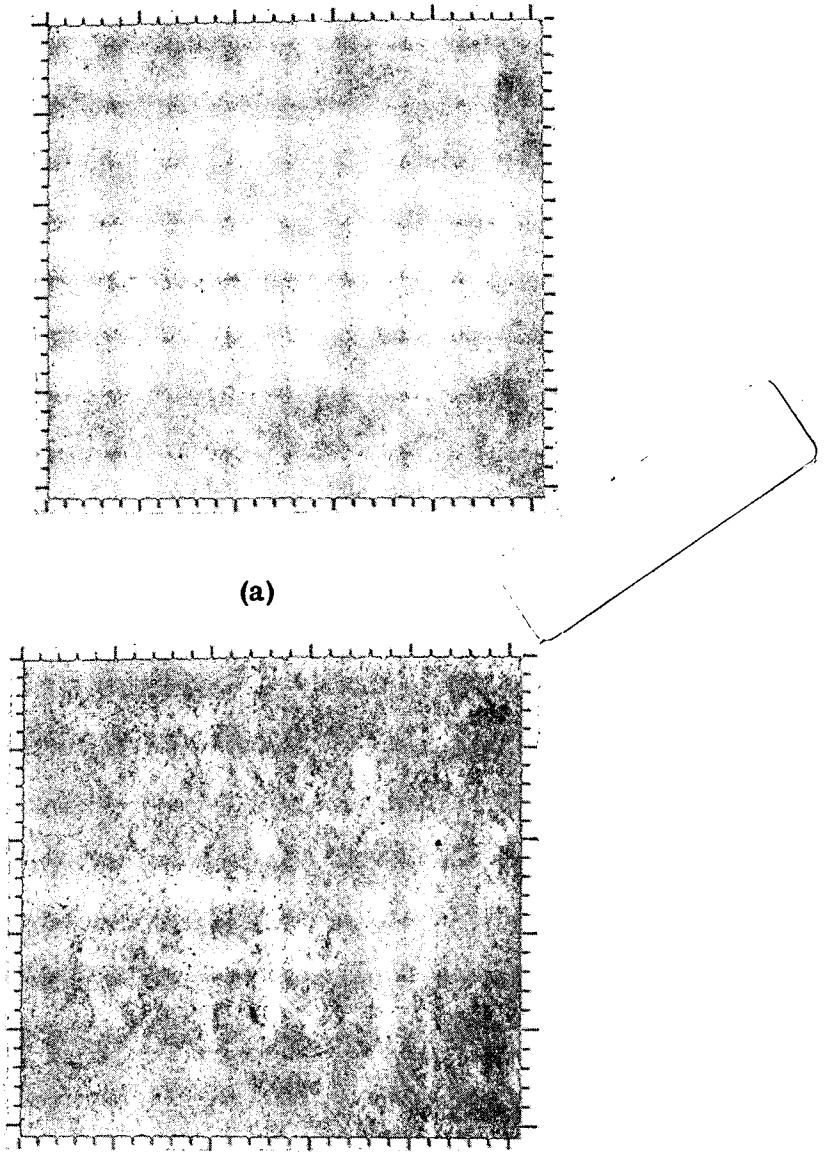

(a)

(b)

Figure 4-9 (a) Selected portion of Figure 4-5;
(b) Result of applying one-dimensional inverse filter to (a).

4.2.1.1 --Continued.

As part of the study of spot size and spacing the 650 x 700 picture shown in Figure 4-7(c) (the result of applying stretch 3 to the original) was processed and displayed so as to approximate the results of having used different parameters in the original scan. Figures 4-10(a) and (b) and Figure 4-11(a) and (b) show respectively every second point and every third point of Figure 4-8(c) in both direct and complement mode. The pictures were all enlarged to the same size but note the change in the number of samples that are displayed. Figure 4-7(c) shows a 75 percent sample overlap, Figure 4-10 shows 50 percent overlap and Figure 4-11 shows about 25 percent overlap. Figure 4-12(a) shows the result of stretch 3 applied to every fourth point of the entire original scan (Figure 4-3). This picture then represents the original data as scanned by a 10μm spot with no overlap. As a final result of varying the spot size and spacing, Figure 4-12(b) was obtained by dividing Figure 4-12(a) into square neighborhoods and generating a picture where each point is the average over a 2x2 neighborhood. Again note the reduction in the number of samples displayed. This figure corresponds to an original scan done with a spot approximately 20μ and no spot overlap.

The detailed study of the noise (see Section 2) indicates that no increased resolution is obtained by processing the pictures with overlapping spots with the scanning systems being used. Furthermore, as discussed in Section 6 (see in particular Table 6-4), the amount of CPU time required to filter a picture larger than 256 x 256 makes such processing unacceptably expensive. Therefore the 256 x 256 section of Figure 4-12(a) (before applying stretch 3) which included the major flaws was chosen for further two dimensional filtering. This section is shown in Figure 4-13. Figure 4-13(a) shows the original, 4-13(b) shows the complement of (a) after stretch 3 and 4-13 (c) shows (a) after inverse filtering. Note that although the images in (c) are sharper, there is an increase in the 'speckeling' due to boosting the noise. The histogram of 4-13(c) was used to determine the stretches to be applied to the filtered picture. The best results of either the positive and negative displays are shown in Figure 4-14.

4.2.1.2 Information International, Incorporated.

Area 2A (number 17 of Table 4-1) was scanned from the 1.0 density film by I.I.I. using their 3:1 lens. The entire original file was rerecorded by I.I.I. and is shown in Figure 4-15; Figure 4-16 is the histogram of the data shown in Figure 4-15.

2

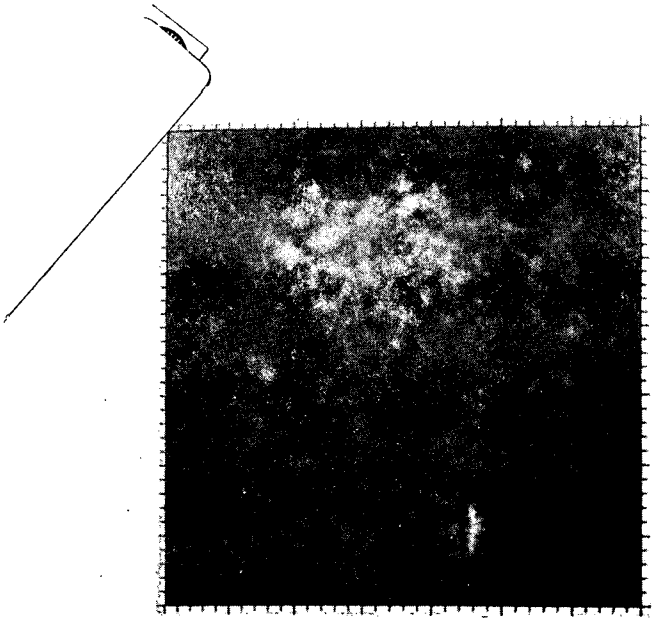

(a)

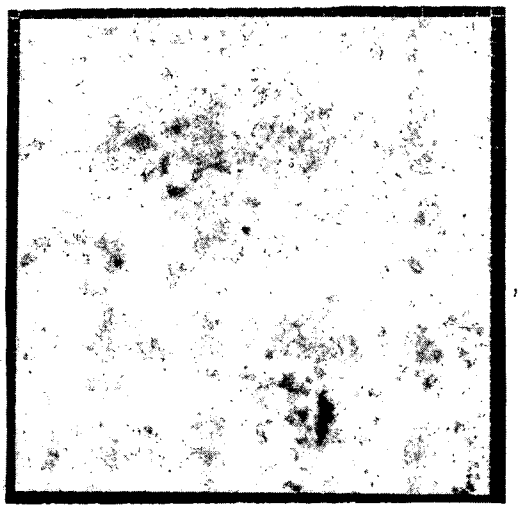

(b)

Figure 4-10. (a) Every second point of Figure 4-7(c);
(b) Complement of (a).

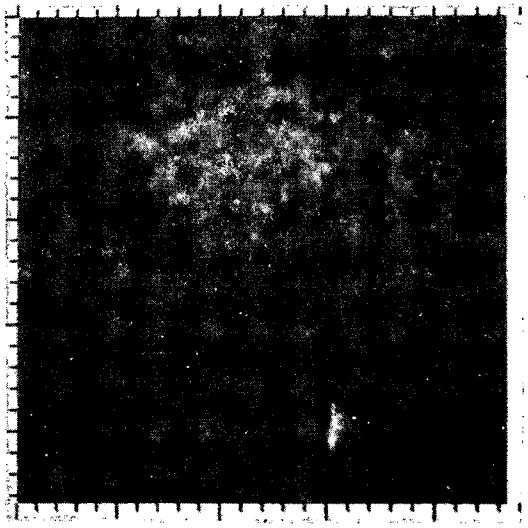

(a)

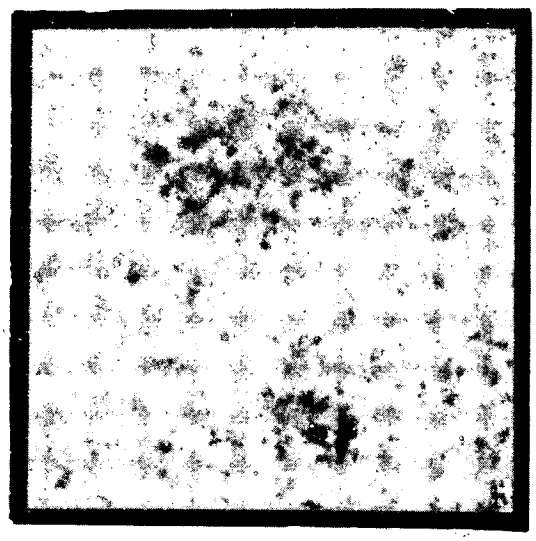

(b)

Figure 4-11. (a) Every third point of Figure 4-7(c);
(b) Complement of (a).

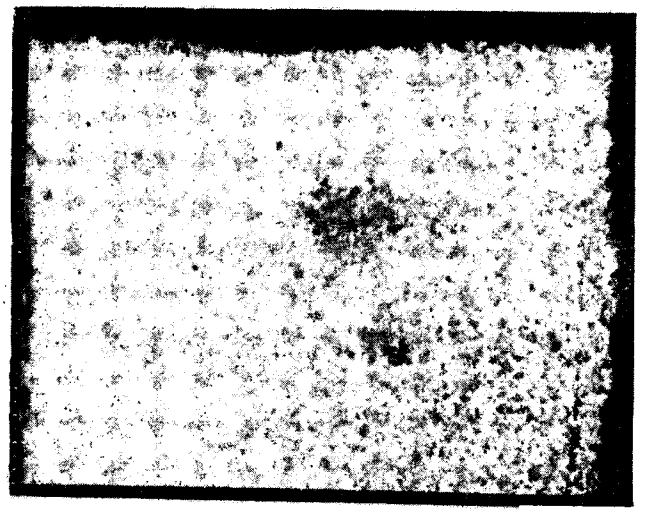

(a)

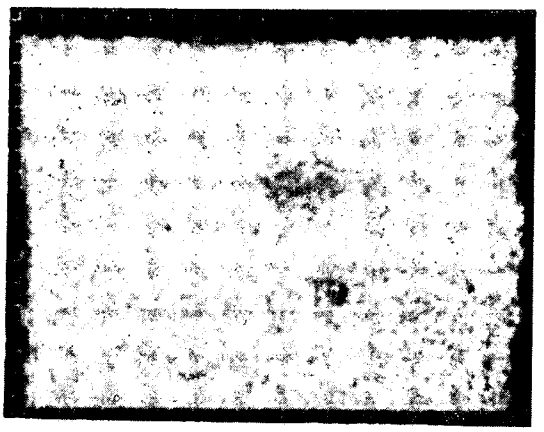

(b)

Figure 4-12. (a) Every fourth point of Figure 4-7(c);
(b) Average over 2x2 neighborhoods of (a).

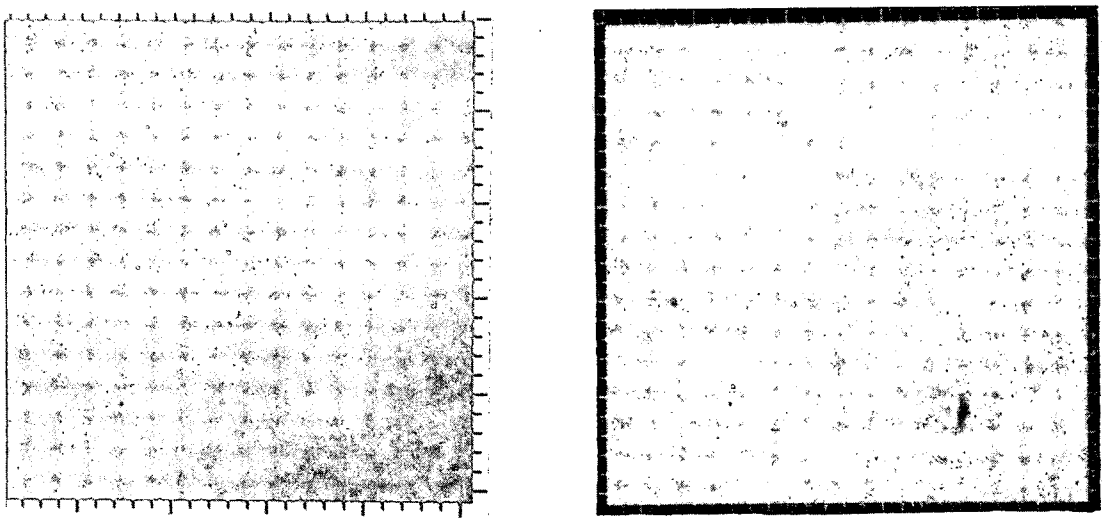

(a) (b)

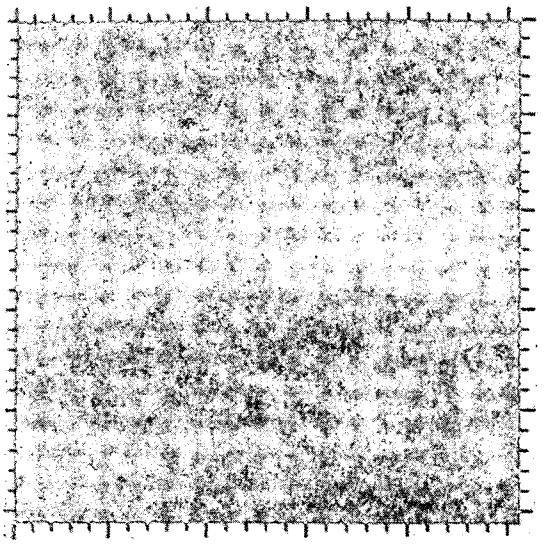

(c)

Figure 4-13. (a) Section of Figure 4-12(a) showing every fourth point;
(b) Result of the complement of Stretch 3 applied to (a);
(c) Result of inverse filtering of (a).

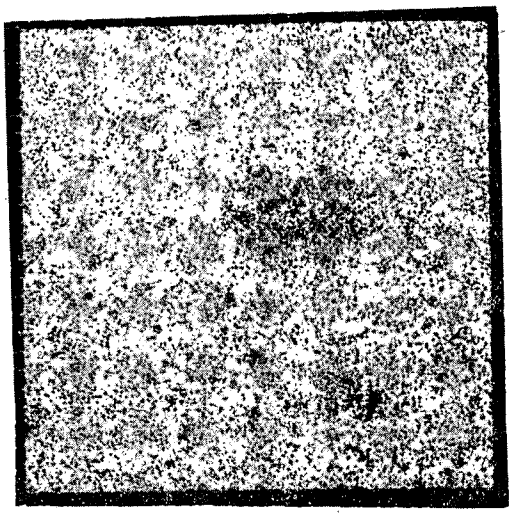

(a) Complement of Stretch 2

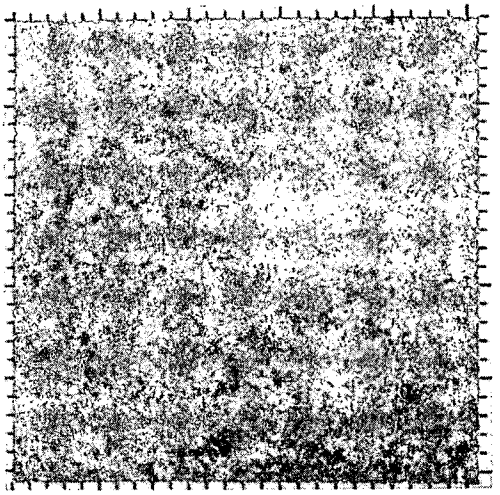

(b) Stretch 4

Figure 4-14. Stretches of Figure 4-13(c).

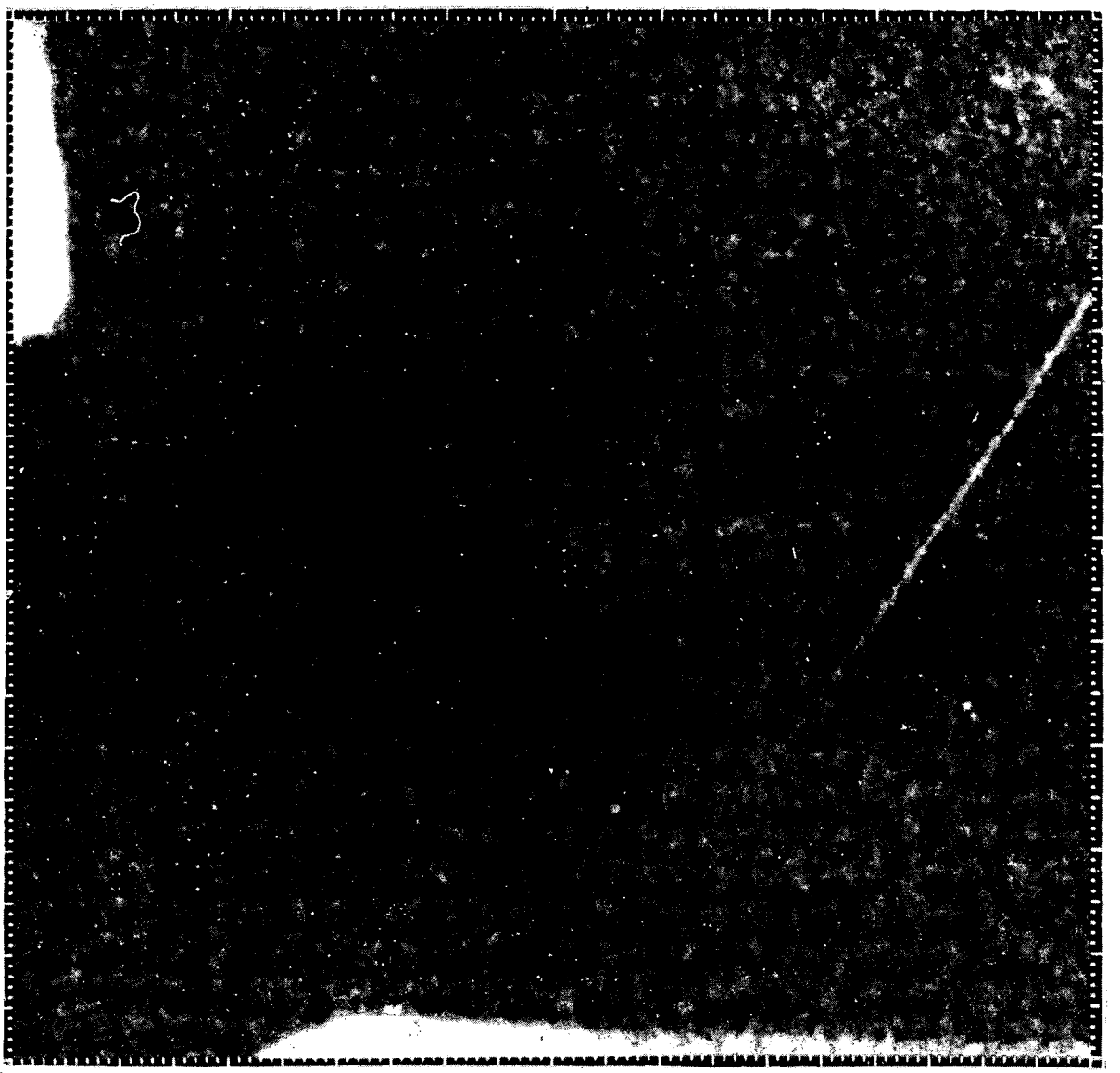

Figure 4-15. Film recording by I.I.I. of scan of Area 2A with the I.I.I. 3:1 lens.

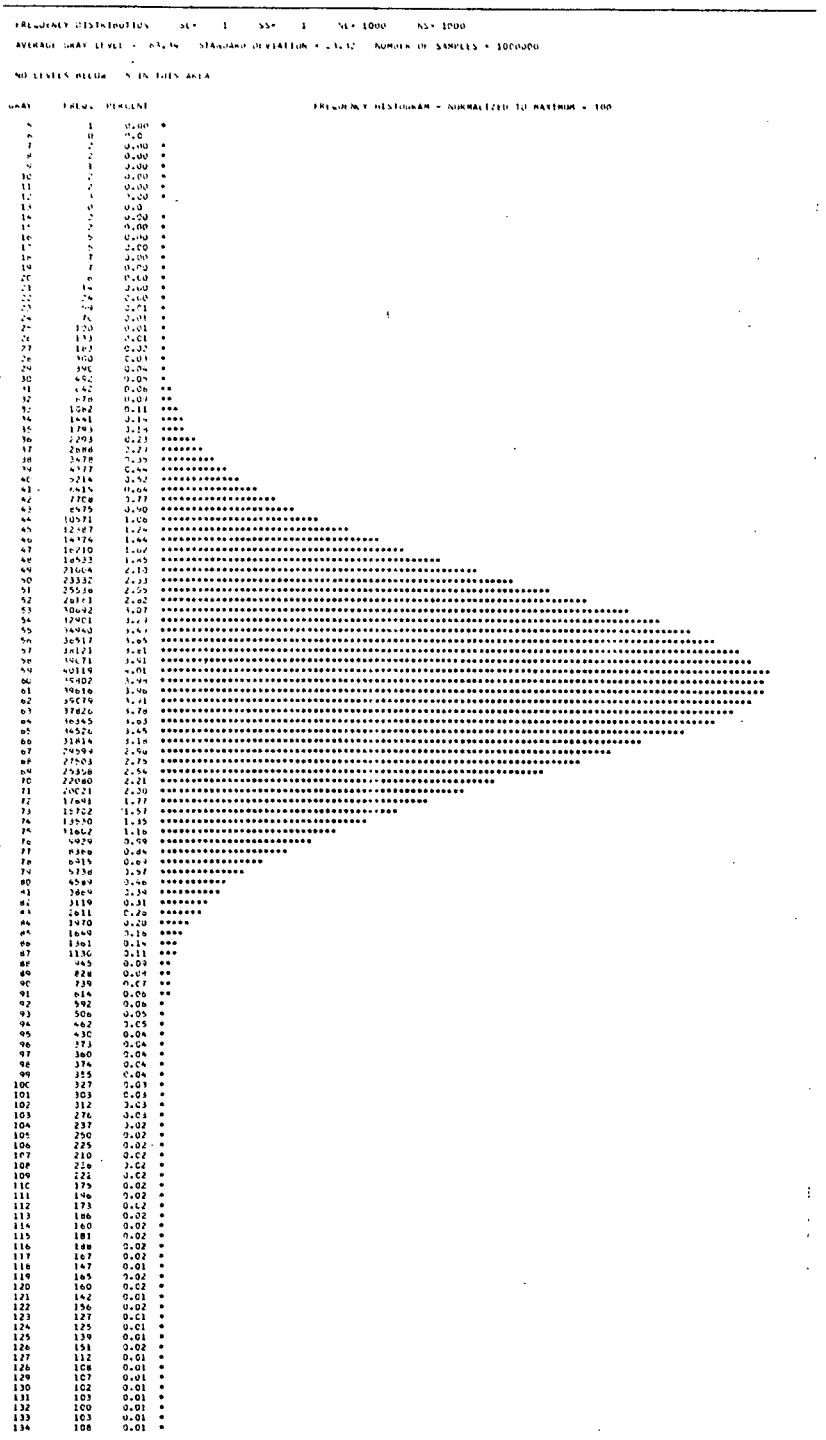

Figure 4-16 Histogram of Figure 4-17

4.2.1.2 --Continued.

The light sections on the edges are the ink marks specifying the area on the film. The line on the right half of the picture is a scratch on the film. To obtain consistency, the recording was done in the complement mode of that from Link. Therefore the pictures in this section will be shown in the complement to allow direct comparison with Link scanning.

It is of interest to visually compare the scans made of area 2a by the three different systems. The following steps were taken to display pictures with roughly the same scale, i.e., the same number of resolution elements per unit length. The I.I.I. scan of area 2a with the 3-to-1 lens has a spot size of approximately 6μm and 50% overlap. In order to give visual comparison with the Link scan shown in Figure 4-12(a), every other sample was selected to approximate a 6μm scan with no overlap and then the average over a 2x2 neighborhood was taken. This result is shown in Figure 4-17(a). An approximation to the Dicomed data (1 mil spot with no overlap, Figure 4-24) can be made by taking every second point and averaging over 4x4 neighborhoods. This is shown in Figure 4-17(b).

Note the general blurring that is produced by averaging points. Although the transfer function determined from the I.I.I. resolution chart indicates high system noise and an irregular inverse function, an attempt was made to improve the resolution by inverse filtering. Figure 4-18(a) shows the unenhanced original data with abutted spots. Figure 4-18(b) shows the filtered picture and 4-18(c) displays the best stretch of the filtered picture.

It is clear from a comparison of the filtered and unfiltered pictures that while the filtering has sharpened up some of the fine detail (e.g., compare the scratch in Figure 4-18(a) with that in Figure 4-18(c)) the noise has masked most of the fault area itself.

4.2.1.3 Dicomed.

Area 2A (number 3 of Table 4-3) was scanned by Dicomed on the 0.8 density film. Figure 4-19(a) shows a print made from the negative that Dicomed scanned. This scanning was performed with a one mil spot and a 50% overlap along a scan line but no overlap in the other direction. The fault was scanned to 6 bits, i.e. 64 gray levels. The most information can be seen in the picture using stretch 4. This picture is shown in Figure 4-19(b). Because of overlap in one dimension only, the area shown is geometrically distorted. Taking every second sample along a line removes this distortion as is seen in Figure 4-19(c). The transfer

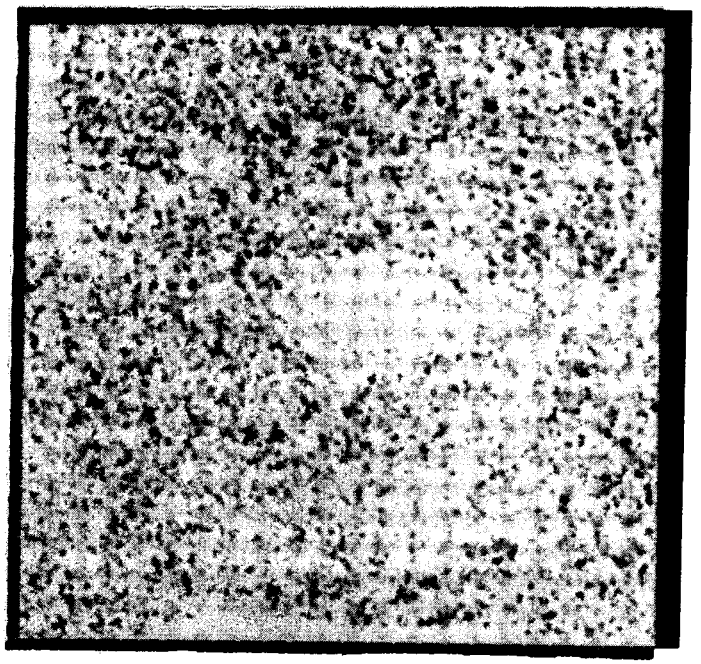

(a)

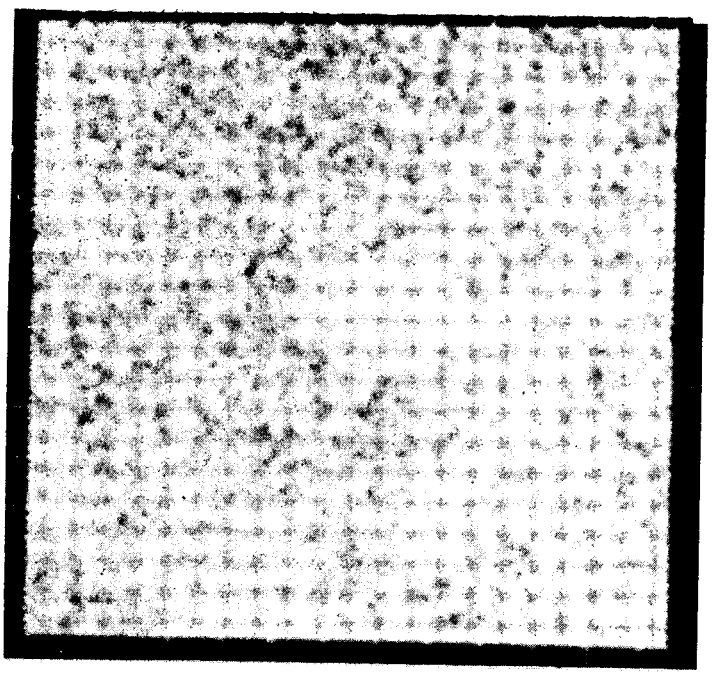

(b)

Figure 4-17. (a) Approximates a 12μm spot with no overlap; (b) Approximates a 24μm spot with no overlap.

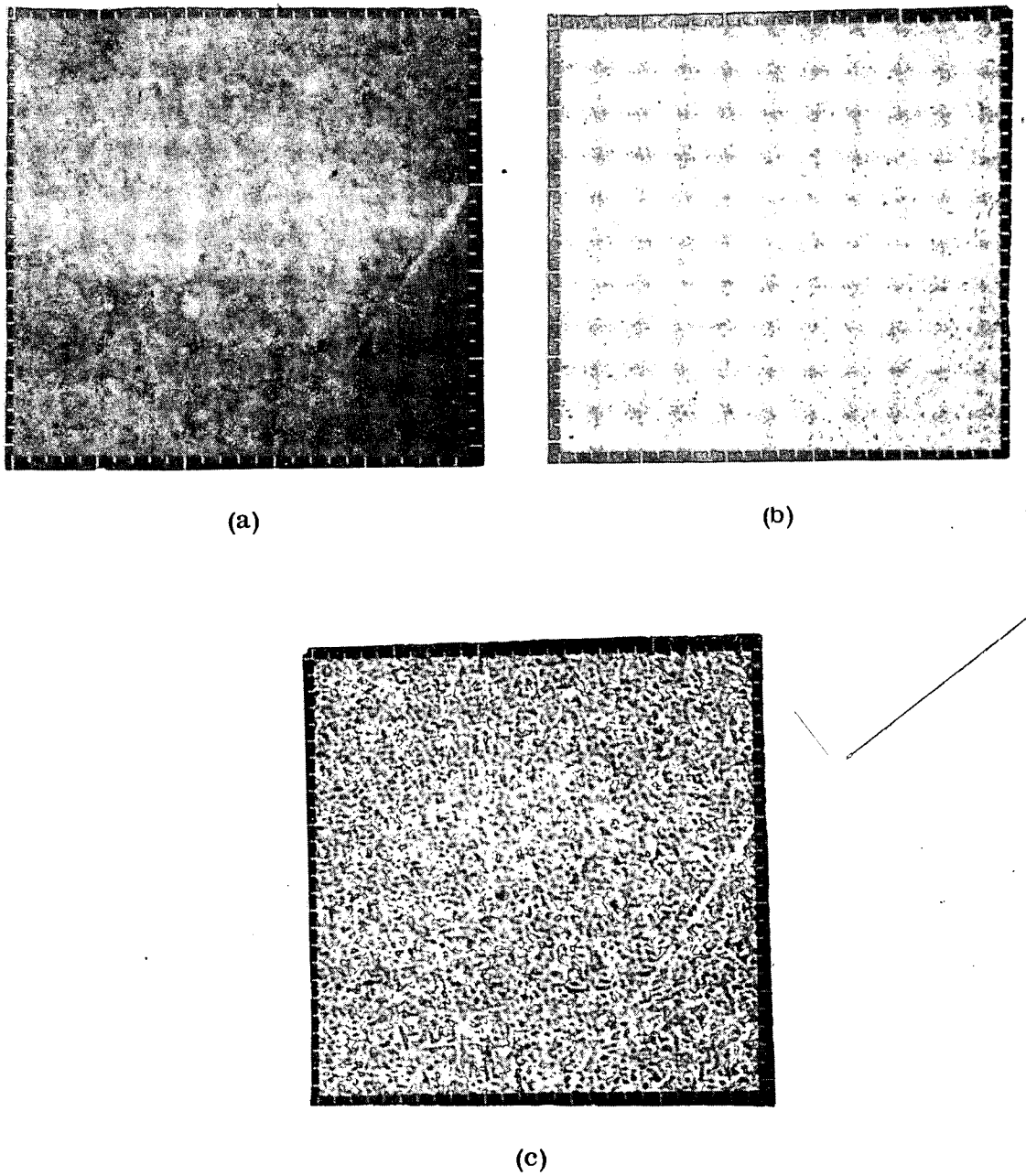

Figure 4-18. (a) Section of original picture with spots abutted;
(b) Inverse filtered version of (a);
(c) Stretch 3 applied to (b).

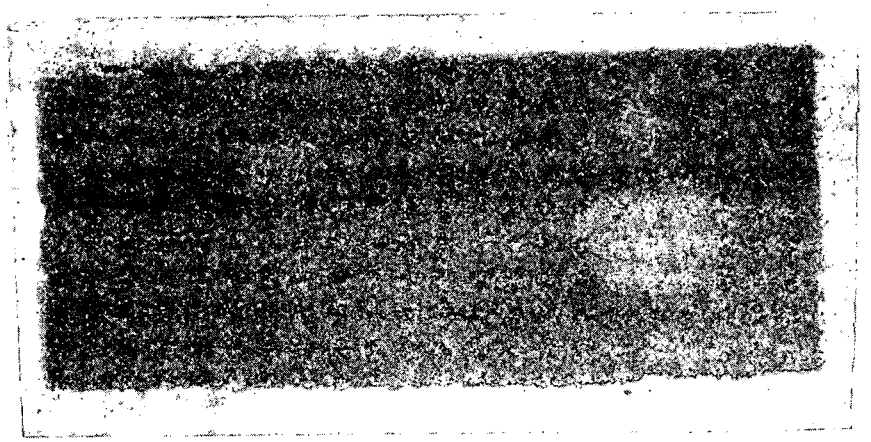

(a)

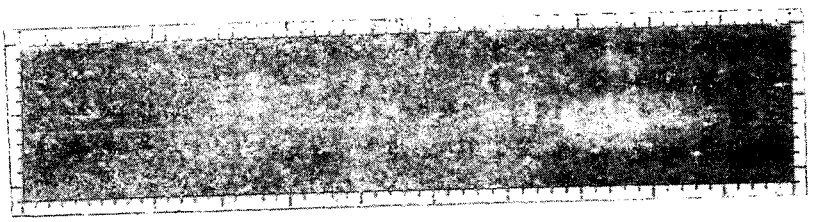

(b)

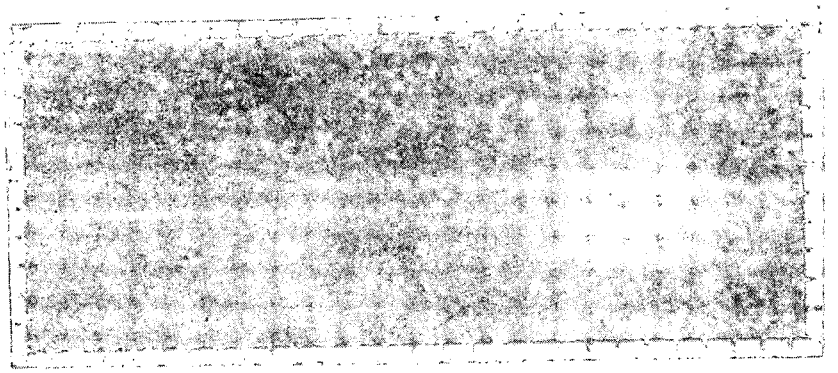

(c)

Figure 4-19. (a) Print from original radiograph;
(b) Original scanned data with 50 percent overlap along a line after stretch 4;
(c) Every second point on a line of (b).

4.2.1.3 --Continued.

function for the Dicomed system indicates resolution that is too low and irregular to warrant processing the Dicomed data with either convolution or Fourier filtering techniques. A higher resolution image dissector tube will be available for future Dicomed scanning. It will permit scanning with a 1/2 mil spot.

4.2.2 Results of Processing Area 2B.

4.2.2.1 Link.

Area 2B (number 4 of Table 4-3) was scanned by Link with the 3:1 lens with a spot diameter of approximately 10μ and 75% overlap. A study of a set of standard stretches (which required 24 Dicomed photographs) revealed no areas that could firmly be identified as a tailed porosity. An attempt to locate the fault was made using the Link 3:1 inverse filter for a 10μ non-overlapping scan. The original spot-abutted picture is shown in Figure 4-20(a) and the filtered unstretched picture in 4-20(b). As can be seen in Figure 4-20(c) the best of the stretches on the filtered picture still leaves doubt as to the identification of any faults in the picture.

4.2.2.2 Information International, Incorporated.

Area 2B (number 18 of Table 4-1) was scanned by I.I.I. from the same film (density 1.0) and with the same spot size and spacing as area 2A. However, only preliminary processing was applied to this picture because of an apparent problem with the focus on the scanner. I.I.I. could not explain the out-of-focus condition. Because of the strong interest MSFC has expressed in being fully advised of problems that affect the quality of digitizing, a section of the original data for area 2B is shown in Figure 4-21. A comparison of the apparent focus difference can be made against Figure 4-5 which was done with the same scanning parameters and from the same film.

Area 2B had previously been scanned by I.I.I. from the 2.4 density film. Difficulties in locating any areas that might correspond to the flaws that can be seen on the negative resulted in having I.I.I. rerecord this data. A careful study of their photograph suggested two possibilities:

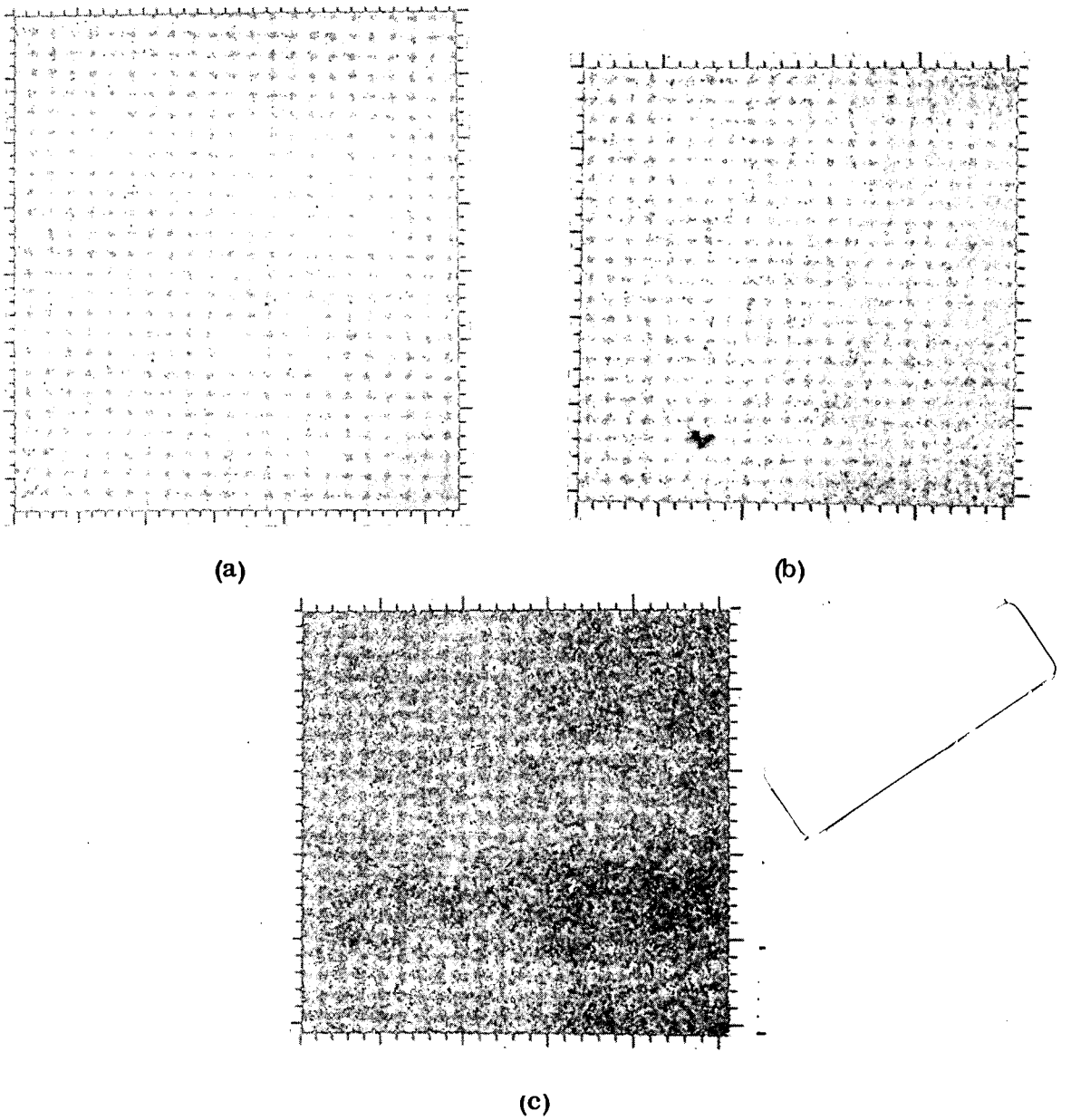

Figure 4-20. (a) Original scan of Area 2B by Link with abutted spots;
(b) Inverse filtered version of 256 x 256 portion of (a);
(c) Stretch 4 applied to (b).

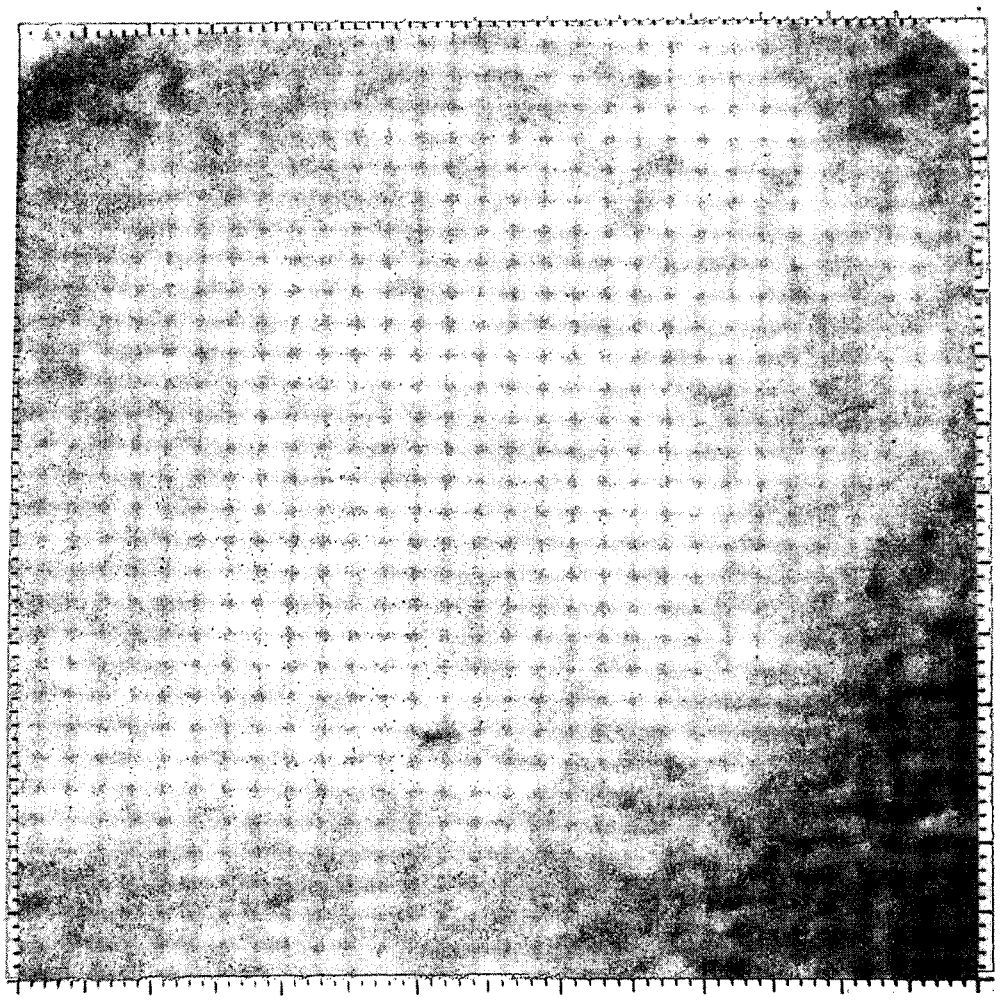

Figure 4-21. Original scan of Area 2B as scanned by I.I.I.

4.2.2.2 --Continued.

(a) the noise completely masked the data, or

(b) the wrong area had been scanned.

Therefore, no further processing was performed on this picture.

4.2.2.3 Dicomed.

Area 2B (number 4 of Table 4-3) was scanned by Dicomed from the same film and with the same scan parameters as 2A. Figure 4-22(a) shows a print from the radiograph and 4-22(b) shows the scan with spots abutted in both directions after stretch 3 had been applied. No faults could be identified and the resolution was not sufficient to warrant filtering.

4.2.3 Results of Processing Area 1.

4.2.3.1 Link.

Area 1 (number 5 of Table 4-2) was digitized by Link with the 3:1 lens (10μ spot) and a fifty percent overlap. The most interesting section of the display with non-overlapping spots was selected for processing. Figure 4-23(a) shows this area before processing and (b) shows the unstretched result from inverse filtering. Figure 4-23(c) and (d) shows the best of the stretches applied to 4-23(b) in either the normal or complement mode. The one porosity displayed was the most clearly defined in the entire fault area.

4.2.3.2 Information International, Incorporated.

The fault (number 4 of Table 2-3) was scanned from the 2.4 film with a 0.5 mil spot using the 3 to 1 lens. This scan was performed early in the contract and there is reason to believe that hardware problems caused a higher noise level than the optical transfer function curve from the 3 to 1 lens scan of the resolution chart indicates. The pictures showed no clearly defined porosities.

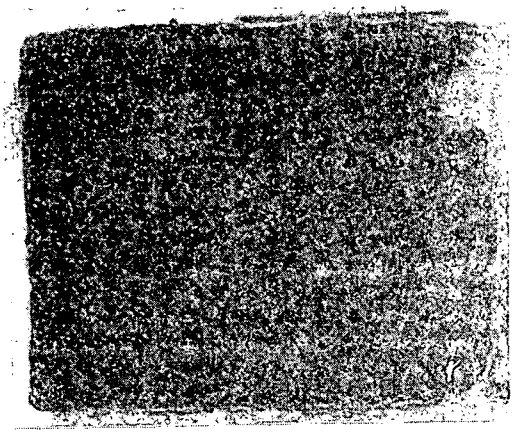

(a)

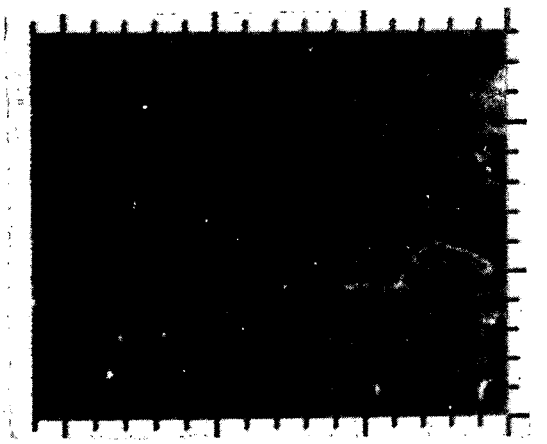

(b)

Figure 4-22. (a) Print made from the original radiograph of Area 2B; the light markings are from the ink outline on the film.
(b) The best stretch (number 3) applied to the scanning of (a) by Dicomed.

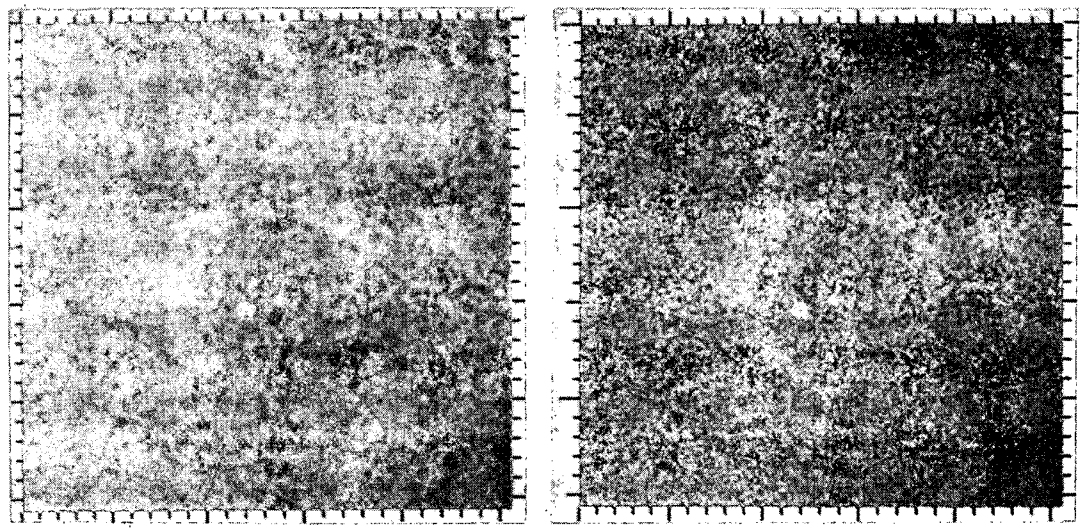

(a) (b)

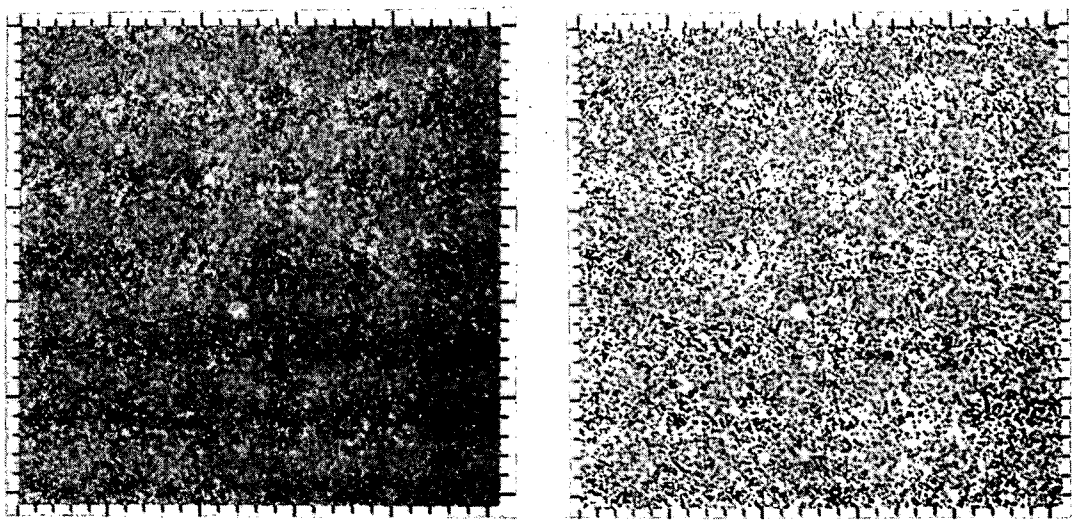

(c) (d)

Figure 4-23. (a) Original Link scan of Area 1; spots abutted
(b) Result of inverse filtering (a)
(c) Stretch 4 applied to (b)
(d) Stretch 5 applied to (b).

4.2.3.3 Dicomed.

This relatively large area was scanned by Dicomed with 50% overlap along a line. A print from the original radiograph is shown in Figure 4-24(a). The original scan is shown in Figure 4-24(b) and the best stretch in 4-24(c). Although no pores are clearly defined this series of pictures is included because they show the best results obtained from scanning with a one mil spot.

4.2.4 Results of Processing Area 3 Scanned by I.I.I.

Area 3 (number 7 of Table 4-1) is an example of a weld fault containing known cracks. Figure 4-25 shows a print made from the radiograph of the crater cracks. Because the crater cracks of Area 3 cover a large area on the film it was necessary for I.I.I. to scan the area in two files, each with over 3 million points. This scan was performed on the high density film (2.4). Preliminary processing revealed the most information in the first of the two files, so it was selected to be recorded on film. Figure 4-26 shows the recording of this data by I.I.I.

A series of contrast stretches was applied to portions of Figure 4-33 but no better definition of the crack structure was obtained. The noise in the data and the experience gained from the filtering already described indicated that inverse filtering was not justified.

4.3 Summary.

This section summarizes the steps used to process the pictures shown in the previous section. The method used to select each processing step is discussed and a flow chart showing the relationship between the various steps is given.

4.3.1 Linear Intensity Mappings.

A crucial step in the preliminary processing of any picture, (and particularly of any picture with a low contrast range) is the determination of the portion of the gray level scale that contains the critical data. This determination then allows an intensity mapping which displays the critical data to best advantage. The selection of the parameters to make this mapping can be done in the manner discussed in Section 4.2, however experience with a particular type of negative scanned by any given system will make it possible to eliminate several of the steps shown in Table 4-4.

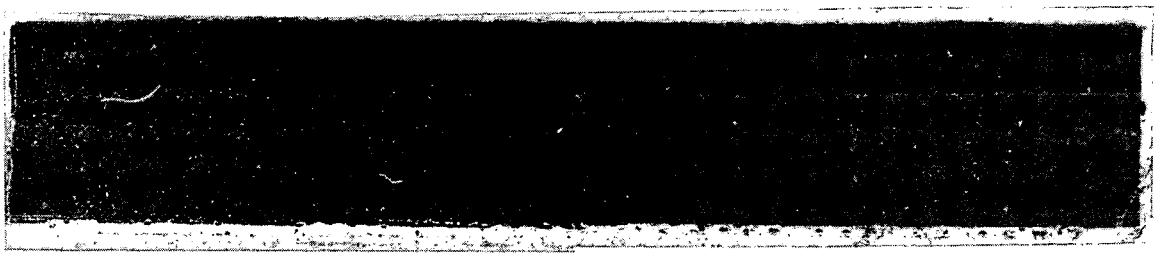

(a)

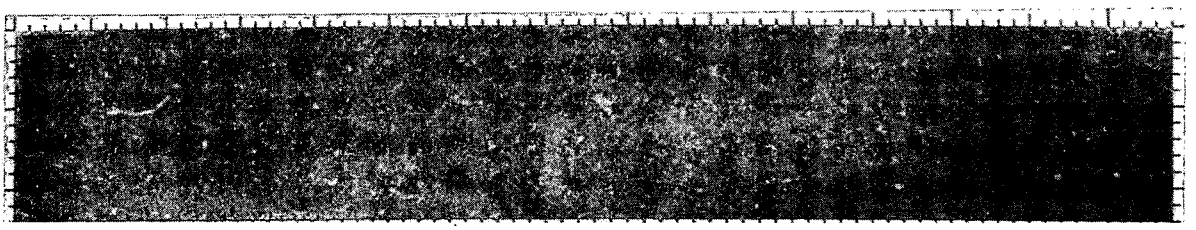

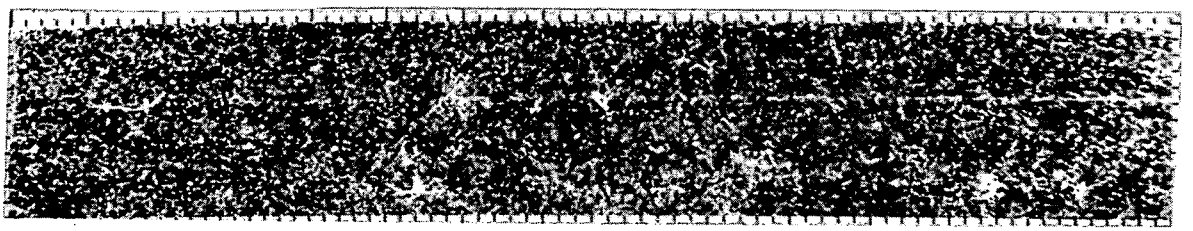

(c)

Figure 4-24. (a) Print from original radiograph of Area 1
(b) Original Dicomed scan of Area 1
(c) Best stretch of (b).

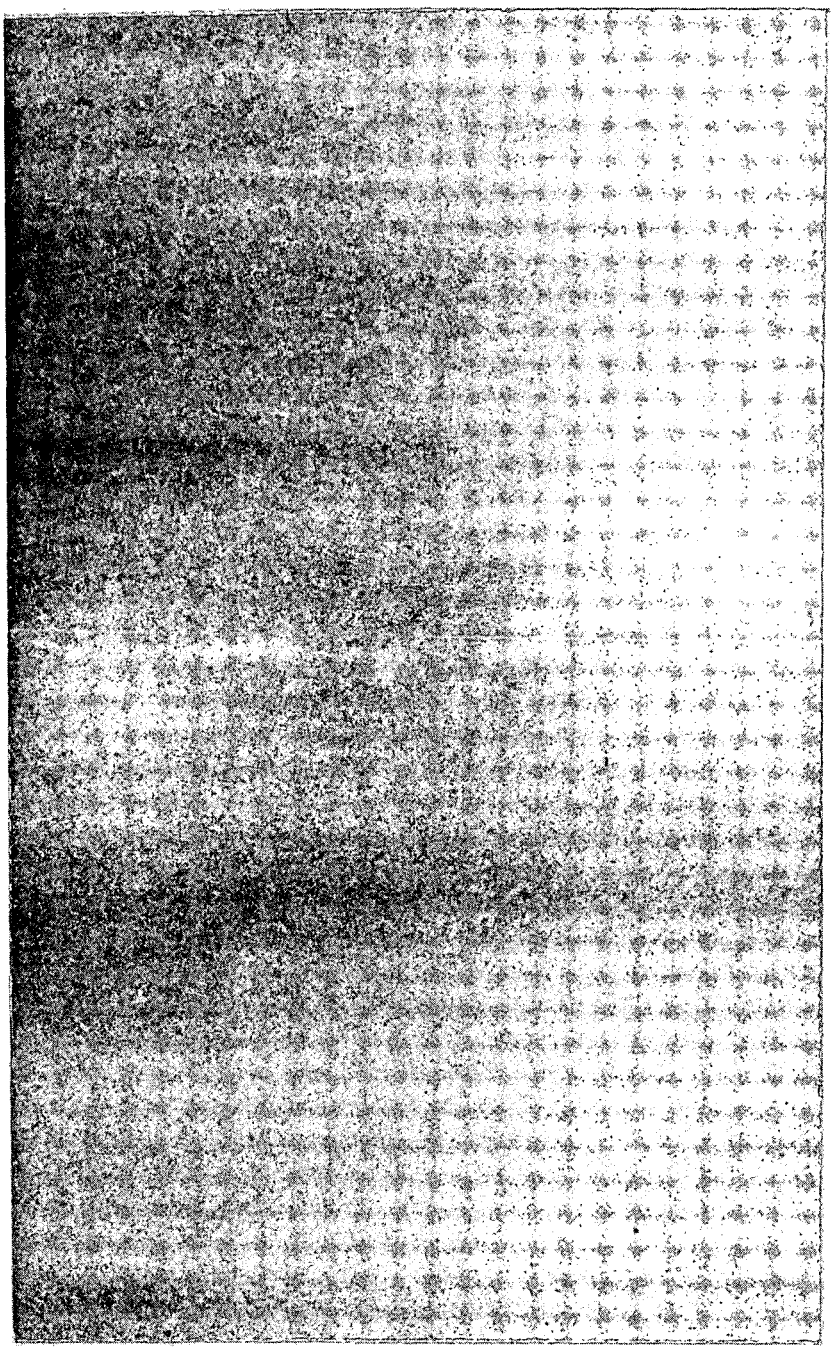

Figure 4-25. Print from the original radiograph of Area 3.

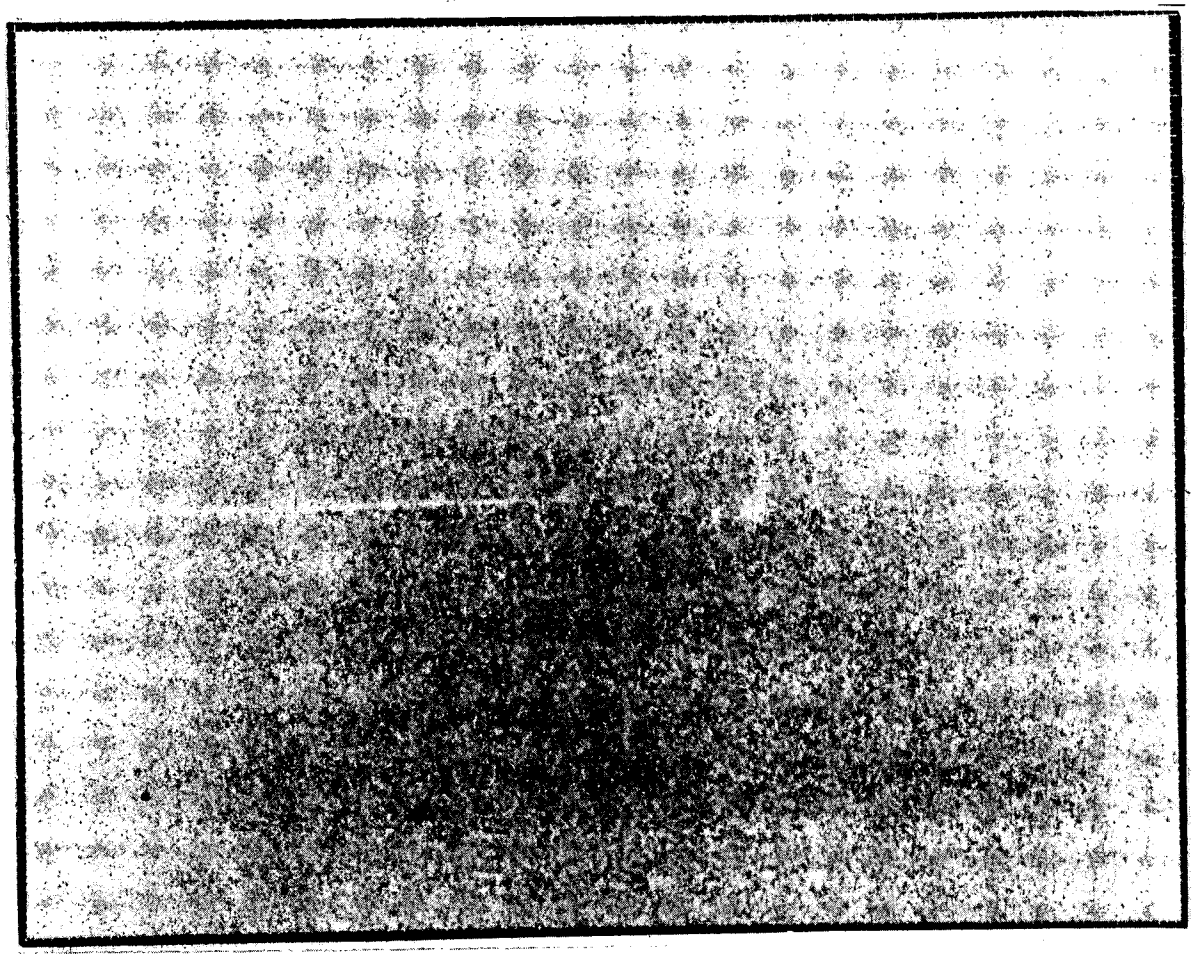

Figure 4-26. Film rerecording by I. I. I. of scan of Area 3 with the I. I. I. 3:1 lens.

4.3.2 Sample Reduction.

Several examples are shown in Section 4.2 of the effect of reducing the number of samples to display a certain area from the film. Processing time and cost can be greatly reduced by keeping only the number of samples necessary to give the needed detail resolution. Experience will aid in making this determination and will also affect the selection of the scanning parameters for future scanning. For a prelininary study of large areas it may always be desirable to reduce the number of samples so that the entire picture can be displayed as a whole. Since scanning is both time consuming and costly it is recommended that the original scan be done with as small a spot and as fine spacing as may be needed. However, this decision too depends on the system configuration, the number of pictures being processed and many of the other factors discussed in Section 6.

4.3.3 Inverse Filtering.

The physical process by which a radiograph is formed imposes limits on the resolution. Increasing the resolution of the radiograph can be formulated as the solution of a convolution type integral equation but this is extremely difficult if noise is present. The sources of noise are typically high frequency and the transform of the noise sequence may be constant or may increase with frequency. When this is the case inverse filtering may amplify the noise so much that the signal is obliterated.[4] Examples of noise boosting show up in some of the filtered pictures shown in Section 4.2 as speckling effects.

It is important to reduce the system noise. However it may also be worthwhile to investigate new techniques for solving the convolution-type integral equations to allow inverse filtering of data in which system noise is still present.[4]

4.3.4 Processing Flow.

The flow chart in Figure 4-27 shows the relationship of the enhancement steps applied to the radiographs that were processed for this study. Note that the steps shown up through the best stretched picture could be done by digitizing with a scanner with a selectable density window as discussed subsequently in Section 6.5. Note that, although non-linear filtering is indicated in Figure 4-27, only linear intensity mappings and linear filtering techniques were applied to the pictures shown in Section 4.2.

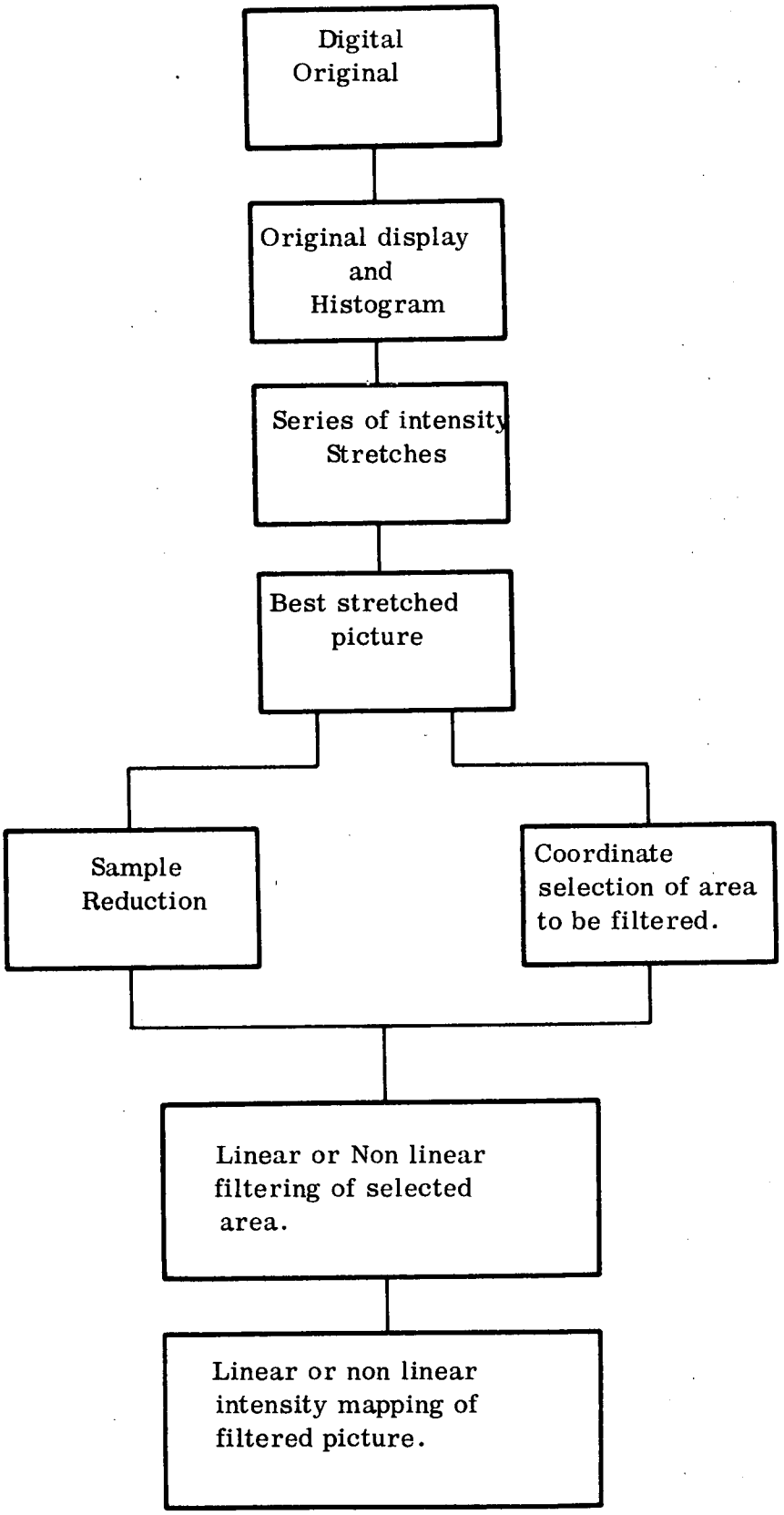

Figure 4-27. Flow Chart Processing Steps.

5. SOFTWARE.

The enhancement software used under this contract will be discussed in Section 5.2. The executive routines required for the use of these programs are functionally described and flow charted in Section 5.1. The actual program write-ups will appear in a separate volume to facilitate easy access.

5.1 Executive Routines.

The enhancement software used for processing the weld data was designed to operate under the VICAR system. Executive subroutines called by these routines must be written in order to run these programs on any system other than an IBM System 360 Model 44. The following sections outline the necessary functions and concepts involved.

5.1.1 Read.

The READ subroutine is used to read data into core. The coding is done in assembly language to allow for more efficient packing of data and elimination of control words written during FORTRAN I/O. The READ program has the following calling sequence.

CALL READ (Param 1, Param 2, ··· , Param 8)

PARAM	Parameter List	Description
1	Indicator	Contains status of request upon return.
2	Data Set Reference Number	Logical Data Set Number
3	Record Number	Zero = Sequential Read Non-zero = Random Record Number
4	Format Code*	Zero = Byte/Byte Transfer One = Halfword/Byte Transfer
5	Abbreviation*	Number of bytes to be skipped at beginning of record.

5.1.1 -- Continued.

PARAM	Parameter List	Description
6	Byte Count	Number of bytes to be read in. A count less than record length results in truncation.
7	Data Buffer	Address of READ buffer (full word alignment results in decrease of transmit time, core to core, by factor of four.
8	Auto Check **	Zero = Return after completion of request with status code in indicator cell. One = Return immediately after issue of read.

* Only applicable for double buffering.
** Auto check code of zero (0) is mandatory for double buffering.

The indicator, upon return, has the following meaning:

00 - Normal return
$4X_{16}$ - Invalid request, where X is the word in the parameter list deemed invalid.

Should the status be returned in the indicator, it would be:

04_{16} - End of File

08_{16} - Permanent Transmission Error

$0C_{16}$ - Operation Terminated, No Transmission

10_{16} - Invalid Request

The Data Set Reference Number is the logical data set number assigned by the problem programmer. When running the enhancement routines in a batch mode,

5.1.1 -- Continued.

the data set reference number merely would refer to which system unit was being used.

The Auto Check bit allows the problem programmer to issue the system read and return immediately to program control. This allows the user to perform computation while data is being read.

The format code is used when input data is packed in one point per byte. In this case, the data is unpacked into a halfword for processing. When data is not packed, the transfer is simply a byte-to-byte transfer

The logical flow of the READ routine used in the processing is shown in Figure 5-1.

5.1.2 WRITE.

The WRITE routine used in the enhancement programs is also coded in assembly language to provide efficient data transfer without the control word found under FORTRAN I/O routine. The calling sequence is:

CALL WRITE (Param 1, Param 2, · · · , Param 8)

PARAM	Parameter List	Description
1	Indicator	Contains status of request upon return.
2	Data Set Reference Number	Logical Data Set number.
3	Record Number	Zero = Sequential Write Non-Zero = Random record number.
4	Format*	Zero = Byte/byte transfer One = Half Word/byte transfer.
5	Abbreviation *	Number of samples to be skipped at beginning of record
6	Sample Count	Number of bytes to be written (a count less than record size results in truncation).

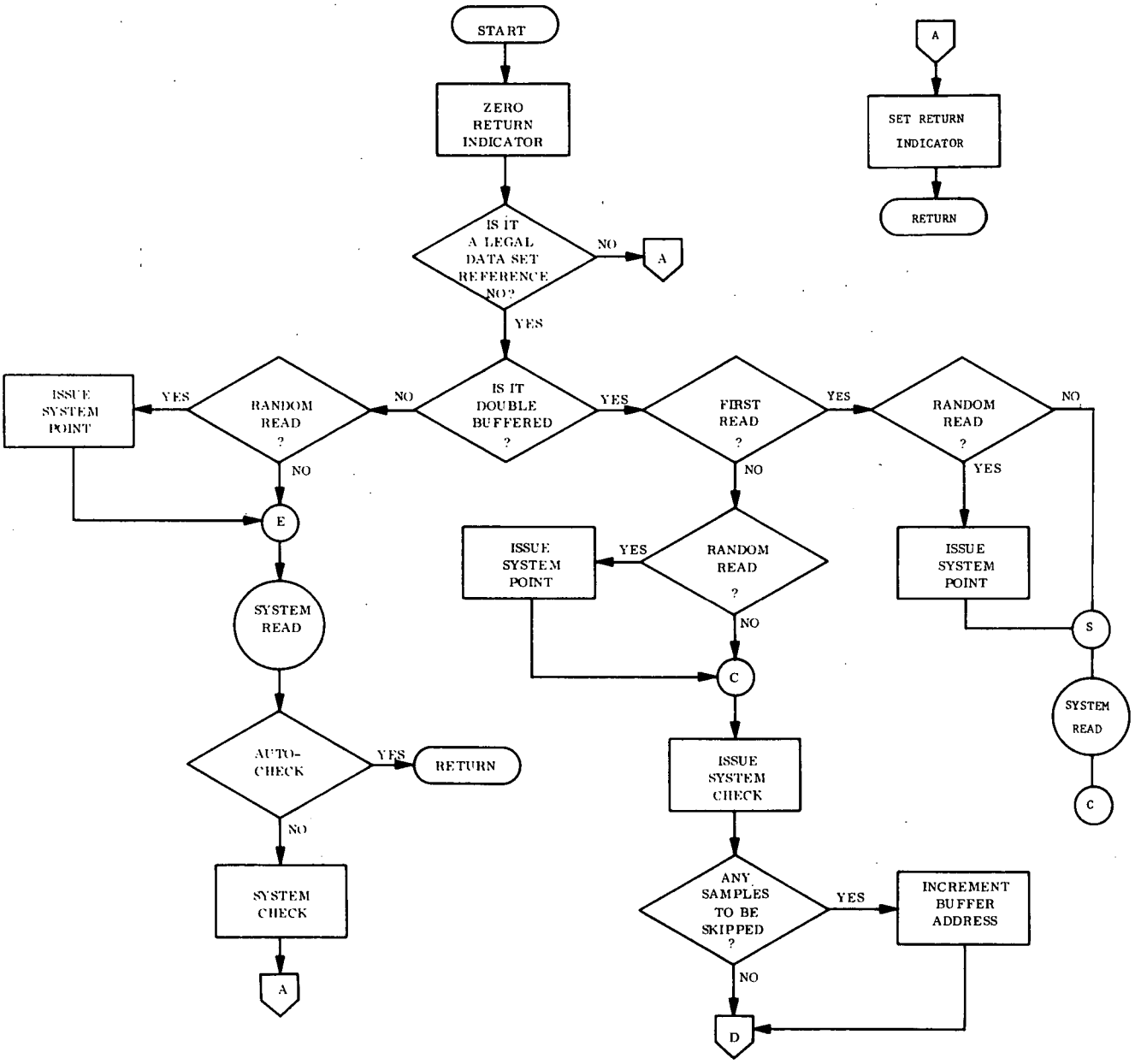

Figure 5-1 READ Routine

5.1.2 -- Continued.

PARAM	Parameter List	Description
7	Data Buffer	Address of output data buffer (full-word alignment decreases time of core transmits in double buffering by a factor of four).
8	Auto Check	Zero = Return to problem program after operation complete with status in indicator. One = Return to problem program immediately after write issued.

* To be used with double buffering only.

The indicator, upon return, has the following meaning:

00 - Normal Return
$4X_{16}$ - Invalid request, where X is the word in the parameter list deemed invalid

Should the status be returned in the indicator, it would be:

04_{16} - End of Extent

08_{16} - Permanent Transmission Error

$0C_{16}$ - Last Operation Terminated, No Transmssion

10_{16} - Invalid Request

The parameters used are the same as those discussed in Section 5.1.1. The logic flow for the WRITE routine is shown in Figure 5-2.

5.1.3 Other Support routines.

Other special routines used include

PARAM	PRINT
OPEN	END
CLOSE	ABEND

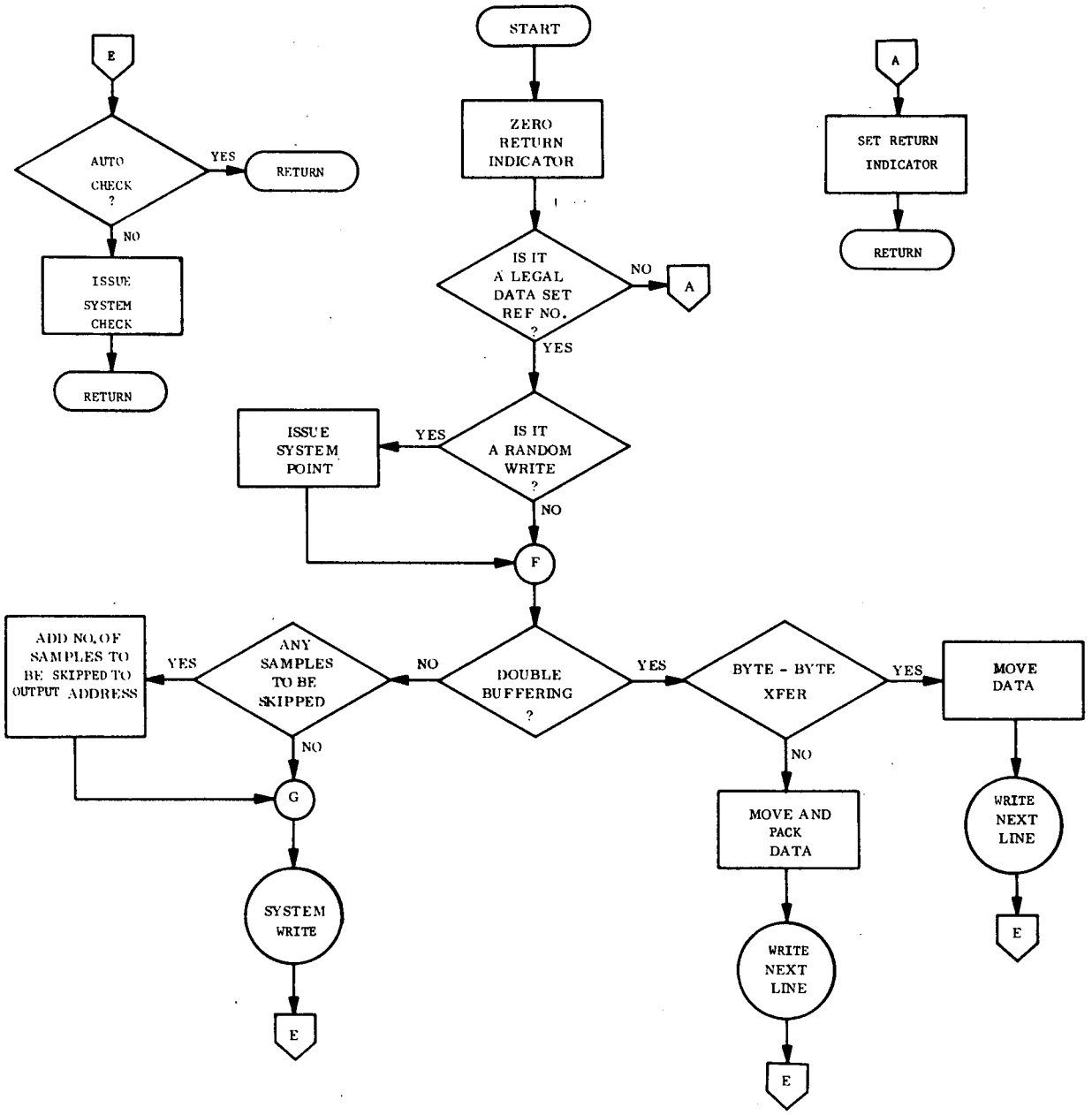

Figure 5-2 WRITE Routine

5.1.3 -- Continued.

Other system routines necessary are

CHECK
POINT

The calling sequence and logic flow of the special routines follow. These routines can however be reduced to a simpler form than that required in the ESL processing system.

The PARAM routine is used to pass user parameters to the program being executed.

The calling sequence for this routine is:

CALL PARAM (Param 1, Param 2, Param 3)

PARAM	Parameter List	Description
1	Indicator	Contains the stutus of the request upon return.
2	Buffer Address	Location of the parameter table buffer in problem program (full-word boundary) into which parameters are to be loaded.
3	Parameter Count	Number of full-words to be transmitted into the problem program.

The indicator, upon return, has the following meanings:

00 - Valid request
$4X_{16}$ - Invalid request where X is the word in the parameter list that was deemed invalid.

When running the enhancement routines in a batch mode no PARAM routine is necessary. The required data can be obtained by using a FORTRAN read in the problem program and input parameters will be read from cards.

The user, in that case, must supply 20 words (integers) that describe the data sets being used. Those words are supplied automatically by the PARAM subroutine, which is shown in Figure 5-3.

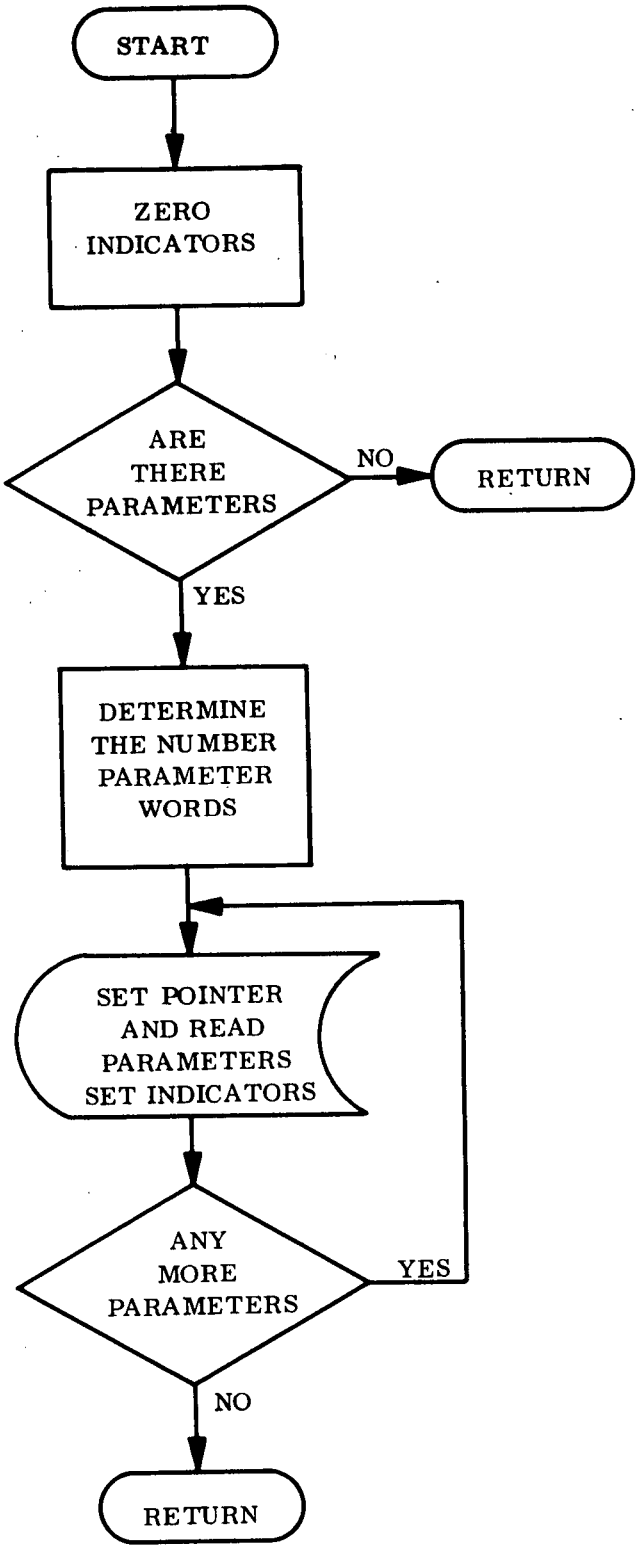

Figure 5-3 PARAM Routine

5.1.3 --Continued.

The OPEN request sets up the Maintenance Control Blocks for future I/O requests on this data set.

At this time, the data set will be defined as input or output, the data set can be repositioned if specified, single or double buffering will be noted and alternate buffers and their lengths are defined.

If double buffering is specified, the alternate buffer will receive all read records from the input data set. The buffer specified by the READ call has the data transmitted core to core from the alternate buffer. This allows an anticipated record to begin I/O while another record is being processed.

An open request is required for each data set to be used. The Data Set Reference Number used is the logical number.

The calling sequence for this routine is

CALL OPEN (Param 1, Param 2, · · · , Param 6)

PARAM	Parameter List	Description
1	Indicator	Contains status of request upon return.
2	Data Set Reference Number	Logical Data Set number
3	Input/Output	Zero = Input One = Output
4	Repositioning	Zero = No Repositioning One = Repositioning (do not use repositioning on data sets that have had label processing).
5	Alternate Buffer	Address of alternate buffer (full word boundaries on READ buffer result in increase of speed of core to core transmit by factor of four).
6	Alternate Buffer Length	Length of alternate buffer in bytes. Zero = Single buffering.

5.1.3 -- Continued

The indicator, upon return, has the following meanings:

NN - Normal return, where NN ($< 40_{16}$) is number of label records

$4X_{16}$ - Invalid request, where X refers to the word in the parameter list which was deemed invalid.

The OPEN routine is not required if the enhancement routines are run in a batch mode. The label processing usually done in the CALL OPEN will not be required because there is no system to handle the labels. Routines using random access, however, will require a value (zero) returned to indicate the number of label records found. The OPEN routine is shown in Figure 5-4.

The CLOSE routine is the counterpart of the CALL OPEN routine. This CALL will prevent any further I/O on the designated data set until another CALL OPEN is executed. A double EOF is written on tape and an EOF on disk for each close.

The calling sequence for this routine is:

CALL CLOSE (Param 1, Param 2, Param 3)

PARAM	Parameter List	Description
1	Indicator	Contains status of request upon return.
2	Data Set Reference Number	Logical Data Set number
3	Repositioning	Zero = No repositioning One = Repositioning (Rewind).

The indicator, upon return, has the following meanings:

00 - Valid request

$4X_{16}$ - Invalid request, where X refers to the word in the parameter list deemed invalid.

The CALL CLOSE routine is not required when running in a batch environment. The system I/O routines will issue the proper close or EOF message on the I/O units used. The CALL CLOSE routine is shown in Figure 5-5.

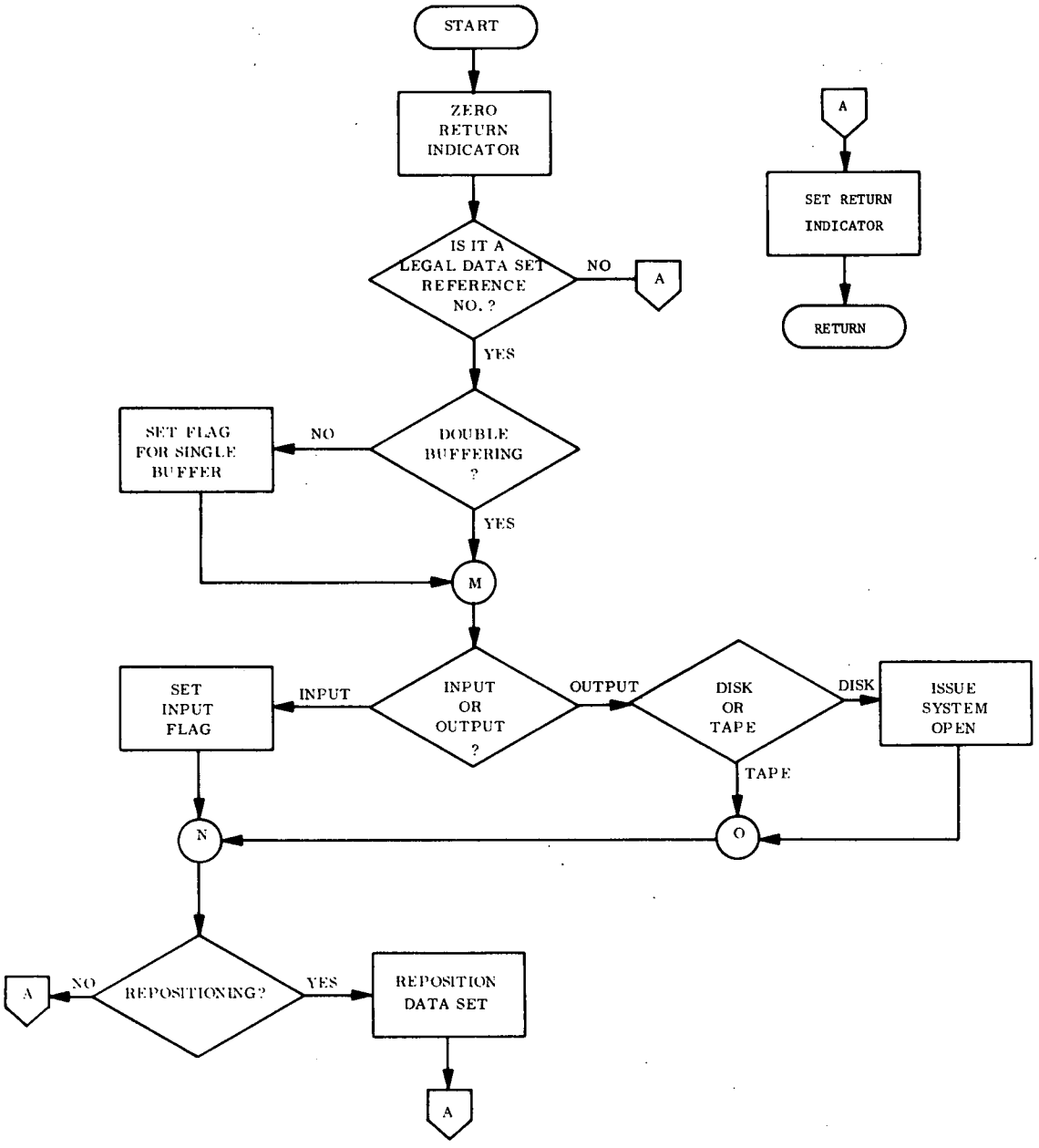

Figure 5-4 OPEN Routine

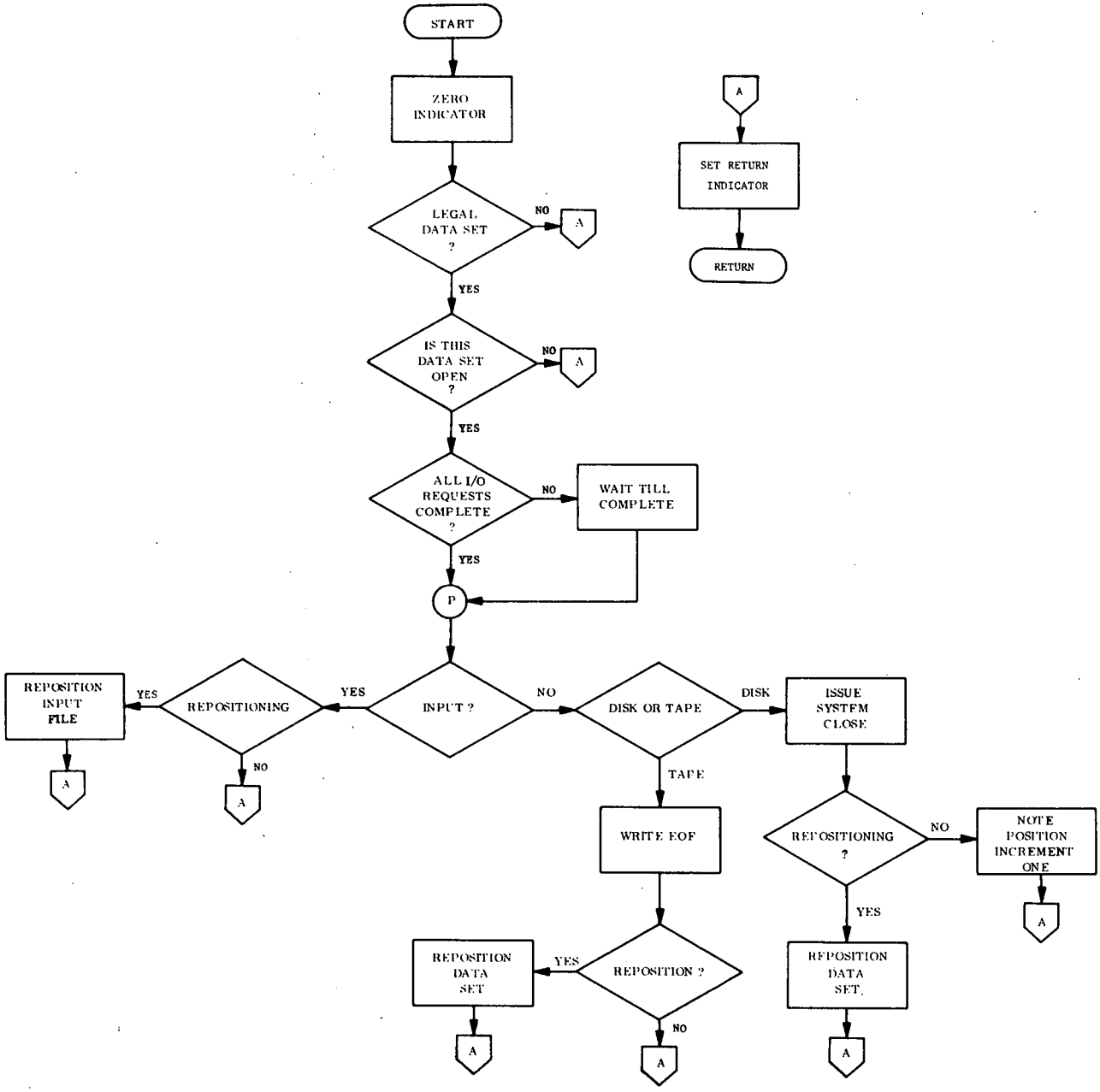

Figure 5-5 CLOSE Routine

5.1.3 -- Continued.

The PRINT routine is used for on-line messages. These messages can be printed on the typewriter and/or the printer. Since messages are not considered as output data sets, an OPEN is not required.

Data is printed as 8-bit printer graphic characters (EBCDIC). It is the responsibility of the programmer to get the data into the proper format for printing.

Restrictions: -

(1) Output to the printer should have a carriage control character as the first character.

(2) A maximum of 132 characters should be printed on the printer.

(3) A maximum of 120 characters should be printed on the typewriter.

(4) Only operator pertinent messages should go to the typewriter.

The calling sequence for this routine is:

CALL PRINT (Param 1, Param 2, · · · , Param 4)

PARAM	Parameter List	Description
1	Indicator	Contains status of request upon return.
2	Device	Zero = Typewriter One = Printer Two = Typewriter and Printer
3	Byte Count	Number of data bytes to be printed (include carriage control).
4	Data Buffer	Address of data to be printed.

The indicator, upon return, has the following meaning:

00 - Normal return
$4X_{16}$ - Request ignored, word X of parameter list deemed invalid.

The CALL PRINT routine was written to provide a means for the problem programmer to output to the printer and console. This was necessary because the VICAR system was written so that it could not handle the normal FORTRAN

5.1.3 -- Continued.

READ and WRITE software. All functions performed by PRINT can be accomplished using FORTRAN I/O routines. The PRINT routine is shown in Figure 5-6.

The CALL END routine is used when a program has completed normally. The calling sequence for this routine is:

```
CALL END
```

No parameters are associated with this call.

The CALL END routine is used only to return control to the job control processor at the end of the routine. When running the enhancement routines in a batch mode a return or stop is sufficient.

The ABEND routine is called when abnormal termination of a task is required. The calling sequence for this routine is:

```
CALL ABEND
```

No parameters are associated with this call.

The ABEND routine is not necessary when the OPEN and CLOSE routines are not used. Equivalent results are obtained by writing an error message with FORTRAN I/O and returning to the system. The ABEND routine is shown in Figure 5-7.

5.1.4 Relocatable Routines.

Various relocatable subroutines are called by the enhancement software. The principal routines are those used to check the status of an OPEN, CLOSE, READ, WRITE, or PRINT call. These routines can all be replaced with FORTRAN tests on the status of the return indicator. In the case of the OPEN, CLOSE and PRINT routines, no checks will be necessary if the calls are eliminated.

The RLPRNT, BINBCD and BINBCX routines are frequently used to convert data in core into EBCDIC so that it can be printed using CALL PRINT. The use of FORTRAN I/O will eliminate any need for these routines.

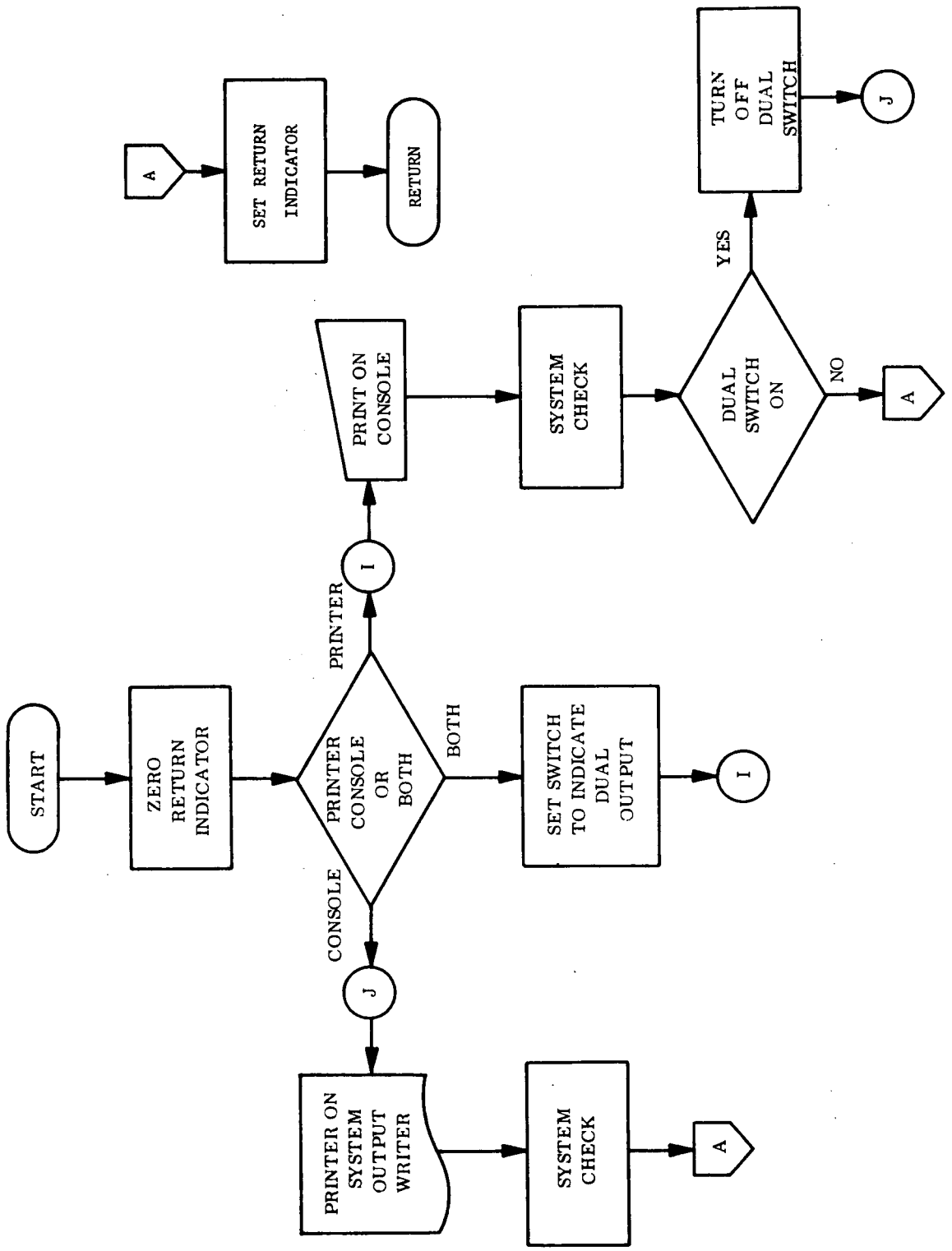

Figure 5-6 PRINT Routine

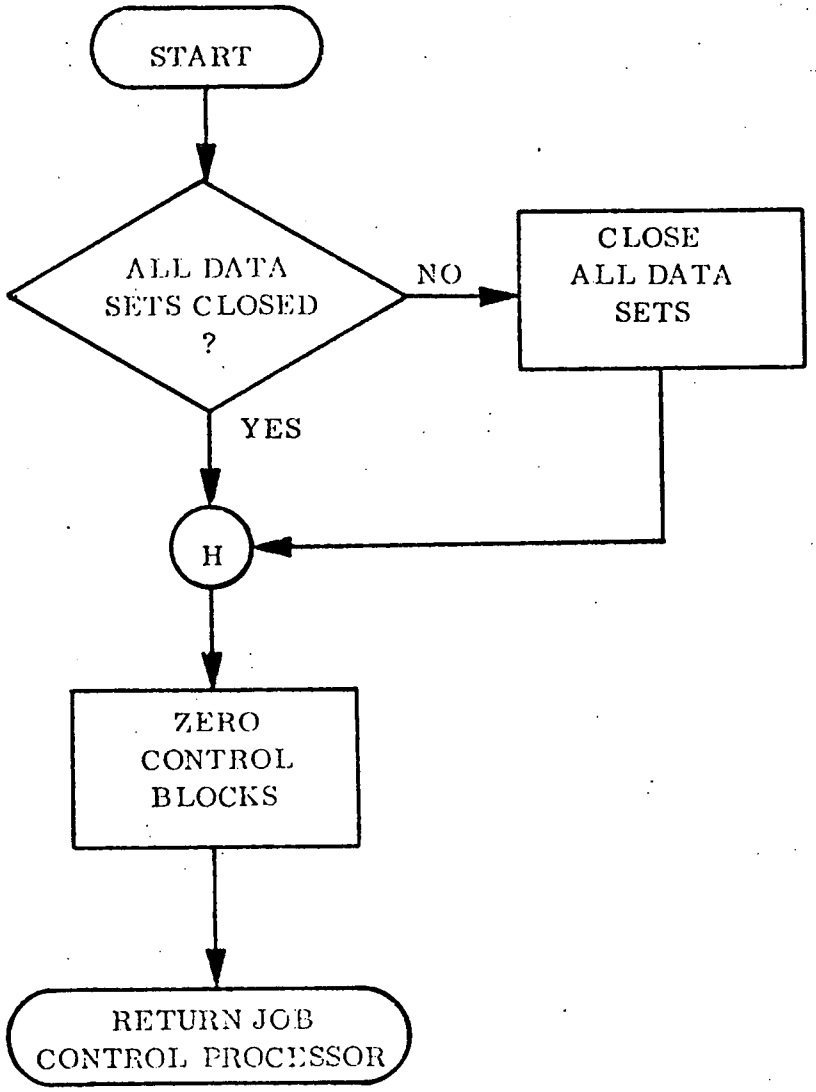

Figure 5-7 ABEND Routine

5.1.5 Control Blocks.

The executive routines require the use of control areas for input and output data sets. The control blocks contain information related to

Double buffering
Format (Packing)
Random or Sequential Processing
Data set open or closed
Address of alternate buffer
Byte count

The format of these control blocks must be designed and built around the computing system used.

5.2 Enhancement Software.

Enhancement software is divided into six groups:

(1) Fourier filtering,

(2) Convolution filtering,

(3) Filter generation,

(4) Equipment and/or data evaluation,

(5) Picture modification (point selection, contrast change),

(6) Data scaling.

Groups (3) and (4) are closely related, as equipment performance is a major determinant of the optimum filter selection. Also, groups (1) and (2) depend on the generation of filters for their functioning.

A general discussion of the six groups is given in this section; the program listings and details of their use are given in the programer's manual (Volume II of this report).

5.2.1. Fourier Filtering.

Fourier filtering is suited for use when

(1) the area of interest is represented by $2^n \times 2^m$ points (n, m integers),

(2) rotation or axis translation is time-feasible, and

5.2.1 -- Continued.

(3) there are no large gray-level transitions implied by the left-right or top-bottom edges. (Boosting of higher spatial frequencies will cause ringing, as a black-white transition already contains strong high spatial frequencies.)

The technique used to filter pictures in the Fourier domain follows.

The Fourier transform of the input picture is multiplied by filter weights and the result is inverse Fourier transformed. Seven routines are required:

(1) FFTF1 performs row by row one-dimensional Fourier transforms of the input pictures. It alternately multiplies the picture elements by +1, -1 to center the Fourier transform (the DC element is at the point ($\frac{1}{2}$ NL + 1 , $\frac{1}{2}$NS + 1), where NS = the number of samples, and NL = the number of lines.

(2) ROTATER performs 90-degree (right-handed) rotation on the output of FFTF1.

(3) FFTF2 performs row by row Fourier transforms of the (complex) input data set. After steps 1, 2, 3, the result is the Fourier transform of a 90-degree (RH) rotation of the input picture. A real data set is also output, containing the absolute value of the Fourier components for optional displays, with the DC term set to zero.

(4) CFILTER multiplies any two complex data sets and outputs the product. In Fourier filtering, this is the "filtering" step.

(5) FFTI1 performs row by row inverse Fourier transforms of the result of the filtering and outputs a complex data set.

(6) ROTATEL performs a 90-degree counterclockwise rotation.

(7) FFTI2 performs row by row inverse transform of the input data set. It also performs alternate multiplication by +1, -1 to restore the original convention (see FFTF1, above). The output is a real data set, containing either the real part or the absolute value of the complex output (the desired option is selected by a parameter).

5.2.2 Convolution Filtering.

Convolution filtering is computationally slower than Fourier filtering, but can be used to advantage if

(1) filter size is small, or

(2) Fourier filtering cannot be used due to size or edge gray level considerations (see Section 5.2.1).

One routine is required for convolution, CONVOL. This routine applies the filter to the integer input picture and outputs, as real data, the result of convolving the input picture and the filter.

The algorithm used does not assume axial or point symmetric properties for the filter. Unfolding is used on the edge areas to eliminate the large gray transitions possible.

5.2.3 Filter Generation.

The filters for both Fourier and convolution filtering are generated in the same manner: the generation of complete (two-dimensional, elliptically symmetric) Fourier filter coefficients. In the case of convolution filtering, an additional step is required: inverse Fourier transforming and the application of two weighting factors. The inverse transforming is done by FFTI1, ROTATER, and FFTI2, routines described in Section 5.2.1.

5.2.3.1 MTF Correction Filters.

It is desirable in many cases to correct the scanner's response to higher spatial frequencies. One must first obtain a measure of the scanning system's spatial frequency response. The MTF routine does this (see Section 5.2.4). As a user option, the MTF routine will also create one dimensional inverse Fourier filter. The filter thus created will correct the response of all spatial frequencies less than the smallest spatial frequency where the scanner's response is less than 20 percent. All higher spatial frequencies are multiplied by 5.0. This is done to avoid over-enhancement of the system noise.

After the MTF program has created the one-dimensional inverse Fourier filter for both horizontal and vertical directions, the routine TWOFLT is used to do

5.2.3.1 -- Continued.

elliptical fitting for the off-axis points. The output of this routine is the complete two-dimensional inverse Fourier filter.

5.2.3.2 Gaussian Fourier Filters.

The routine GAUSWTG will generate a Fourier filter with elliptical symmetry. For a low pass filter, the filter is of the form

$$F(x,y) = A\, e^{-(a_1 x^2 + a_2 y^2)}$$

For the high pass filter the filter is of the form

$$F(x,y) = A + B[1 - e^{-(a_1 x^2 + a_2 y^2)}].$$

The user specifies the high frequency gain, DC gain, and half power points on each axis.

5.2.3.3 Convolution Filters.

To generate a convolution filter equivalent to the Fourier filter we use the following property of Fourier filters:

if $g(x,y)$ is the original function,

$G(w_x, w_y)$ is the Fourier transform of the original function,

$F(w_x, w_y)$ is the Fourier filter,

then

$$g(x,y) * F^{-1}[F(w_x, w_y)] = F^{-1}[G(w_x, w_y)\ F(w_x, w_y)]$$

where * represents convolution and F^{-1} represents inverse Fourier transform.

Thus $F^{-1}[F(w_x, w_y)]$ is the convolution filter.

FFTI1, ROTATER, and FFTI2 are used to generate a complete convolution filter from the equivalent Fourier filter. However, a filter as large as the picture is prohibitive and extravagant. In the case of high pass filtering, usually a 15x15 or smaller filter is sufficient. The routine WTGEN selects a user chosen size filter, computes certain weights required by the filter and prints out one quadrant of the convolution filter.

5.2.4 Equipment Evaluation.

The routine MTF is used to determine the modulation transfer function (MTF) of a given scanning system. This routine is given a black-white edge digitized by the scanning system in question. Using the following relationship:

$$MTF(w_1) = \left| H(w)_{|w=w_1} \right| ,$$

the MTF may be determined.

H(w), the system function, may be found by differentiating the response to a step input. It has been found that H(w) is real and positive for the scanners used; thus MTF(w) = H(w).

The MTF routine prints the MTF of the system for each spatial frequency present in the edge. The highest spatial frequency is the point-to-point spacing frequency.

The routine NOISE calculates the standard deviation of the data over an all black or all white area.

The routine SIZE calculates the required number of gray levels vs. detail size. It requires the standard deviation calculated in NOISE, the spot spacing and the S/N level of threshold visibility as parameter inputs. SIZE combines the MTF and noise evaluation and therefore provides a way to compare the performance of scanner systems.

5.2.5 Picture Modification.

Two routines were used in modifying the pictures by means other than filters:

(1) contrast change (GAMMA),

(2) point selection (PIXPIK).

5.2.5.1 Contrast Change.

GAMMA is a routine which changes, under user parameter control, the contrast of selected points of the intensity scale of a picture. Both input and output are 8-bit picture elements.

5.2.5.2 Point Selector.

PIXPIK is a routine which allows the user to select elements from a picture. Every Nth element from every Mth line is output, where N and M are user parameters. Both input and output are 8-bit pictures.

5.2.6 Data Scaling.

The program SCALE accepts the real output from the filter routines and converts and scales the real numbers from 0 to 255 (8-bit picture elements). Input is real; output is 8-bit integer picture elements.

6. HARDWARE.

The special- and general-purpose hardware discussed in the following sections is designed to provide a digital weld radiograph enhancement capability for analyzing weld faults.

6.1 System Requirements.

The process of enhancing radiographic data places several requirements on the processing system. Figure 6-1 shows the functional components of a weld radiograph enhancement system. Each of these components must be chosen carefully to meet the requirements of the enhancement process.

The system must be capable of handling data with 4K x 4K resolution elements. The system will provide a Fourier transform capability for data up to 1024 x 1024 resolution elements. Larger transforms may be done but are not cost effective due to the extensive I/O requirements of Fourier transform algorithms. Convolution codes should be capable of handling images up to 4K x 4K resolution elements with a 15 x 15 filter function. Other non-filtering algorithms should be capable of handling images 4K x 4K comfortably with a quick turn around time. Facilities for image input and output must be available. A soft copy display for intermediate results is essential.

6.2 Central Processor.

The Central Processing Unit (CPU) is the central control of the weld radiograph enhancement system. The CPU will perform all computational functions required, handle all communication with the peripheral devices and control the flow of processing functions. The critical performance characteristics which affect the overall system are:

(1) size,

(2) instruction times,

(3) indexing capability,

(4) software, and

(5) I/O structure.

In choosing a CPU, these factors have to be considered carefully. In the following discussions these factors will be discussed in detail.

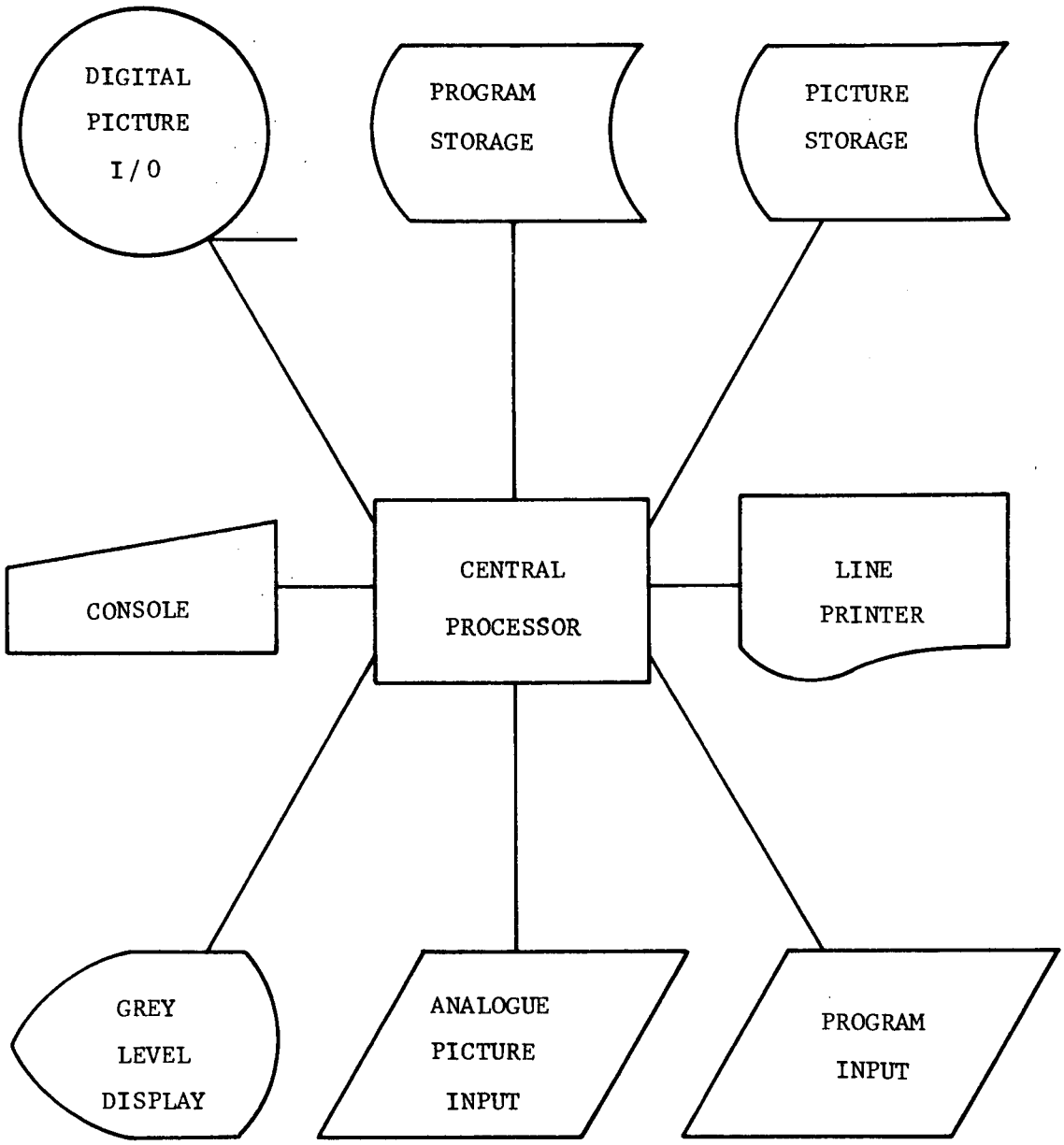

Figure 6-1 Functional Components of a Weld Radiograph enhancement System.

6.2.1 Size.

The minimum core size for the enhancement of weld radiograph data is 32K words. Enhancement systems can be operated on smaller systems but the loss of flexibility severely restricts the speed and capacity of the system.

The 32K word core allows the handling of records 4096 characters in length conveniently and allows the programmer to use double buffering techniques to speed up the processing time. For algorithms that have one input and one output this means that 8192 words are required for double buffering. In cases where multiple inputs or outputs are used, the amount of core required increases 4096 words per data set for single buffering and 8192 for double buffering. With three data sets, we are only left with 8K words for the supervisor and problem program when double buffering. Table 6-1 shows the amount of core required for different input and output combinations of records 4096 words long.

Table 6-1. Core Requirements.

No. of Inputs	No. of Outputs	Core Required (Words) Single Buffering	Double Buffering
1	0	4096	8192
0	1	4096	8192
1	1	8192	16384
1	2	12288	24576
2	1	12288	24576
3	1	16384	32768

The core resident portion of the operating system and core resident processing supervisor will occupy a significant portion of the core. In a dedicated system, the system supervisor can be reduced in size by deleting unneeded options. The executive routines use 1000 words of core and are resident at all times during the actual processing. The processing algorithms use from approximately 400 words to approximately 3000 words of core not including the arrays discussed above.

6.2.1 --Continued.

The data used in the processing is supplied in an eight-bit format. As a result, the data fits well into 16-bit words. If machines with 24- or 32-bit words are used, it is economical to pack two data points into each word and use half-word arithmetic. The double buffering routines can take advantage of this fact for all eight-bit data and thereby reduce the amount of core used for double buffering. There is nothing to be gained in using 32- or 24-bit arithmetic instructions when the input is only eight bit. As a result, it is recommended that all arithmetic instructions be 16-bit operations to optimize the use of the core and reduce the cost.

The processing of weld radiographs can be comfortably accomplished in a 32K 16-bit core. A 32K 32-bit word machine with half-word arithmetic can be programmed so that it will use fewer words than the 32K word 16-bit machine. Table 6-2 shows the core requirements for a 32K 32-bit word machine using packed 8-bit data.

Table 6-2. Core Requirements.

No. of Inputs	No. of Outputs	Core (K Words) Single	Double
0	1	2048	3072
1	0	2048	3072
1	1	4096	6144
2	1	6144	9216
1	2	6144	9216
3	1	8192	12288

6.2.1 --Continued.

When performing Fourier transform algorithms it is necessary to store a complex line which is two full words for each picture point. For a 4096 word picture this means that each entry in Table 6-1 is doubled and no packing can be used as in Table 6-2. One means of avoiding the situation is to use convolution filtering in place of the Fourier filtering.

The implementation of the Fourier transform and convolution filtering algorithms require large portions of core. In the case of convolution filtering, the software retains m lines in core, where m is the number of lines in the filter.

The algorithm can be performed by retaining only partial lines in core, but the I/O time will increase accordingly. Table 6-3 shows the maximum size convolution filter that can be used on pictures of different sizes assuming a core size of 32K 16-bit words.

Table 6-3. Maximum Convolution Filter Sizes.

No. of Elements per Line (m)	Filter Size (n x n)
64	Full*
128	Full*
256	85
512	43
1024	21
2048	9
4096	5

*The picture can be convolved with a convolution filter as large as the picture.

6.2.1 --Continued.

From Table 6-3 we can see that to perform convolution filtering on the weld radiographs we are severely limited as to our filter size as the picture size increases. By splitting up the lines and retaining only portions of each line in core we can use larger filters.

The Fourier transform algorithms use complex arithmetic and therefore require two full words per picture point. In a machine using a 24- or 32-bit word, the 32K word core is sufficient to process 4096 x 4096 areas one line at a time. In a 16-bit machine, the floating point arithmetic is handled with double words so the core requirements for the data arrays are doubled. All Fourier transform algorithms are implemented one line at a time, rotated, and applied again. If done in core the core requirements are too large to be practical.

The complex rotation algorithm creates a critical problem in the process of the Fourier transform. Because of the large amounts of data, the rotation can only be done using partitioning schemes and temporary I/O storage. On the IBM System 360 Model 44 the rotation ran 6 minutes for a 256 x 256 area. The run time will be approximately proportional to N^2, creating a severe restriction on picture size. A possible solution to the problem would be the use of slow-speed addressable core which could be used to bring in larger partitions and reduce the I/O time required.

In general, larger pictures are handled most conveniently using convolution techniques. Reasons for this are the reduced core requirements and the fact that neither the intermediate picture rotation nor the floating point arithmetic is required. When considering special-purpose hardware, the convolution techniques are also easier to implement for the above reasons.

6.2.2 Speed.

The speed of the Central Processor is a limiting factor in the performance of the overall system. The speed of the system is an intricate combination of software, hardware and peripheral support. Critical factors affecting the processing of picture data are:

6.2.2 --Continued.

(1) instruction times,

(2) index registers,

(3) core size,

(4) software, and

(5) peripheral support.

The following discussion will isolate the crucial concepts and discuss possible tradeoffs.

The process of filtering a picture is accomplished through the use of Fourier transform or convolution techniques. Both algorithms require significant computational time and thereby limit the overall speed of the system.

The introduction of the Cooley-Tukey algorithm for performing the Fourier transform in a digital computer has made the application of the Fourier transform possible. Computational requirements for the Fourier transform of a two-dimensional picture are proportional to $n^2 \log_2 n$, where n is the number of samples per line. As discussed in Section 6.2.1, large amounts of core are required to perform the Fourier transform on the entire image. The approach used to reduce the core requirements is to apply the transform to each line of the data, rotate or transpose the resulting complex array and apply the transform again. This technique allows the user to work with data sets up to 4096 x 4096 in a 32K word core. The rotation, however, requires a significant amount of I/O time and thereby limits the performance of the system on large pictures. Alternatives to the slow rotation are (1) more core to allow faster rotation of larger partitions, or (2) the use of addressable low-speed core so that the processing can be performed on the entire picture in core. The slow core is available at significantly lower cost than the regular high-speed core, but the large amount of core required is still in excess of 32 million words of core for a 4096 x 4096 picture. Reductions in core requirements are possible if we only retain half of the Fourier domain but this still requires 16 million words of core.

The enhancement routine used to perform the Fourier transform at ESL is implemented by using two one-dimensional Fourier transforms with a 90-degree rotation or transpose between the two transforms. The computation times for the Fourier transform in one dimension on the IBM System 360 Model 44 are shown in Table 6-4. Projected timings for other IBM computers are shown in Tables 6-5, 6-6, and 6-7. The times required for the rotation of the complex array are

Table 6-4. Computational Times for One-Dimensional Fourier Transform of Pictures n x n for IBM System 360 Model 44.

n	CPU HOURS
128.	0.0034
256.	0.0154
512.	0.0694
1024.	0.3083
2048.	1.3566
4096.	5.9197

Table 6-5. Computational Times for One-Dimensional Fourier Transforms of Pictures n x n for IBM System 360 Model 67.

n	CPU HOURS
128.	0.0013
256.	0.0061
512.	0.0276
1024.	0.1224
2048.	0.5389
4096.	2.3515

Table 6-6. Computational Times for One-Dimensional Fourier Transforms of Pictures n x n for IBM System 260 Model 75.

n	CPU HOURS
128.	0.0008
256.	0.0039
512.	0.0173
1024.	0.0770
2048.	0.3388
4096.	1.4782

Table 6-7. Computational Times for One-Dimensional Fourier Transforms of Pictures n x n for IBM System 370 Model 165.

n	CPU HOURS
128.	0.0003
256.	0.0012
512	0.0055
1024.	0.0244
2048.	0.1072
4096.	0.4680

6.2.2 --Continued.

shown in Table 6-8. The software used to implement the rotation is designed to operate in a 32K word core, so times could be improved by increasing the number of points rotated in each phase. The routines used under this contract were implemented using floating point arithmetic.

It should be mentioned at this point that the Fourier transform process has to be performed twice to filter a picture. The result is that the entire Fourier filtering process will take four passes through the one-dimensional Fourier transform algorithm and two passes through the rotation algorithm. Application of the filter and scaling algorithms will add additional computation time, but their contribution is insignificant in comparison to the actual transformation algorithms.

Timings for the convolution filter algorithm are shown in Tables 6-9 through 6-12. These times are based on the full convolution with four degrees of freedom. By reducing the filter to a radially symmetric filter with only one degree of freedom the times can be reduced by 20 per cent. Additional reductions in time are available by coding the inner loops in assembler language and making careful use of integer arithmetic.

As discussed in Section 6.2.1, the convolution algorithm retains m lines of core, where m is the number of lines in the filter. The algorithm is designed this way to minimize the I/O time required. Larger filters can be implemented at a reduction in overall speed by only reading in a portion of each line. In the case of the 4096 x 4096 picture, reading in half of each line into core would allow the use of a filter 21 x 21. As the number of cuts increases, the I/O time will increase at the rate of k*m, where k is the number of partitions used on each line and m is the number of filter lines. In either case, the program must maintain m lines or partial lines in core. If this is not done, the I/O time will make the convolution process unrealistic.

In both the Fourier and convolution techniques, significant time savings can be obtained by coding the inner loops in assembly language. In the case of the convolution, a savings of about 50 per cent is available over the times in Tables 6-9 through 6-12.

Table 6-8. Times for Complex Array Rotation.

n	Time (Minutes)
128.	1.5
256.	6.0
512.	24.0
1024.	96.0
2048.	384.0
4096.	1536.0

Table 6-9. IBM System 360 Model 44 Computational times (in hours) for convolution filtering with an n x n filter and m x m picture.

m/n	3	5	7	9	11	13	15
128.	0.0036	0.0099	0.0194	0.0320	0.0479	0.0668	0.0890
256.	0.0142	0.0395	0.0775	0.1281	0.1914	0.2674	0.3559
512.	0.0570	0.1582	0.3101	0.5126	0.7657	1.0694	1.4238
1024.	0.2278	0.6328	1.2403	2.0502	3.0627	4.2776	5.6951
2048.	0.9112	2.5311	4.9610	8.2009	12.2507	17.1105	22.7803
4096.	3.6448	10.1246	19.8442	32.8036	49.0029	68.4421	91.1212

Table 6-10. IBM System 360 Model 67 Computational times (in hours) for convolution filtering with an n x n filter and m x m picture.

m/n	3	5	7	9	11	13	15
128.	0.0014	0.0039	0.0077	0.0127	0.0190	0.0266	0.0353
256.	0.0057	0.0157	0.0308	0.0509	0.0760	0.1062	0.1414
512.	0.0226	0.0628	0.1232	0.2036	0.3042	0.4248	0.5656
1024.	0.0905	0.2514	0.4927	0.8144	1.2166	1.6992	2.2623
2048.	0.3620	1.0055	1.9707	3.2577	4.8665	6.7970	9.0492
4096.	1.4479	4.0219	7.8829	13.0308	19.4658	27.1878	36.1968

Table 6-11. IBM System 360 Model 75 Computational times for convolution filtering with a n x n filter on a m x m picture.

m/n	3	5	7	9	11	13	15
128.	0.0009	0.0025	0.0048	0.0080	0.0120	0.0167	0.0222
256.	0.0036	0.0099	0.0194	0.0320	0.0478	0.0668	0.0889
512.	0.0142	0.0395	0.0774	0.1280	0.1912	0.2670	0.3555
1024.	0.0569	0.1580	0.3097	0.5120	0.7648	1.0682	1.4221
2048.	0.2275	0.6321	1.2388	2.0479	3.0592	4.2727	5.6885
4096.	0.9102	2.5282	4.9553	8.1915	12.2366	17.0908	22.7541

Table 6-12. IBM System 370 Model 165 Computation times for convolution filtering with a n x n filter on a m x m picture.

m/n	3	5	7	9	11	13	15
128.	0.0003	0.0008	0.0015	0.0025	0.0038	0.0053	0.0070
256.	0.0011	0.0031	0.0061	0.0101	0.0151	0.0211	0.0281
512.	0.0045	0.0125	0.0245	0.0405	0.0605	0.0845	0.1126
1024.	0.0180	0.0500	0.0981	0.1621	0.2421	0.3382	0.4502
2048.	0.0720	0.2001	0.3922	0.6483	0.9685	1.3527	0.8009
4096.	0.2881	0.8004	1.5688	2.5933	3.8740	5.4108	7.2037

6.2.2 --Continued.

The critical instructions for both filtering techniques are the floating point add, floating point multiply, integer add, and integer multiply. The times for these instructions on the IBM System 360 Model 44 are:

AE	Floating add short	4.56 μs
ME	Floating multiply short	14.81 μs
A		2.25 μs
M		16.89 μs

The enhancement speed of any Central Processor is greatly affected by these times and is to be weighed heavily in choosing a CPU. The times for convolution and Fourier filtering show the vast difference in performance on different computers. The control processor used should be as fast as possible for the money available. The critical instructions are:

(1) floating point add,

(2) floating point multiply,

(3) fixed point add,

(4) fixed point multiply,

(5) load, and

(6) store.

In the case of floating point instruction, it is essential that these be done using floating point hardware.

Processing image data requires the use of index registers. The use of other addressing techniques is unacceptable due to the large amounts of data involved. The use of other techniques would result in a loss of 20-30 percent in overall speed.

3

6.2.3 Input/Output Structure.

The processing of image data depends heavily on the speed and capacity of the peripheral devices. The I/O structure of the Central Processor can make a significant difference in the overall system performance. Without the proper I/O structure the Central Processor will therefore be slow and inefficient in processing image data.

The most critical element is the Direct Memory Access(DMA) channels available to the system. The magnetic tapes, random access devices and special purpose hardware all require DMA channels. Other peripherals such as the film scanner and grey level display will require two additional DMA channel when connected on-line. The number of available DMA channels will be the most limiting factor if there are less then 3 or 5 when the display and scanner are on-line. It should be noted that some processors have a DMA which can be assigned to n different I/O channels, thereby reducing the actual number of DMA channels but supplying an equivalent on n DMA channels.

6.3 Peripheral.

The peripheral devices are critical in the overall enhancement system because of the volume of data handled. Peripheral components must be carefully chosen to provide adequate speed and size. The standard peripherals such as card reader, punch, printer and console are assumed and will not be discussed.

6.3.1 Magnetic Tape Units.

Magnetic tapes are used as a permanent storage medium and in some cases an interface medium. The speed, density and number of tracks are critical factors affecting their use.

The speed of the tape unit will be a contributing factor in the overall speed of the system. If the number of pictures processed is small, i.e., one a day, and a dedicated system is being used, then the tape speed is not critical. The higher speed drives become important when the system is being used to process several pictures a day which require use of a tape drive.

A minimum of two nine-track tapes are required for efficient operation. A seven-track should be used only if it is needed for interfacing with other equipment. It is often convenient to have a third drive available to copy or merge tapes, but its presence is not mandatory.

6.3.1 --Continued.

Tapes are best used by the system to perform long-term storage. Tapes can be used as intermediate storage, but they are limited in that they only operate sequentially. The random access devices provide a more convenient intermediate working storage mode because multiple data sets can be retrieved from the same device conveniently and in any order. When an interface is required between the central system and an off-line device the magnetic tape is the only logical choice.

6.3.2 Random Access Devices.

Many forms of random access devices are available for use in a weld enhancement system. The use of a random access device gives the fast random access intermediate storage and a fast and efficient medium for program storage. Random access devices are used rather than using magnetic tapes because of the increased ease of operation and their ability to do random accessing necessary in Fourier filtering algorithms. Specifically, one disk can be used to store multiple data sets which are to be used during one task whereas the magnetic tape cannot be used effectively without many tape drives. The random access mediums also provide a quicker access to the program library where the enhancement routines are stored.

The weld enhancement facility will require an extensive program library. A disk operating system and storage of enhancement routines on a random access device will enable the user to have fast and efficient use of the facilities of the system. Other modes of program storage involve cumbersome operator intervention and reduce the overall efficiency of the system. The actual random access device used in the enhancement facility can be picked from any of the available devices. The requirements are only that it contain enough storage for the operating system and program storage required. The speed of the program storage device is not critical and may be chosen to meet other needs of the system. In most cases, the random access device can be used as both an intermediate storage area and a program storage area.

Intermediate storage plays an essential role in the efficiency of the system. The processing of large pictures will require many temporary work areas to store interim results. In the case of the Fourier and convolution filtering, the speed of the data transfer plays a critical role in the time required to process an image.

6.3.2 --Continued.

As shown earlier, the Fourier transform requires a time consuming matrix rotation which proves to be a limiting factor in processing large images. Random access devices are essential in keeping these times to a minimum and the device should be as fast as possible within reasonable budget constraints.

Slow speed core will provide the fastest data access but will generally be more expensive than other devices. The fixed head disk or drums will again provide rapid data access but the cost is high. The moving head disks and drums provide a slower data transfer yet provide significantly more data storage at an equivalent cost to the other systems. This additional storage is important in that it provides an area for program storage, an operating system and multiple intermediate data sets.

6.3.3 Display Devices.

The process of enhancing a weld fault requires the display of processing results. Results can be displayed by recording the results on the scanning/recording hardware or they can be displayed on some quick-look gray level device. The use of a quick-look device increases the effectiveness of the system by allowing the user an immediate check on his success whereas the recording procedure causes a delay in evaluating the results.

Several quick devices are available for use in the enhancement system. One common device used is a Conrac TV monitor. These units can be set up either to be refreshed by disc, as is done by Data Disc, be refreshed by core or the user can simply take a polaroid time exposure as the image is painted on the screen. Television type displays are currently limited to a raster size of about 512 x 512. In the case of Data Disc, they are also restricted to sixteen gray levels as an off-the-shelf item. In general, the gray level displays currently available do not offer sufficient grey levels, a large enough raster and they suffer from excessive flicker due to the refresh rate.

Storage tube displays have been shown to be capable of displaying adequate gray level pictures. In particular, the Dicomed Corporation markets a sixty-four gray level 2048 x 2048 display. The display provides a large enough display area to enable convenient display of large pictures. The Dicomed display can be operated off-line using a magnetic tape to transfer information from the central system. The interface required is similar to that of a nine-track tape unit and is available from Dicomed.

6.3.3 --Continued.

The on-line display gives the user an immediate indication as to the success of his efforts; however, it always ties up the system while he is creating the picture. The off-line unit allows the user to create tapes and play back pictures later. This system allows the user to analyze results at any time. However, the added delay in viewing the picture delays the processing of the picture.

6.4 Special-Purpose Hardware.

The process of enhancing weld radiographs involves the handling of large arrays of data. In several cases, the processing is limited by the speed of a critical inner loop calculation. Both the Fourier and convolution filtering techniques fall in this category.

There are many special-purpose Fourier transform processors available. The need for these units has arisen primarily due to the needs of signal processing and are therefore only capable of handling one-dimensional input. As discussed earlier, the two-dimensional Fourier transform can be obtained by taking two one-dimensional transforms, one on the rows and one on the columns. Depending on the design of the hardware, the FFT hardware can process a line of 1024 samples in from 1 ms to 5000 ms. This is a considerable improvement over the times indicated in Section 6.2 which were implemented by software. The rotation times, however, still pose a serious limitation to processing of large arrays.

The convolution algorithm makes use of the operation known as the sum of products. The implementation of the required operations by hardware has been done many times in one dimension. Unlike the Fourier filtering, the convolution algorithm can be easily implemented in two dimensions. The actual hardware used to do the Fourier transform is often used to do the convolution filtering and the reduction in processing time is correspondingly about the same.

The process of convolution and Fourier filtering are known to be equivalent when the convolution weights used are of the same dimension as the filter used. The computational speed of the convolution algorithm when processing such a large set of weights is, however, significantly longer than the Fourier transform itself. Even when using smaller filters, it is found the convolution time is longer than that of the Fourier. By using a folded filter and only allowing one degree of freedom the convolution code can be shown to be faster than the Fourier techniques for a filter less than 7 x 7. The accuracy of the resulting filter, however, is usually only about 40 to 50 percent, thus leaving considerable question about its use.

6.4 --Continued.

The Fourier techniques on the other hand give extremely accurate results with errors only in round-off and floating point precision. Implementation, however, is very difficult on large pictures, as has been discussed previously. The result is that the user must choose between the two techniques in each situation. It should be mentioned that the Fast Fourier techniques can only be used on pictures that have lines and line length that are a power of two. The convolution techniques can be applied to pictures of any size.

The need for a special purpose processor is determined by the usage of the system. The special purpose hardware will play an essential role in increasing throughput when the system is used excessively for filtering picture data. Large pictures will also be more easily handled with the use of special purpose hardware. The performance of the system will be significantly improved with the use of special purpose hardware but there is no stringent need for this hardware until the enhancement system either has too many welds to process or the need arises to process large pictures frequently.

6.5 Scanner/Recorder.

The acquisition of high quality scanning and recording of weld radiographs has proven to be a critical and complex process. The capabilities of the scanners studied under this contract as operated by the companies involved, were shown to provide inadequate results for the accurate analysis of weld radiographs. Because the scanning is the limiting factor in the enhancement process, the specifications for the hardware used must be clearly defined.

6.5.1 Operating Environment.

The scanner/ recorder should be off line and should be operated in a clean room environment. It should be adequately shielded against radio frequency or vibration interference.

6.5.2 Quantization Requirements.

A scanning system should provide as many gray levels as possible in the density range containing the information. This implies that a means is required to place the available gray levels in a specified density range since the density range containing the information can vary.

6.5.2 --Continued.

For example, if the film has an average background density of 2.0 and if the information lies in a density range of ±0.2, then it would be optimum to place the 2^N gray levels obtainable from N bits of data in the density range from 1.8 to 2.2. Placing the available gray levels in the density range of interest requires considering the following two scanning options.

6.5.2.1 Selectable Density/Transmittance Window.

One requirement on converting a specified density range into a desired number of intensity steps (gray levels) is that the scanner have a "selectable window". This implies that the scanner could be adjusted by setting a baseline density and density increments, or, equivalently, by setting the minimum and maximum density and maintaining linear or non-linear steps to the desired number of bits. Linear and non-linear steps correspond to scanning in transmittance and density modes, respectively (see Section 6.5.2.2).

All the scanning done in this study by I.I.I. was done in the density mode with 2^N equal density steps in a "density window" of 1.8 density units. The range of 1.8 density units could not be narrowed but it could lie centered about a specified density value. For data lying in a very narrow density range the fixed width of 1.8 units is too great to allow sufficient discrimination of critical information..

The scanning done by Link was in transmittance mode with a "transmittance window" determined by adjusting the scanner so that the maximum gray level (63 for 6 bit data, 255 for 8 bit data) was achieved when scanning through the open aperture, i.e., in the absence of film. Using this method the "transmittance window" covers transmittance values from 1.0 to .016 for 6 bits and 1.0 to .004 for 8 bits. These ranges correspond to density values of 0 to 1.8 and 0 to 2.4 for 6 and 8 bit data respectively. Clearly this method also in not adequate when scanning for critical data in a very narrow density range.

It is assumed that weld fault information is recorded on the X-ray film. For purposes of this study, no minimum size was established by NASA MSFC for critical weld flaws. Therefore, to cover all possibilities, it is necessary to obtain a digital representation of the image which discriminates the smallest density changes as possible. However, the smallest density change containing fault information is not known. Consequently, it is not possible to specify the

6.5.2.1 --Continued.

"optimum" width of the density window based on a theoretical analysis. Furthermore, the optimum width cannot be specified empirically using the scanning done under this study. Thus, to arrive at an empirical specification, the state-of-the-art in film scanners must be investigated to determine if a sufficiently narrow window exists in a scanner with a low enough noise level and a small enough spot to provide the quality of data required for a weld enhancement system; none of the three CRT scanners used in this study have these features.

From Figure 6-2 it is seen that equal transmittance steps are not equal density steps. In particular, the first three gray levels (corresponding to transmittance of 0, 1/64 and 2/64) occur for density values of infinity, 1.8 and 1.5, respectively. Thus when digitizing is performed in equal transmittance steps on high density film all information that lies in a relatively wide density range below the maximum level will be mapped into very few gray level steps.

The desirability of digitizing in equal density steps when the film has a high average density and a narrow density excursion containing information can be seen from Figure 6-3. This figure shows a curve for equal density steps versus gray level for a film with maximum density of 2.4 digitized with a 6-bit system. In this mode each gray level corresponds to 0.0375 density units.

The digitizing performed by both Link and Dicomed was done in equal transmittance steps. All digitizing done by I.I.I. was done in equal density steps. Based on the above considerations, it was expected that the I.I.I. scans would be more sensitive to the small excursions made by the information on the film, but excessive system noise masked this anticipated effect.

It is recommended that the scanner used for digitizing radiographic films have one of the following capabilities (in order of preference):

(1) transmittance-mode scanning with a density window having a selectable width and center;

(2) density-mode scanning with a density window having a selectable width and center;

(3) transmittance-mode scanning with a density window having a fixed width but selectable center;

(4) density-mode scanning with a fixed density window.

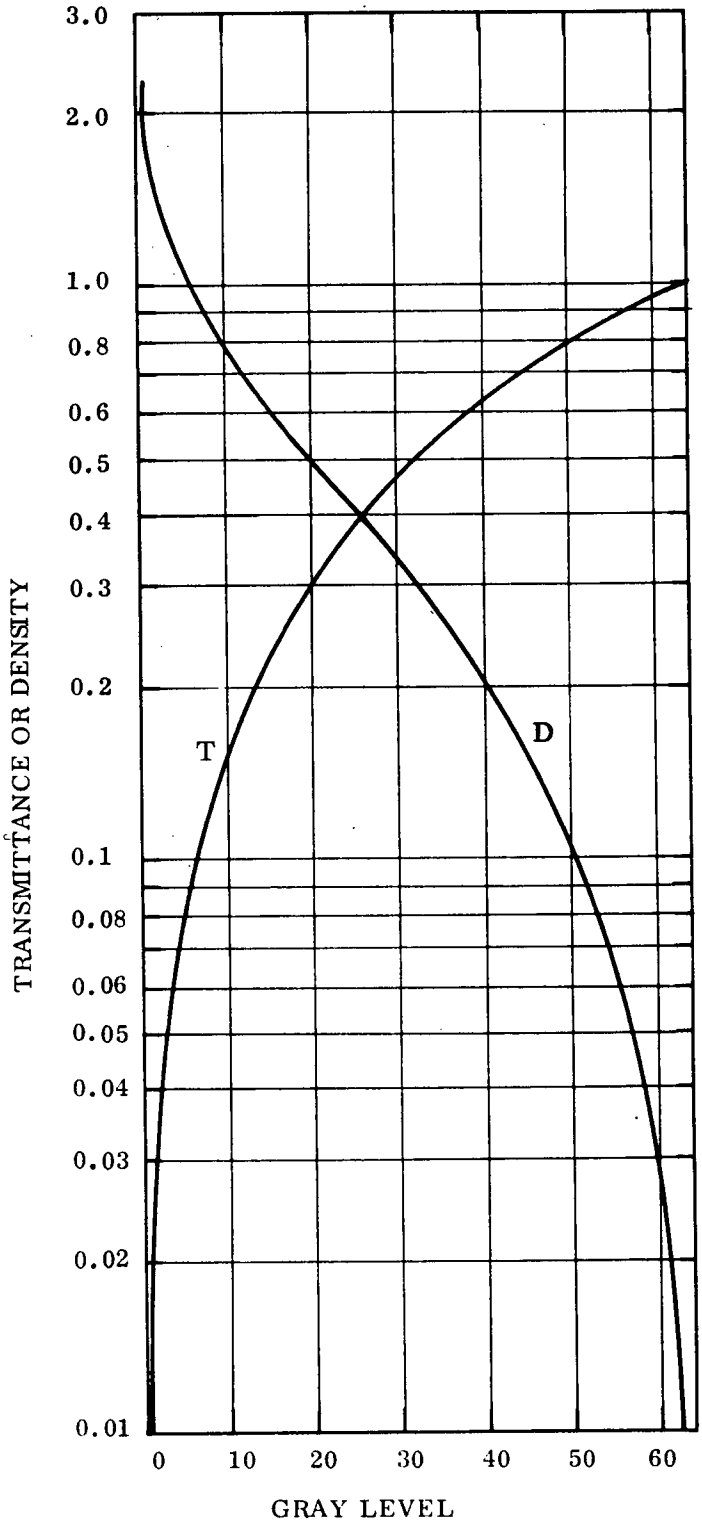

Figure 6-2. Response curves. T shows equal transmittance steps versus gray level and D shows the corresponding density steps.

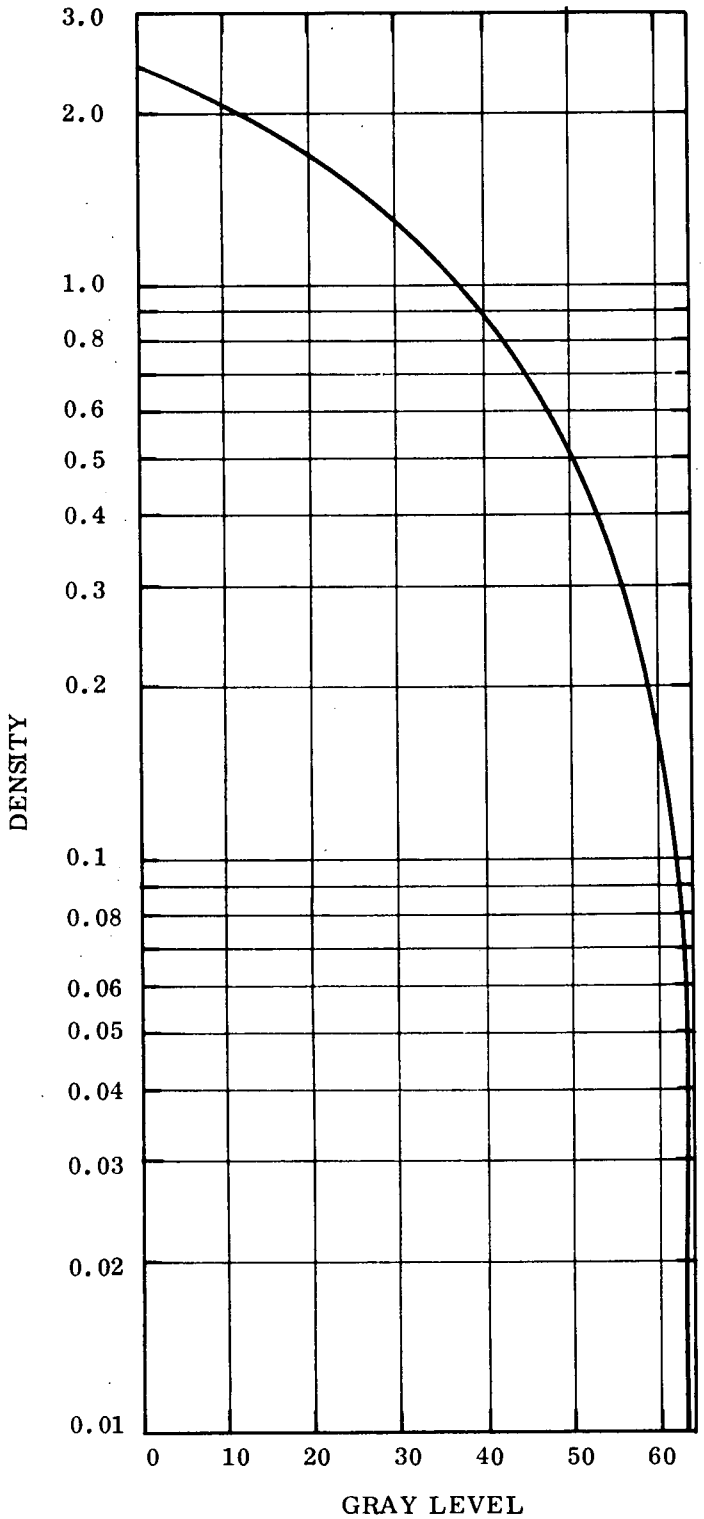

Figure 6-3. Response curve for equal density steps versus gray level for a film density of 2.4 and 6-bit digitization.

6.6 Configuration and Recommendations.

The process of digital enhancement of weld radiographs requires a large number of straight forward operations. As a result, the computing facility is designed to handle a lot of data but not perform as a general purpose computing facility for other applications. The Central Processor and peripherals must meet certain specifications and these are:

The system shown in Figure 6-4 is designed to provide an enhancement facility for the processing of weld radiographs. With this configuration the user will enter the picture data on the magnetic tape drive. The tape will provide an interface between the off-line scanning system and the central computing facility. The second and third tape drives can be added as needed. The facility will function with only one drive but the use of two or more drives is recommended for efficiency. The tapes should be capable of transferring data at 30Kb for a tape density of 800 bpi. Higher speed drives should be used only when usage demands.

The intermediate storage must provide an average access time of less than 50 milli-seconds and a transfer rate of 200Kb. Faster transfer rates are not required because the longest records used are only 32K bytes. The intermediate storage medium will provide at least 100,000,000 bytes of storage. The device will be random access and can be obtained as a disk, drum or slow core.

Program storage will be done on either punched cards or a random access device. Punched cards will only be used when the system is run with no special purpose processing system. The use of the intermediate storage device for program storage will enhance the performance of the system even when operating in a batch mode. The use of a processing language and processing supervisor will require the use of a random access device for program storage. The efficiency of the system is greatly enhanced by the use of a processing system stored on a random access device. The use of the punched cards with no processing system on the other hand becomes extremely cumbersome when processing large amounts of data.

Some form of gray scale display must be provided to output results. Output can be stored on tape and rerecorded on the scanning recording system but the cost and time required restrict its frequent use. A more adequate solution is to provide an on or off-line quick look display for evaluation of processing results. Various forms of displays are available on the market but a trade-off must be made of speed against raster size and gray scale. Several systems are available as off-the-shelf items which utilize TV monitors and obtain a

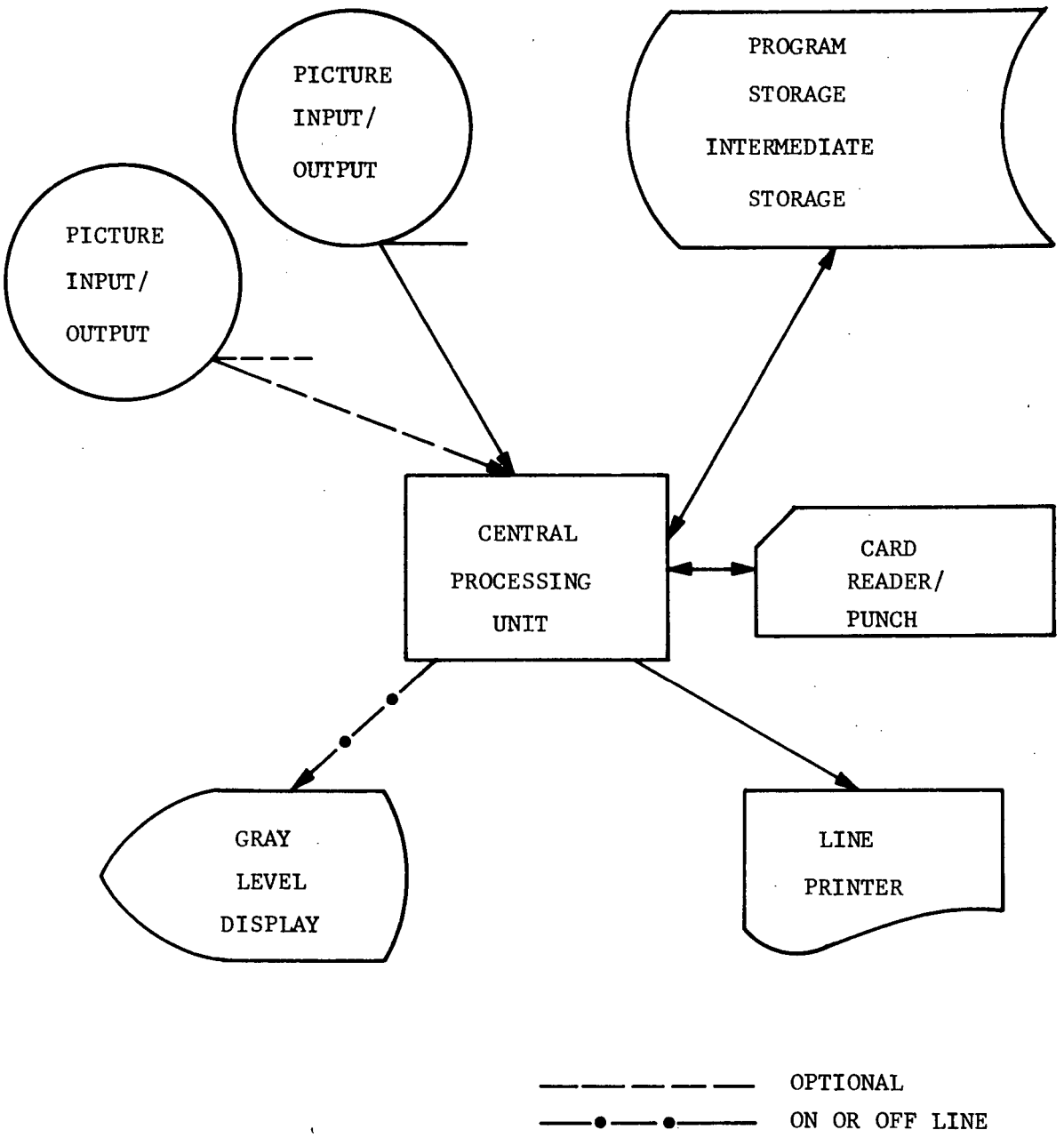

Figure 6-4 System Configuration

6.6 --Continued.

512 x 512 raster size with 16 gray levels. The raster size however is too small to provide an adequate viewing area. Storage tube displays on the other hand are available up to a 2048 x 2048 raster with 64 levels of gray. The small dynamic range and slow speed are limiting factors for the storage tube but the large viewing area provides a positive advantage. On-line devices provide an immediate check on processing but tie up the system while viewing pictures. The off-line display slows down the viewing process but pictures can be displayed often without any effect on the computational system. A possible solution is the development of a unit which will operate in either mode.

The Central Processing Unit (CPU) is the most critical component. Because of the nature of the data and the operations performed, the speed of the CPU is extremely critical. To provide adequate turn around the processor must have the following capabilities:

(1) $\leq 1\ \mu s$ cycle time
(2) $\leq 15\ \mu s$ floating multiply
(3) $\leq 5.0\ \mu s$ floating add
(4) 32K 16 bit words
(5) index registers
(6) support random access devices
(7) 200KB transfer rate, and
(8) support magnetic tape drives.
(9) a sufficient number of DMA channels to support peripheral devices

These qualifications can be met by many manufacturers in the minicomputer field which will reduce the cost of the overall system.

Special purpose hardware should only be added when the processing load is too large to handle otherwise. It is recommended that if special purpose hardware is used that it be aimed at providing adequate facilities for convolution filtering techniques due to the fact that it is more practical to implement in two dimensions than the Fourier transforms.

The scanning/ recording hardware should be operated off-line using magnetic tape as an interface to the central system. In systems where the scanning is computer controlled, the computer can be used to perform elementary enhancement techniques and pictures utilities. In this case, the sophisticated processing could be reserved for the central computing system.

APPENDIX A

ANALYTICAL CONSIDERATIONS

This appendix provides the theoretical background for the work described in Sections 1 - 7 of the report. It is divided into three main topics. Section A.1 gives an overview of the scanning and recording operation, Section A.2 discusses scanner evaluation techniques and Section A.3 presents the analysis of film grain and gray level quantization.

CONTENTS

A.1 OVERVIEW OF SCANNING AND RECORDING.

Because of their fundamental role in the digital processing of radiographs, the general nature and operation of film scanner/recorders are described in this section. A description of the scanner/recorder operation is given in Section A.1.1, and Section A.1.2 is concerned with noise and accuracy considerations.

A.1.1 Description of Film Scanner/Recorder Operation.

There are five principal methods for optical scanning and reading of photographic film. These are: cathode ray tube flying spot scanning, mechanical aperture scanning in a drum-type densitometer, direct electron beam reading, laser scanning and image dissector (vidicon). All but the image dissector may also be used for signal recording on photographic film. Since cathode ray tube flying spot scanners were selected for evaluation in this study, only this type of device will be discussed to illustrate general principles.

Figure A-1 illustrates the use of a digital flying spot scanner/recorder for digitizing a transparency. The deflection, intensity and spot size circuits of the flying spot scanner CRT are all controlled by a digital computer to scan the light spot on the phosphor face in a controlled raster pattern. A small fraction of the image light of the scanner spot is sampled by a beam splitter and collected onto a reference photomultiplier. The reference photomultiplier output is fed back through a digital correction circuit to compensate for spatial and temporal variations of the CRT spot brightness over the surface of the tube, thereby assuring uniform illumination of all points in the scanned transparency.

The main portion of the forward-directed light output from the scanned CRT spot is imaged through a lens onto the transparency being scanned. As the CRT spot scans its pattern, its image scans across the transparency. The light from this spot image that is passed by the transparency is collected and imaged onto a photomultiplier tube. The photomultiplier current is integrated over the dwell time of the spot upon a position in the transparency. The output of the integrator is then divided by the reference photomultiplier, so that the net output is always proportional to the fraction of the incident light transmitted by the transparency, i.e., to the transmittance. This measured transmittance is then digitized and stored on magnetic tape for input to the simulation. In some cases it is desirable to digitize the logarithm of the transmittance.

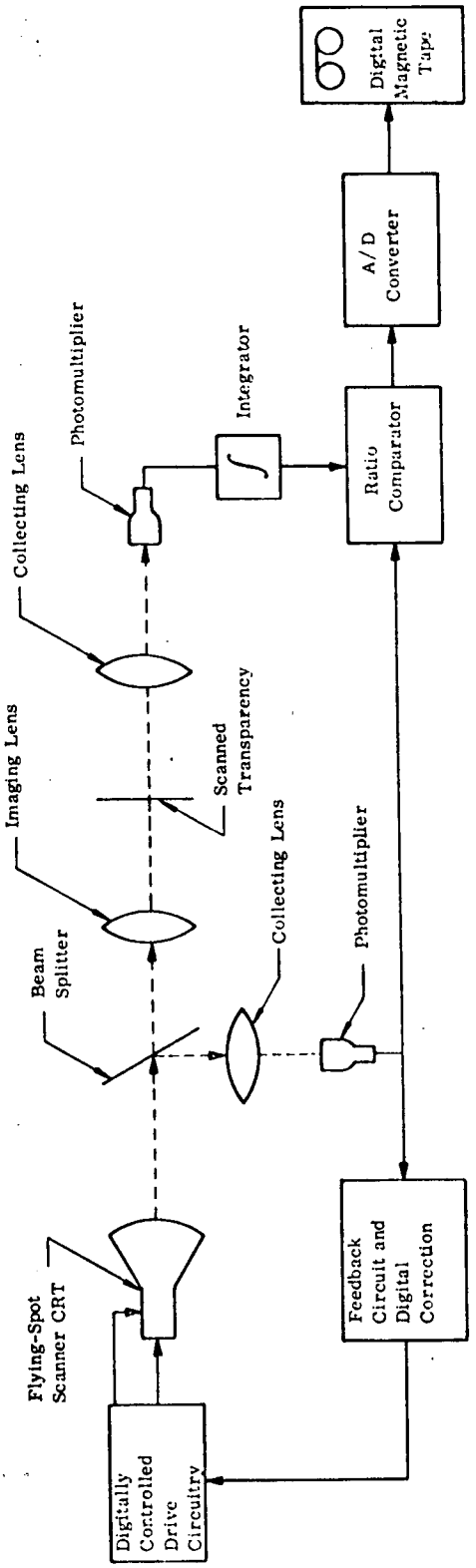

Figure A -1 Film Scanner Operation

A.1.1 -- Continued.

Figure A-2 illustrates the use of a film scanner/recorder for recording digital images on photographic film as a hard-copy visual output. The digital data is converted to a set of analog signals which are used to drive the various circuits controlling the flying spot scanner CRT. Again, the image of the output spot is sampled by a beamsplitter and imaged onto a reference photomultiplier in a feedback path to the drive circuitry. The CRT spot dwell time is proportional to the desired intensity or transmittance of the output picture at each point. The feedback circuit compensates for nonuniform phosphor and electron beam response and may also be used to compensate for nonlinearities in the recording film D-log E curve. The thereby regulated CRT spot is imaged onto the film being exposed, with the exposure of each spot having been properly controlled.

The use of commercially available film scanner/recorders to obtain hard copies of a large number of intermediate pictures is expensive and time consuming. Consequently, for this study almost all hard copies were obtained by photographing a video display of the digital image. The Dicomed 30 unit is used to obtain video displays at ESL. This unit has a roster size of 1024x1024, 64 gray levels, and, despite an undesirably small dynamic range, is adequate for the majority of the pictures.

A.1.2 Qualitative Considerations of Noise and Accuracy.

The types of noise found in film scanning and digitizing equipment may be classified according to whether or not they are correctable through calibration. The noise due to non-correctable sources may be considered to be the noise that remains after calibrations have been applied.

Examples of scanning noises that can be corrected for by calibration are: CRT spot halation, phosphor noise, lens flare, photomultiplier nonlinearities at high gains, and positionally dependent intensity variations. These effects are corrected by adjusting the intensity output of the photomultiplier on a point-by-point basis using a prerecorded digital calibration array. This calibration array is obtained by scanning a neutral density filter of highly uniform known transmittance and by measuring the resultant position-dependent output. It is believed that, after correction, the calibratable noise sources would not contribute significantly in the eighth or higher bit of the digital output.

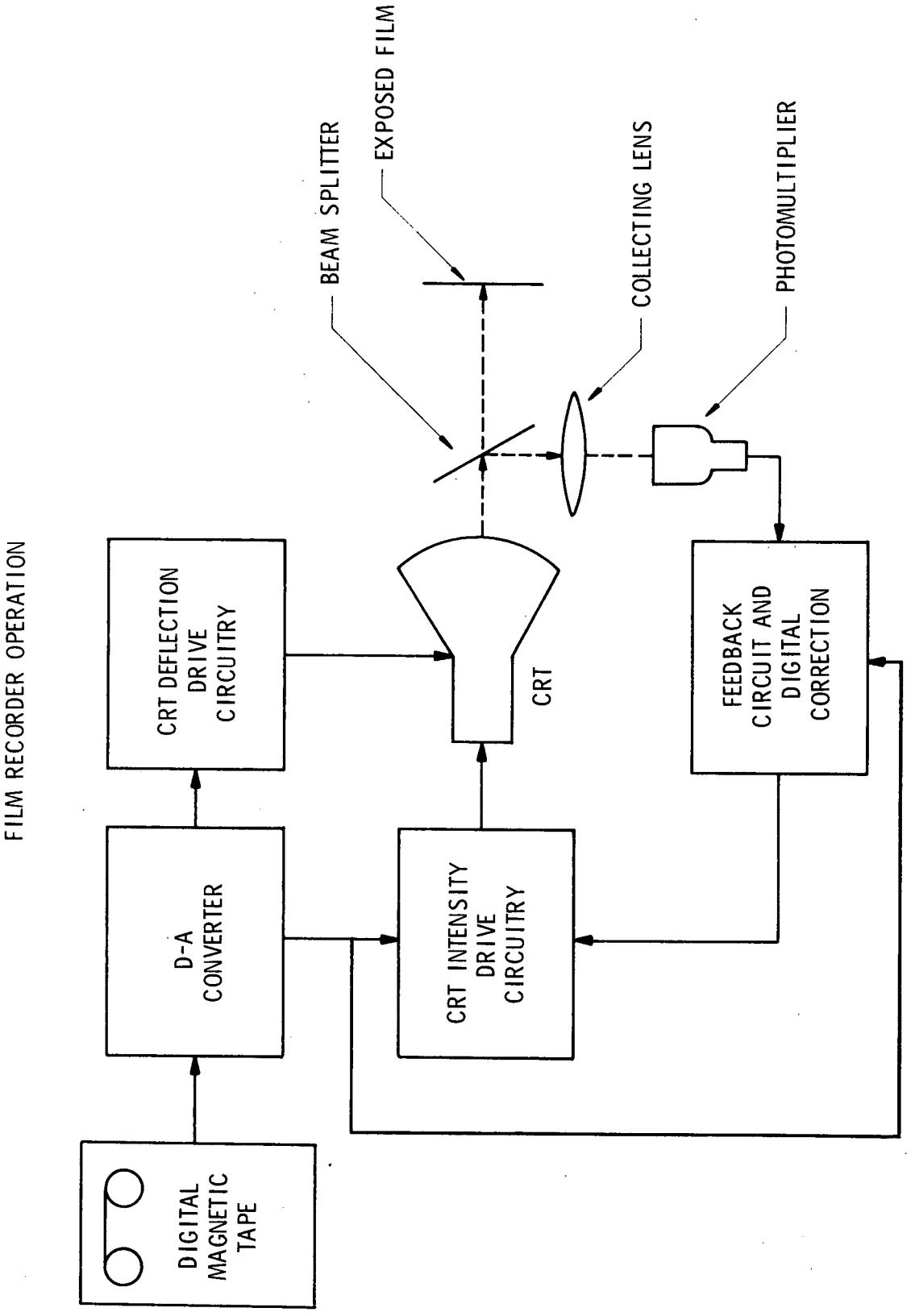

Figure A -2 Film Recorder Operation

132

A.1.2 -- Continued.

Non-calibratable noise sources include CRT beam intensity fluctuations, RF interference affecting the CRT drive circuitry, and photomultiplier dark-current (thermal noise). RF interference can cause errors in spot size, intensity and position. However, by properly screening the film scanner and by filtering the electrical power inputs, RF interference can, for all practical purposes, be eliminated. The effects of time-varying beam intensity fluctuations can be minimized by feedback regulation through the reference photomultiplier. The thermal noise level in the photomultiplier can be lowered by cooling the photocathode, if necessary. The combined effect of these noise sources is commonly held negligible in the sixth significant bit and, by exercising the necessary precautions, eight-bit precision is achievable.

Other factors which must be considered in film scanner accuracy are linearity and reproducibility. Linearity is a measure of the positioning accuracy of the scanner. It is expressed as a ratio whose numerator has the value of the maximum allowed positioning error in spot diameters over a given distance. The given distance as measured in spot diameters is the denominator of the ratio. Linearity figures typically cited for scanners are 0.05 percent, or ± one spot diameter out of 2,048.

The reproducibility of the scanner is expressed in two ways: in terms of spot position, and in terms of gray level. The scanner is instructed to place a known pattern of spots on the film, and those spots out of position are counted. Color discrimination is used to measure the number of misplaced spots. The gray level accuracy is measured by digitizing a calibrated neutral density filter, counting the number of spots which do not have the proper gray value, and establishing the percentage of spots in error. Typical reproducibility numbers cited for scanners at six-bit digitization are: (1) a positional uncertainty that 0.025 percent of the spots may be out of their correct position by as much as one spot diameter, and (2) an intensity uncertainty that up to 0.05 percent of the spots may be in error by as much as one gray level out of 64.

A.2 Scanner Evaluation Techniques.

The performance of a film scanner is primarily determined by its spatial frequency response (SFR) and its noise characteristics. Procedures were used to measure both the SFR and the noise from a digitized Air Force three-bar resolution chart. The SFR and noise are used to define the limitations of the

A.2 -- Continued.

scanning hardware and to determine the Fourier filter to correct for the system degradation. Section A.2.1 describes analytically the SFR and Section A.2.2 details noise evaluation analysis.

A.2.1 Spatial Frequency Response.

The point spread function (PSF) describes how each element of an optical system spreads or distorts the image of a point object. The point spread function is the normalized diffraction pattern formed by a point object. When the lens is perfect (that is, diffraction-limited), then the diffraction pattern consists of a bright central disk (the Airy disk) surrounded by a series of progressively fainter rings. If the lens is less than perfect the size of the central disk and the spacing of the surrounding rings stays about the same, but the central disk is less bright. The light that is lost by the central disk reappears in the surrounding rings.

In the film the image of a point is spread by scattering, reflections, and the grains themselves. In an image tube spreading is caused by the granular structure of the photosensitive surface, charge leakage, the finite size of the scanning beam, and perhaps electrical bandwidth. At any rate, we can measure (and sometimes calculate) the point spread function for each element of the film scanner.

Figure A-3 shows some typical spread functions for a lens, film, and an image tube. The spread function is a plot of the illuminance of the image as a function of distance in the image plane. Actually each element of the scanner system will have a series of spread functions for different positions off the optical axis. And, in general, only a spread function for a point on the optical axis will be symmetrical.

If, instead of a point, our optical system images a line, then we obtain the line spread function. We can consider the line spread function as a series of point spread functions added together to form the line.

Knowing the point spread functions for an optical system, we can plot the illuminance of any image by adding together the point spread functions that correspond to the points in the object or target. This summation process can be represented by what is called a convolution integral. To illustrate, if we have an object

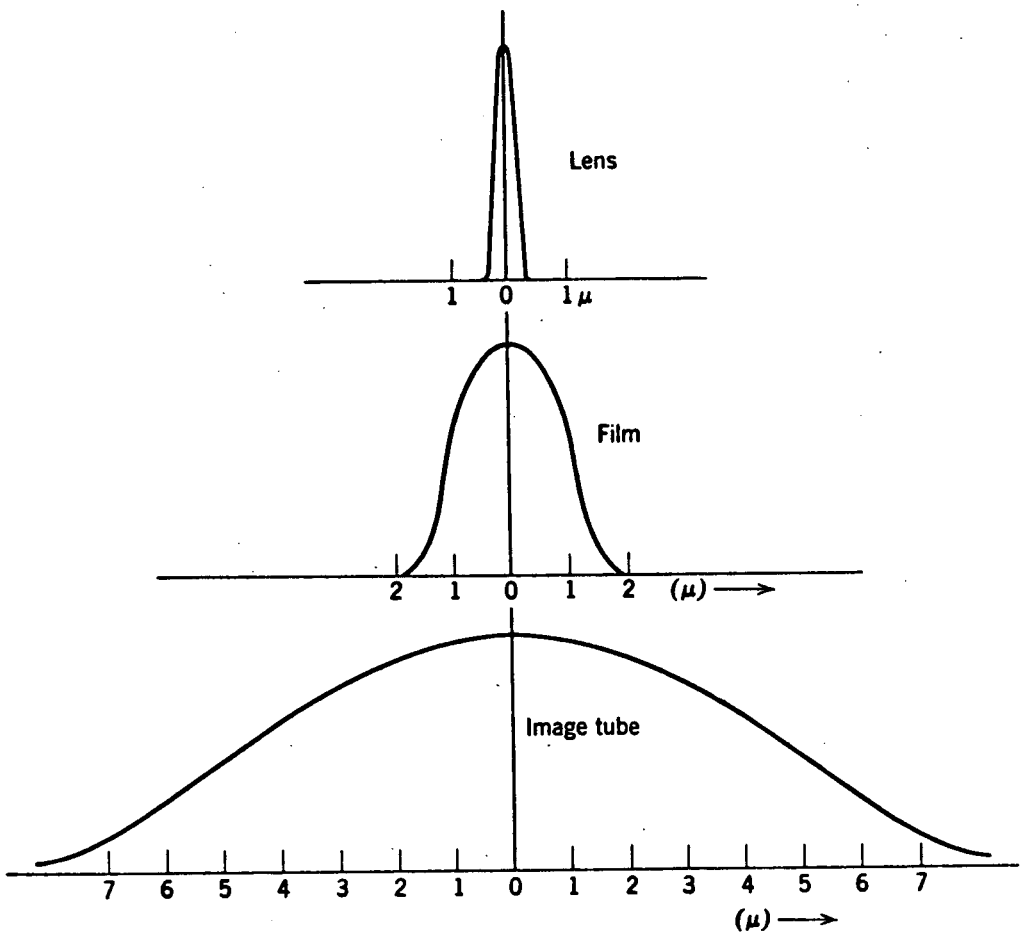

Figure A-3. Typical spread functions for a lens, film, and image tube.

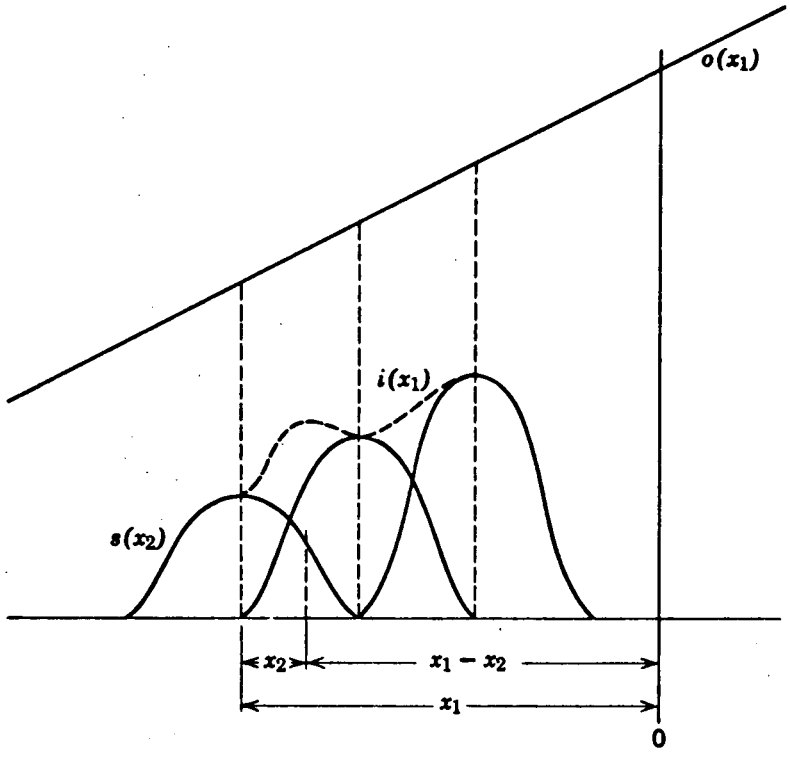

Figure A-4. Illustrated convolution of an object function $o(x_1)$ and a spread function $s(x_2)$ to produce the image function $i(x_1)$.

A.2.1 -- Continued.

defined by a function $o(x_1)$ and a spread function $s(x_2)$, then the illuminance of the image $i(x_1)$ is given by the convolution of these two functions:

$$i(x_1) = \int_{-\infty}^{\infty} s(x_2)\, o\,(x_1 - x_2)\, dx_2 \ . \qquad \text{(A2-1)}$$

In an actual optical system optical aberrations, such as pincushion distortion or coma, cause the point spread function to be a function of position in the image plane. The inclusion of these detailed nonuniformly spatially dependent effects in the modeling of the optical system makes the computations very expensive, and, consequently such computations are done only for very demanding optical system designs where the expense can be justified. Fortunately, these aberrations are third order effects, for the systems covered in this study, i.e., these effects can be neglected relative to the first order uniform magnification of the optical system. Therefore, the assumption that the spread function is constant as a function of position in the image plane is valid for this discussion. Figure A-4 illustrates the convolution integral.

On taking the Fourier transform of both sides of Eq. (A2-1) it is found that

$$I(\omega) = S(\omega)\, O(\omega) \ , \qquad \text{(A2-2)}$$

that is, the Fourier transform of the image function, $I(\omega)$, equals the product of the Fourier transforms of the point spread function, $S(\omega)$, and the object function, $O(\omega)$. Rearranging, we get

$$S(\omega) = \frac{I(\omega)}{O(\omega)} \ . \qquad \text{(A2-3)}$$

This is analogous to the definition of the transfer function in circuit analysis. (O'Neill[5] points out that it is unfortunate that, in optics, the symbols I and O for image and object have the opposite relation in circuit analysis, where they stand for input and output.) When normalized, the Fourier transform of the spread function is called the optical transfer function (OTF). Denoting the normalized transform by $\tau(\omega)$, we have

$$\tau(\omega) = \frac{\int_{-\infty}^{\infty} s(x)\, e^{-i\omega x}\, dx}{\int_{-\infty}^{\infty} s(x)\, dx} \qquad \text{(A2-4)}$$

The above expression for the optical transfer function contains both an amplitude term and a phase term. Usually the phase term is important only when considering coherent illumination, as in a laser. However, in most photographic film-

A.2.1 -- Continued.

scanning analysis the illumination is incoherent, so only the amplitude term is important. The transfer function is then called the modulation transfer function (MTF), and it is designated T(k) where $2\pi k = \omega$:

$$T(k) = |\tau(\omega/2\pi)|. \qquad \text{(A2-5)}$$

In the ideal but unrealizable case, the OTF will show a unity response for all spatial frequencies up to the limits of diffraction. Using the OTF and an Air Force resolution chart we have a means of quantitatively measuring the performance of different scanning systems. By scanning and digitizing a high-contrast edge from the test chart, the so-called edge trace response of the scanner system may be recorded. The line spread function can be obtained by taking a one-dimensional spatial derivative of the edge trace measured for a sharp black-to-white transition. If the system did not degrade the original image, the image of this transition would be identical to the input, and the line spread function would be a delta function. The scanning system, however, does introduce high frequency degradations and the resulting edge will be degraded as shown in Figure A-5. As a result, the impulse function of the degraded edge will not be an ideal impulse function but might be as shown in Figure A-6. By taking the Fourier transform of the impulse function, and scaling the DC term to one we obtain the MTF of the scanning system, Figure A-7.

A.2.2 Noise Evaluation.

The introduction of noise in the scanning procedure produces a significant effect on the resulting MTF. From the physical properties of the lens and the spot energy distribution we know that the MTF will be a monotonically decreasing function. When noise is introduced however, we find that the MTF is not monotonic. The non-monotonic behavior was introduced when we took the spatial derivative of the input. The effect of the derivative was to multiply the noise present by a sine function in the spatial frequency domain.

That a sine function in the magnitude of the Fourier coefficients is the result of differentiating the input is seen from the following.

Define the discrete Fourier coefficients of the original input as

$$A_n = \sum_{k=0}^{N-1} x_k \, e^{2\pi i(kn/N)} \qquad \text{(A2-6)}$$

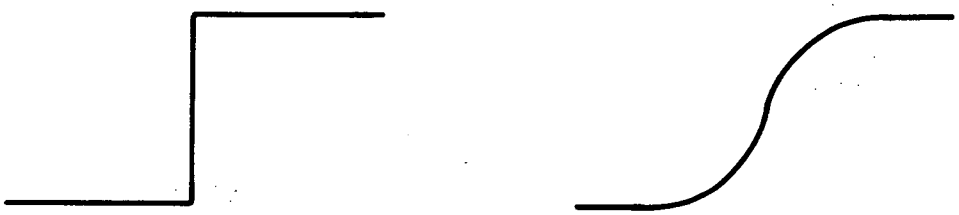

Figure A-5. (a) Perfect black to white edge;
(b) Degraded black to white edge.

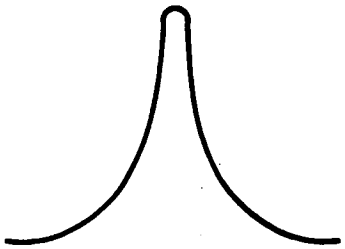

Figure A-6. Impulse function from a degraded edge.

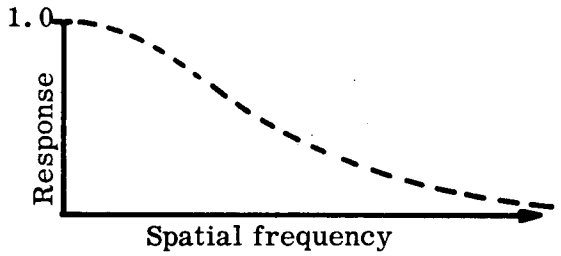

Figure A-7. Typical OTF determined from a degraded edge.

A.2.2 -- Continued.

Then the Fourier coefficients of the point by point differences of the original input are defined as

$$B_n = \sum_{k=0}^{N-1} y_k \, e^{2\pi i(kn/N)} \quad , \tag{A2-7}$$

where

$$y_n = x_n - x_{n+1} \qquad \text{for } n = 0, 1, \cdots, N-2 \quad ,$$

$$y_{N-1} = x_{N-1} - x_o \quad .$$

Equation (A2-7) can be written as

$$B_n = \sum_{k=0}^{N-1} x_k \, e^{2\pi i(kn/N)} - \sum_{k=1}^{N-1} x_{k+1} \, e^{2\pi i(k-1)/N} - x_o \, e^{2\pi i(N-1)n/N} \quad . \tag{A2-8}$$

Since $e^{2\pi i(N-1)n/N} = e^{-2\pi i(n/N)}$ for an integer n, Equation (A2-8) becomes

$$B_n = \sum_{k=0}^{N-1} x_k \, e^{2\pi i(kn/N)} - \sum_{k=0}^{N-1} x_k \, e^{2\pi i(k-1)n/N} \quad , \tag{A2-9}$$

which can be reduced to

$$B_n = \left[\sum_{k=0}^{N-1} x_k \, e^{2\pi i(kn)/N} \right] \left(1 - e^{-2\pi i(n/N)} \right) \quad . \tag{A2-10}$$

Combining Equations (A2-6) and (A2-10) gives

A.2.2 -- Continued.

$$B_n = A_n \left(1 - e^{-2\pi i(n/N)} \right) \qquad \text{(A2-11)}$$

and

$$|B_n| = |A_n| \, 2 \sin \frac{n\pi}{N} \quad . \qquad \text{(A2-12)}$$

The solid line in Figure A-8 illustrates the non-monotonic behavior of the Fourier transform of the noisy data and the dashed line in Figure A-8 shows the noise constant times the above sine wave. The noise-free MTF is the result of subtracting the values of the dashed curve from the values of the solid curve and is illustrated in Figure A-9.

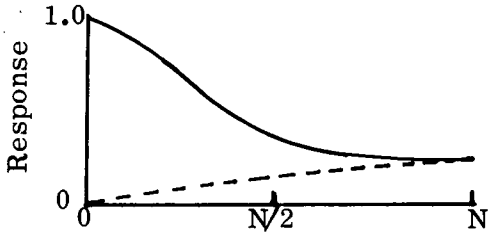

Figure A-8. The solid curve shows the typical Fourier transform of the first order differences of a black/white transition from a system with noise. The dashed curve shows the noise constant times 2 sin ($n\pi/N$).

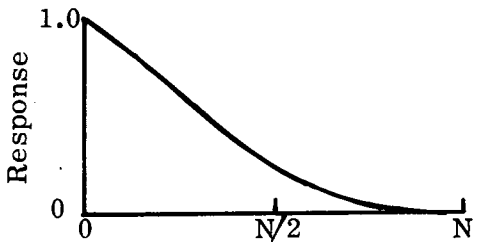

Figure A-9. The noise-free MTF obtained by subtracting the dashed curve in Figure A-8 from the solid curve.

A.2.2 -- Continued.

It is desirable to obtain a noise-free response curve for use in both system evaluation and inverse filter generation. An analytical study of averaging and curve fitting techniques should be made to determine the best method to correct the MTF for noise.

A.3 Effects of Film Grain and Gray-Level Quantization.

Graininess is defined as the visual impression of nonuniformity of density in a radiograph (or photographic) image. With fast films exposed to high kilovoltage radiation, the graininess is easily visible to the unaided eye. With slow films exposed to low kilovoltage X-rays, moderate magnification may be needed to make it visible. In general, graininess increases with increasing film speed and with increasing energy of radiation.

The "clumps" of developed silver which are responsible for the impression of graininess do not each arise from a single developed photographic grain, since each grain is far too small to be seen by the unaided eye. Rather, the visual impression of graininess is caused by the random, statistical fluctuations in the number of grains exposed and developed per unit area. These fluctuations, in turn, create noise-like variations in the nominal density level, thus giving a grainy appearance to the developed image and also leading to measurement errors in any attempt to determine the relative brightness of two points in the object scene.

The dependence of graininess on film speed arises from the fact that the silver bromide crystals in a slow film are smaller than those in a fast film, so that the crystals in a slow film will produce less light-absorbing silver when they are exposed and developed. However, at low kilovoltages, one absorbed quantum will expose one grain, of whatever size. Thus more quanta will have to be absorbed in a slower film than in the faster film to result in a particular density.

The increase in graininess of a particular film with increasing kilovoltage can also be understood on this basis. At low kilovoltages each absorbed quantum exposes one photographic grain; at high kilovoltages one quantum will expose several, or even many, grains. At high kilovoltages, then, fewer absorption events will be required to expose the number of grains required for a given density than at lower kilovoltages. The fewer absorption events, in turn, mean a greater relative deviation from the average, i.e., a greater clumping of exposed grains, and hence greater graininess.

A.3 -- Continued.

It has been experimentally verified that over adequately large regions of uniform exposure, the fluctuations in the optical density of a photographic or radiographic emulsion exhibit a distribution of the deviations from the mean density that are well approximated by a Gaussian probability law.[6] The standard deviation σ_D of the density is often referred to as the RMS granularity of the emulsion. σ_D is a function of the mean density and of the size of the scanning spot. Falconer[7] has derived an expression for σ_D given by

$$\sigma_D = \frac{\sqrt{a\, D/2.3}}{d} \qquad \text{(A3-1)}$$

Here a is the mean absorption cross section per silver grain in the emulsion, and d is the diameter of the scanning spot with which the measurement of σ_D is made. This formula indicates that the observed granularity increases as the square root of the mean density (Eyer's law),[8] and decreases inversely as the spot diameter d (Selwyn's law).[9] Unfortunately the value of a is not available for Kodak radiographic films.

In practice, film manufacturers measure the RMS granularity of their emulsions with a scanning densitometer at a specified optical density and scanning aperture and then use Eyer's and Selwyn's laws to convert them for use at other densities and other resolutions. In particular, if σ_o denotes the RMS granularity measured at film density D_o, and with a scanning aperture d_o, then the granularity σ_D expected at a mean optical density $\bar{D}$ and with a scanning spot diameter d is given by

$$\sigma_D = \sigma_o\, (d_o/d) \sqrt{\bar{D}/D_o} \qquad \text{(A3-2)}$$

Higgins and Stultz[10] have verified the Selwyn law for a variety of emulsions and average film densities. They have found the law to be valid over a wide range of aperture sizes which they investigated varying from 7.5 to 384 microns.

The important factors which affect the graininess of radiographic films are:

(1) development time and temperature; longer development and higher temperatures of development result in increased graininess;

(2) higher kilovoltages of exposure result in increased graininess;

(3) lead screens and intensifying screens which increase the graininess.

A.3 --Continued.

These factors affect the graininess by varying the grain clump size which results in variations of the RMS granularity σ. As a result, manufacturers of radiographic films are hesitant to assign specific values of σ_o to individual films.[11] Instead, manufacturers simply rate their radiographic films in order of increasing graininess.

For example, Kodak Industrial X-ray films are listed in order of increasing graininess as follows:

Sub-Class 1	Type R
Class 1	Type M
Class 1	Type T
Class 2	Type AA
Class 3	Medical No Screen
Class 4	Screen types of film exposed with calcium tungstate screens

Nevertheless, if for any given set of conditions the granularity of a radiographic emulsion is measured, the effects upon the graininess of varying the film scanner spot diameter or the film density may be determined from Eq. (A3-1). When more data is available from film manufacturers Eq. (A3-2) will aid in an analytical determination of the optimum spot size.

As indicated in Section A.1.1 the directly measured output of a film scanner is proportional to the average transmittance $\bar{T}$ of the film over the area instantaneously illuminated by the scanning spot. The transmittance T is related to the film density D by

$$D = -\log_{10} T = -k \ln T , \qquad \text{(A3-3)}$$

where $k = 0.43429$. If the output of the film scanner is desired in units of density, it must be derived from the measured film transmittance using Eq. (A3-3). This may also be accomplished by nonuniformly quantizing the output photomultiplier using equal density steps determined according to Eq. (A3-3).

First consider the situation in which the desired output is a quantization in film density of the density range $D_1 \leq D \leq D_2$. A quantizer may be characterized as a device with a "staircase function" input-output characteristic.[12] This characteristic function is referred to as a quantization function, denoted $Q(D)$.

A.3 -- Continued.

With the transmittance range $D_1 \leq D \leq D_2$ quantized into η equal increments of width

$$\epsilon_D = \frac{D_{max} - D_{min}}{\eta} \quad , \tag{A3-4}$$

the quantization function becomes

$$Q(D) = D_{min} + (j - \tfrac{1}{2})\, \epsilon_D \quad , \quad j = 1, \cdots, \eta \quad . \tag{A3-5}$$

The film grain noise and the quantization noise are statistically independent additive noise sources. The variance of the quantization noise is given by[8]

$$\sigma_{QD}^2 = \epsilon_D^2 / 12 \quad . \tag{A3-6}$$

The variance of the quantized distribution is given by the sum of the component variances:

$$\sigma_f^2 = \sigma_D^2 + \sigma_{QD}^2 \quad . \tag{A3-7}$$

From equations (A3-2) and (A3-6) it is found that

$$\sigma_f^2 = \sigma_o^2 (d_o / d)^2 (\bar{D} / D_o) + (D_{max} - D_{min})^2 / 12\, \eta^2 \quad . \tag{A3-8}$$

Equation (A3-8) provides an expression for the variance of the measured density at the output of the film scanner due to the combined effects of graininess in the input radiographic image and of amplitude quantization in the intensity digitization process.

As a measure of the accuracy with which the digital image may be represented, a noise-to-signal power ratio (N/S) may be defined by

$$N/S = \sqrt{\sigma_f^2 + \sigma_{sc}^2} \; / \; \bar{D} \quad , \tag{A3-9}$$

where σ_{sc} is the RMS level of noise introduced by the film scanner operation, as discussed in Section 2.4. The ratio of signal to noise (the reciprocal of Eq. (A3-9) has a profound bearing upon the minimum size of detail that can be

A.3 -- Continued.

seen. It has been shown that for threshold visibility of detail, S/N must be at least 5.[1]

To maximize S/N, the individual components of N/S must be minimized. The N/S component due to film graininess is given by

$$(N/S)_g = \sigma_o \, (d_o/d) \, (1/\sqrt{D_o \bar{D}}) \quad . \tag{A3-10}$$

This varies inversely with $\sqrt{\bar{D}}$, and so the S/N is maximized by exposing and developing the radiographs to high film densities. This provides an analytic basis for the improved performance of quality control technicians when working with high density radiographs.

It is also seen that $(N/S)_g$ varies inversely with the diameter of the film scanner spot aperture, so that the S/N increases with increasing spot diameter. However, as the spot diameter increases, so does the size of the minimum resolvable detail (or weld defect) in the radiograph. Consequently, the S/N will vary directly with the size of the detail sought, and so a tradeoff will be required between the scanner resolution and signal-to-noise ratio due to film grain. Alternatively, since small details and sharp edges are associated with high spatial frequencies in the system MTF, the S/N can be expected to decrease with increasing spatial frequency. This has been observed experimentally.

The N/S component due to digitizer quantization is given by

$$(N/S)_q = (D_{max} - D_{min}) / \sqrt{12} \, \eta \, \bar{D} \tag{A3-11}$$

This is seen to vary directly with the size of the density step and inversely with the mean density of the detail being scanned.

If the output of the digital film scanner is obtained directly in terms of film transmittance, corresponding expressions for the S/N may be obtained.

It can be shown that the probability density function for T may also be adequately represented by a Gaussian:

$$p(T \mid \bar{T}, \sigma_T) = \frac{1}{\sqrt{2\pi}\,\sigma_T} \exp\left[-\frac{1}{2} \left(\frac{T - \bar{T}}{\sigma_T} \right)^2 \right] , \tag{A3-12}$$

A.3 -- Continued.

where

$$\sigma_T = (\sigma_o/\sqrt{k D_o})(d_o/d)\sqrt{\bar{T}(1-\bar{T})} \qquad \text{(A3-13)}$$

is the standard deviation of the departure of the transmittance T in any local region over the neighborhood of a scanner spot from the expected transmittance $\bar{T}$ over that neighborhood in the absence of grain effects. The use of Eq. (A3-13) is valid as long as $N\bar{T}(1-\bar{T}) \leq 10$, where N is the ratio of the scanner spot area to the mean absorption cross section per silver grain.

Suppose that the transmittance range $0 \leq T \leq 1$ is to be quantized into η equal increments of width $\epsilon_T = 1/\eta$. The variance of the transmittance quantization noise is then given by

$$\sigma_{QT}^2 = (\epsilon_T^2/12)(1/12\eta^2) \qquad \text{(A3-14)}$$

The variance of the combined film graininess and quantization noises for film scanner output in terms of equal transmittance steps is then

$$\sigma_f^2 = (\sigma^2/k D_o)(d_o/d)^2 [\bar{T}(1-\bar{T})] + 1/12\eta^2 \quad . \qquad \text{(A3-15)}$$

The noise-to-signal ratio N/S is again given by Eq. (A3-9) but with σ_f^2 now given by Eq. (A3-15)

It should be noted that the first term of Eq. (A3-15)goes to zero for $\bar{T} = 0$ and $\bar{T} = 1$, and at those limits the quantization noise is predominant. The function $\bar{T}(1-\bar{T})$ has a maximum at $\bar{T} = 0.5$, and this is the expected local transmittance that produces a maximum variance in the measured transmittance. Consequently, film grain noise effects will be minimized by working at transmittances much smaller than $\bar{T} = 0.5$ (the low contrast obtained with X-ray films at low densities or high transmittances precludes operation at the other extreme of the transmittance scale). Thus, low average film transmittance or, equivalently, high average density are required for maximum signal-to-noise operation.

REFERENCES

1. "Radiography in Modern Industry", 3rd Ed., Eastman Kodak Co., Radiography Markets Division, Rochester, New York, 1969.

2. C. E. K. Mees and T. H. James, The Theory of the Photographic Process, 3rd Ed., The MacMillan Co., New York, pp 185-187, 1966.

3. J. Johnson, "Analysis of Image Forming Systems", Image Intensifier Symposium, pp 249-273, 1959.

4. B. R. Hunt, "The Inverse Problem of Radiography", Mathematical Biosciences, Vol. 8, p 161-179, 1970.

5. E. L. O'Neill, Introduction to Statistical Optics, Addison-Wesley, Reading, Mass., 1963.

6. C. E. K. Mees and T. H. James, The Theory of the Photographic Process, The MacMillan Company, New York, 1966, p 525-256.

7. D. G. Falconer, "Noise and Distortion in Photographic Data Storage," IBM Jour. Research and Development, Vol. 14, p 521, Sept 1970.

8. J. Eyer, Applied Spectroscopy, Vol. 14, p 4, 1960.

9. G. Higgins, Applied Optics, Vol. 3, p 1, 1964.

10. G. C. Higgins and K. F. Stultz, "Experimental Study of RMS Granularity as a Function of Scanning Spot Size," J. Optical Soc. Amer., Vol. 49, pp 925-929, Sept 1959.

11. R. E. Turner, Radiography Markets Division, Eastman Kodak Company, Rochester, New York. Private Communication.

12. J. T. Tou, Digital and Sampled Data Control Systems, McGraw-Hill Book Company, Inc., New York, pp 83-92, 1959.

148